A NUMERICAL ANALYSIS OF THE EFFECT OF SURFACE FINISH AND CEMENT CREEP IN CEMENTED TOTAL HIP REPLACEMENT

by

D.S. Barker

B.E. (Hons).

A Thesis for the Degree of Master of Engineering Science

Department of Civil and Environmental Engineering

The University of Adelaide

July, 1996

Preface

This thesis, although submitted for a Degree of Master of Engineering Science, is in the field of orthopaedic biomechanics, and as such, contains many medical and anatomical terms. In this light, a glossary of terms is presented at the beginning of the text. These terms are not strict medical definitions, but allow the reader who does not have a clinical background to follow the concepts outlined in the thesis.

Also included in the glossary are the anatomical directions which are used as reference throughout the thesis. The reader is referred to several papers for a more detailed explanation of many of the clinical (non-engineering) aspects of the work.

Throughout the thesis, all techniques, concepts and conclusions obtained from other sources have been acknowledged in the text.

Abstract

The focus of the research presented in this thesis is a numerical investigation of the biomechanical behaviour of cemented total hip replacement (THR). Although the majority of artificial cemented hip joints remain intact for the remainder of the patient's life, a significant number fail leading to costly and potentially dangerous revision surgery.

The implantation of a hip prosthesis leads to a total rearrangement in the strain density field of the femur. Bone remodels under a change of strain and the decay of the upper femur due to 'stress-shielding' has been implicated in the breakdown of THR. The tensile stress distribution within the cement mantle is also of prime concern due to the presence of crack formation found clinically. A three dimensional finite element model was constructed in order to study these phenomena.

Maximum principal tensile stresses in the cement mantle and the distortional strain energy density in the upper femur were calculated for the conditions of; a fully bonded prosthesis-cement interface, a sliding interface between prosthesis and cement with a coefficient of friction of 0.22, and a frictionless prosthesis-cement interface. The effect of cement creep and an air-gap under the prosthesis tip were also studied. A bonded interface between the cement and prosthesis significantly reduced both maximum principal tensile stresses in the cement mantle, and distortional strain energy density levels in the upper femur when compared to the sliding interfaces. The presence of a distal air-gap caused an increase in the maximum principal tensile cement stresses at the tip of the prosthesis for the frictionless case only. The inclusion of viscoelastic cement properties caused only small reductions in the tensile stresses in the cement mantle.

The results of this study provide an indication of the mechanical influence of prosthesis stem surface finish and cement creep in cemented total hip replacement.

Statement of Originality

This thesis contains no material which has been accepted for the award of any other degree or diploma in any university or other institution and, to the best of my knowledge and belief, contains no material previously published or written by another person, except where due reference has been made in the text.

I give consent to this copy of my thesis, when deposited in the University Library, being made available for loan and photocopying.

Signed: Date:....17 - 3 - 1997

Acknowledgments

I am most indebted to my principal supervisor, Dr. Michael Yeo for his advice, time and especially patience throughout the period of my candidature. This project was especially difficult at times due to the large strain on computer requirements and it was Dr. Yeo's suggestions, especially regarding the finite element analyses, which helped the project's completion. I am also indebted to my medical supervisor, Professor Mark Pearcy who provided technical advice throughout and helped in the shaping of the thesis format.

I wish to thank the members of the Department of Orthopaedics and Trauma, Royal Adelaide Hospital, especially Dr. Scott Brumby, for critical advice and support throughout the project. I am also particularly grateful to Scott for the supply of CT scans for the sheep femur.

I would also like to acknowledge Derek Wilson of FEA Ltd., who provided substantial support and advice in regards to the finite element software.

I also thank the fellow postgraduate students for their good nature and friendliness over the years, especially James Pannell for proof reading the thesis. Thanks also to the secretarial staff within the Department of Civil and Environmental Engineering, especially Bernie and Anne for their constant smiles and help. Thanks must also go to Stephen Carr for his expertise in solving the inevitable computer problems which cropped up.

On a personal note, I will always be indebted to my sister Claire and mother Helen for the constant love and support given me to throughout this period. I finally must thank the friends that, although being dubious about the completion, kept me sane when things got tough, especially members of the great Zoom netball team.

Contents

Glossary

acetabulum - the "socket" component of the hip joint, located in the pelvis, (See Figure 1.1).

aseptic loosening - loosening due to reasons other than infection.

anterior - towards the front of an anatomical segment, (See Figure G.1).

arthrodesis - the fusion of a joint preventing motion.

atrophy - (also 'disuse atrophy'), a process whereby there is a decrease in the size of a tissue ie. bone. In this study bone atrophy is due to stress-shielding. The opposite to hypertrophy.

bone necrosis - see 'osteonecrosis'.

bone remodelling - (also 'remodelling'), a process where bone at a particular location alters its external and internal structure due to mechanical stimuli.

bone resorption - (also 'resorption'), a process where the bone stock at a particular location is decreased due to adverse mechanical or biological stimuli.

calcar - see 'femoral calcar'.

cancellous bone - the spongeous bone which is located at the end of long bones such as the femur. Also known as trabecular bone.

cement mantle - the cured or "hardened" bone cement which encapsulates the prosthesis stem.

cement plug - a device used to prevent the bone cement flowing distally into the medullary canal. It also increases the strength of the cured cement mantle.

cortical bone - the hardened bone which comprises the 'casing' for long bones such as the femur.

cortex - the hardened outer region of cortical bone, plural - cortices.

CT scan - computed tomographic X-ray scans which are obtained by compiling two dimensional images at a particular interval ie. 10 mm of a three dimensional structure eg. a femur.

debonding - a break-down of the bond at an interface. In this study, either the stem-cement interface or the bone-cement interface.

distal - towards the end of an anatomical segment, (See Figure G.1).

disuse atrophy - see 'atrophy'

femoral calcar - (also 'calcar'), the most proximal-medial region of cortical bone in the femur. (See Figure 1.2). This region of bone is highly susceptible to stress shielding and resorption.

femoral head - (also 'head of femur), the "ball" component of the hip joint, located at the proximal end of the femur, (See Figure 1.1).

femoral neck - (also 'neck of femur'), the region of the femur containing cancellous bone which joins the shaft of femur to the head of femur. (See Figure 1.1)

femoral shaft - the main body of the femur containing predominantly cortical bone. (See Figure 1.1).

head of femur - see 'femoral head'.

hip joint - the joint where the head of femur articulates against the acetabulum.

hypertrophy - a process whereby there is an increase in the size of a tissue ie bone. In this study bone hypertrophy refers to an increase in the size of bone due to excessive stress. The opposite to atrophy.

in vitro - performed in the laboratory, not on a living specimen.

in vivo - whilst living, performed on a living specimen.

interstitial fluid - fluid within the body which lies outside the vascular system (veins, arteries etc) and is extracellular.

lateral - away from the centre-line of an anatomical segment (See Figure G.1).

macrophage - a type of white blood cell which breaks down foreign particles.

medial - towards the centre-line of an anatomical segment (See Figure G.1)

medullary canal - the "hollow" of the femoral shaft into which the prosthesis is inserted.

neck of femur - see 'femoral neck'.

osteoarthritis - a degenerative disease caused from excessive wearing of a joint or joints.

osteoblast - a cell which leads to the production of new bone.

osteolysis - a process where implant material wear debris causes destructive bone tissue loss.

osteoporosis - a biological phenomenon which involves a "thinning" of bone.

osteonecrosis - (also 'bone necrosis'), death of bone tissue, often caused by excessive heat in THR surgery.

phagocytosis - a biological process where macrophages ingest foreign particles.

PMMA - polymethylmethacrylate, the bone cement used as a load mediator between the prosthesis and bone.

posterior - towards the back of an anatomical segment (See Figure G.1).

prosthesis - an artificial component used in the body. In the present study, the metallic replacement for the head and neck of femur.

proximal - towards the origin of an anatomical segment, (See Figure G.1).

radiograph - an "X-ray", which allows bone tissue to be identified.

remodelling - see 'bone remodelling'.

resorption - see 'bone resorption'.

stress-shielding - a phenomenon whereby the stress levels presenting in a region of bone are reduced from the normal physiological levels. This often occurs as a result of total hip replacement.

tibial epiphysis - the end region of the tibia (main bone in lower limb, articulates at the knee joint).

tibial plateaux - the articulating surface between the condyles of the tibia. The condyles are the bony prominences at the end of long bones. Femoral condyles are shown in Figure 1.3.

total hip replacement (THR) - (also 'total hip arthroplasty'), the replacement of the diseased acetabulum and head of femur with artificial parts.

trabeculae - the individual rods and plates which comprise cancellous bone.

valgus - a position indicating internal or medial rotation. For example, if the tip of a femoral prosthesis is located in the centre of the femoral shaft, the prosthesis is in a neutral position, however if the tip is located adjacent to the medial cortex, the prosthesis is in a valgus position.

varus - a position indicating external or lateral rotation.

SUPERIOR ANATOMICAL POSITION SUPERIOR

ANTERIOR or VENTRAL

POSTERIOR or DORSAL

proximal arm

lateral arm

medial arm

distal arm

proximal leg

distal leg

medial leg

lateral leg

INFERIOR INFERIOR
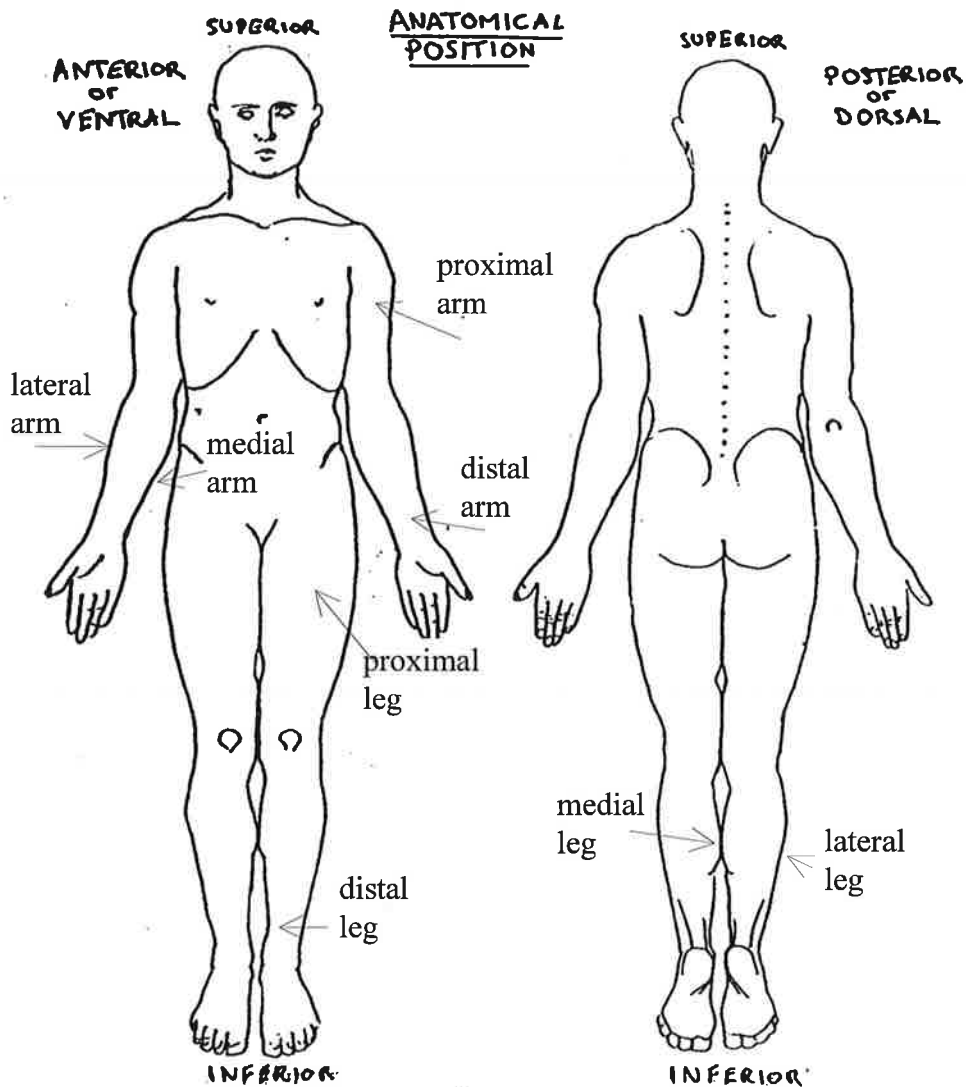
Figure G.1: The anatomical position showing anatomical directions. A segment refers to a body member such as an arm, leg, hand, etc. The origin of a segment is the joint where the segment is connected, closest to the centre of gravity of the body, ie the origin of the leg is at the hip joint, and the origin of the hand is the wrist joint etc. Anatomical directions can be described as: inferior, bottom of a segment; superior, top of a segment; proximal, towards the origin of a segment; distal, towards the end of a segment; lateral, away from the centreline (the imaginary vertical line which bisects the right and left sides of the body) of the body; medial towards the centreline of the body; posterior, the back; anterior, the front. Pairings of these definitions eg. distal/proximal are shown above for various body segments ie the arm and leg.

Examples: The wrist is distal to the elbow.

The shoulder is proximal to the elbow.

The nose is located on the anterior of the body.

The spine can be seen on the posterior of the body.

The thumb is lateral to the index finger.

The big toe is medial to the smallest toe.

Chapter One

Introduction

Total hip replacement (THR) has been described as one of the most successful interventions in orthopaedic surgery. Patients with little function and often great pain resulting from degenerative disorders of the hip joint such as osteoarthritis notice dramatic and immediate improvement after total hip replacement.

Although, generally, the replaced joint performs adequately for the remainder of the patient's life, a significant number 'fail' leading to revision surgery which is both expensive, and dangerous for the patient due to their often advanced age. Actual percentages of failure vary dramatically depending on the type of joint replacement and characteristics of the study group, but figures such as a 9 % failure rate at 15 years post-implantation are typical (McCoy *et al.* 1988). The average age at surgery for these patients was 60 years, and it has been noted that the incidence of failure increases with decreasing age at surgery due to the increased loading on the joint as younger patients are more active.

The sectional anatomy of the intact pre-operative hip joint and the artificial joint is presented in the following figures. A schematic section of an intact hip joint is shown in Figure 1.1 and a section of an artificial hip joint is shown in Figure 1.2. The anatomical features of the intact femur are shown in Figure 1.3 with muscle attachment and the line of amputation.
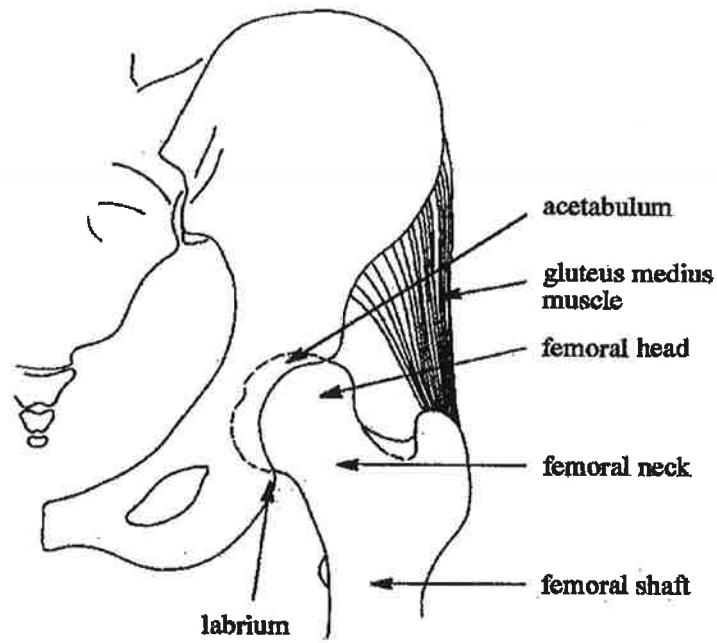
Figure 1.1: The intact human hip joint
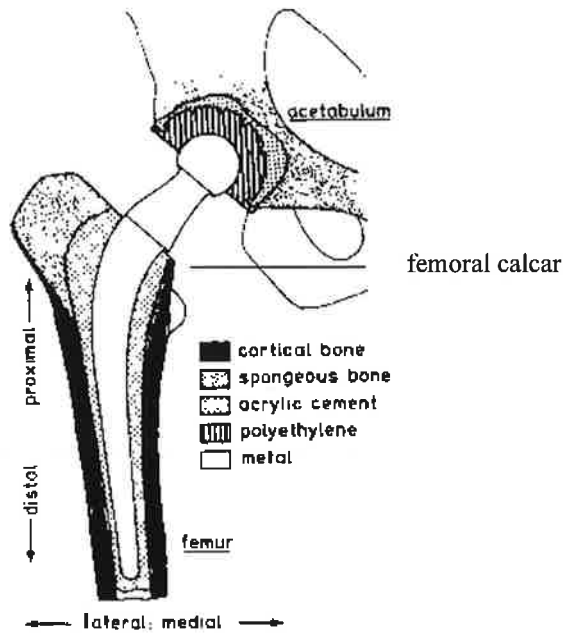
Figure 1.2: Main features and materials of the artificial hip joint. Note the anatomical directions are defined in the Glossary of Terms. *After Huiskes (1980).*

Line of amputation
head
ligament of head of femur
greater trochanter
obturator externus
ischiofemoral ligament
gluteus medius
capsule of hip joint
quadrate tubercle
lesser trochanter
intertrochanteric crest
quadrus femoris
psoas
gluteus maximus
iliacus
adductor magnus
pectineus
vastus intermedius
adductor brevis
vastus medialis
vastus lateralis
linea aspera
adductor longus
biceps femoris (short head)
site of hiatus of adductor magnus
lateral supracondylar ridge
medial supracondylar ridge
popliteal surface
gastrocnemius (medial head)
plantaris
adductor magnus
capsule of knee joint
adductor tubercle
gastrocnemius (lateral head)
medial epicondyle
lateral epicondyle
medial condyle
lateral condyle
intercondylar notch

Figure 1.3: Muscles, ligaments and line of amputation shown on the posterior surface of a right femur. Note: Posterior refers to the back side of a segment whereas anterior refers to the front side. (Refer Figure G.1).

Hip joint replacement surgery involves replacing the worn or diseased ball (head of femur) and socket (acetabulum) with artificial parts. Hip joint replacement can be cemented or non-cemented, however this study focused on cemented systems only. The surgical

procedure involves amputating the head and neck of femur (Figure 1.3) and to some extent reaming and cleaning the 'hollow' of the femur which is known as the medullary canal. A plug is placed into the medullary canal approximately 30 mm distal to the proposed location of the prosthesis tip (the metallic implant, Figure 1.2). Acrylic bone cement is then inserted into the canal in a 'doughy' state under light pressure. The metallic component (prosthesis) is then inserted into the cement-filled canal and the cement cures (hardens) around the prosthesis. The tip of the prosthesis is maintained at the centre of the canal with the use of a centraliser. The acetabulum is also replaced with an artificial material such as ceramic or polyethylene and the prosthesis head is placed into the replaced 'socket'. This study concentrates on the femoral component only, and does not consider the acetabulum.

It is pertinent to state the design objectives of this hip joint replacement system. The major objective is to restore function and remove pain from the patient suffering the hip joint disorder. The joint should perform as closely as possible the range of activities which the joint is subjected to in a healthy pre-operative state. The joint should also have longevity due to the expense and danger of revision surgery. Huiskes (1980) provided an excellent summary of the basic requirements for artificial joints and these requirements were stated as:

"   -The prosthesis and fixation materials should not induce undesirable tissue reactions, as bone necrosis or bone resorption; they should have acceptable wear characteristics and not corrode.

-The surgical procedure should be relatively simple and fast, standardised and reproducible, with minimal surgical trauma.

-The design of the prosthesis, the choice of materials, with reference to strength as well as stiffness properties, should be such as to guarantee adequate mechanical performance in such a way that stress concentrations are avoided and that implant, cement, bone, and the relevant interfaces are not loaded beyond their strength or fatigue limits.

-The implant should have a good salvage potential, meaning that if the system fails, another solution remains possible. Since the ultimate salvage solution is usually arthrodesis

(joint fusion), for instance this means that as little bone as possible should have to be resected.

-Early mobilisation, sterilisation of the components and reasonable costs of the implant should all be possible. "

As with any engineering system, design objectives or requirements are often in conflict, and compromise is inevitable to achieve the optimum result.

In the previously quoted study of McCoy *et al.* (1988) it was stated that 9 % of the replaced joints failed after 15 years. All of these failures involved loosening of the femoral component. Obviously one of the design criteria was not being adequately met and needs to be addressed. The loosening of the femoral component is ultimately a result of a breakdown of the bone-cement interface. During surgery, cement is forced into cavities in the bone and when the cement hardens, there is mechanical locking which forms a bond between the bone and cement. The integrity of this bond is crucial as load must be passed from the prosthesis through the cement to the bone. The intact bone-cement bond allows an even distribution of load, however if the bond breaks down, the resulting movement between prosthesis and bone produces an abnormal load transfer leading to pain and lack of function.

The question is therefore; what are the factors which cause this loosening? This is a controversial question in orthopaedic research with many researchers proposing either mechanical or biological explanations as the predominant cause, and it is generally accepted that it is a combination of these factors which eventually lead to "loosening". The aims of this study were to examine the mechanical behaviour of the cemented total hip joint replacement system, and possible mechanisms of prosthesis loosening. This study used a numerical simulation known as the finite element method to examine the artificial joint behaviour. The non-mechanical cellular influence on loosening, although acknowledged in Chapter Two, is beyond the scope of this work.

In order to detail the biomechanical behaviour of a hip joint replacement, a theoretical framework will be provided in Chapter Two, outlining some of the basic concepts. A review of the literature containing clinical studies, model parameters, and relevant

biomechanical analyses is then provided in Chapter Three. Chapter Four details the mathematical model used to study the artificial hip joint behaviour. Chapter Five then presents the results from the study along with a detailed discussion and comparison of the results. The study is summarised in Chapter Six and the clinical relevance of the results is discussed, along with appropriate recommendations.

Chapter Two

Theoretical framework

In this chapter some of the basic concepts involved with total hip replacement will be outlined as well as introducing the parameters required to construct a numerical model of the system. Firstly, the mechanical and biological issues associated with THR are explored, as well as their interrelationship. The method used for analysing the biomechanics of THR in this study is then prescribed followed by a brief description of the model parameters. Finally the structure of the study is outlined and the format of the results is presented.

2.1 Mechanical issues

The eventual failure of the hip prosthesis system when 'loosening' is evident is defined by a breakdown of the bond at the bone-cement interface, however this is not usually the initiating event. Under normal circumstances the loads that are transmitted through the bone-cement interface are well tolerated. Initial failure often presents as cracks in the cement mantle, usually stemming from voids in the cement or from the prosthesis-cement interface (Jasty *et al.* 1991). The bone cement is inhomogeneous and often contains many air voids due to the low (slightly higher than atmospheric) curing pressure. The curing pressure must be kept low to avoid damaging the bone tissue, a process known as osteonecrosis. Under repetitive fatigue loading these voids act as stress concentrators and crack initiation at these sites is common. These cracks may propagate through to the bone cement interface eventually leading to complete debonding. The stem-cement interface may either be designed as a fixed mechanical bond ie a pre-coated rough surfaced

prosthesis, or a sliding interface ie a polish surfaced prosthesis stem. These interface conditions produce completely different stress distributions within the composite bone-cement-metal structure. If the magnitude of the maximum principal tensile stress within the cement mantle is greater than the capacity of the material to withstand the stress, failure is likely to occur. Tensile stresses are highlighted because acrylic bone cement belongs to a class of materials which are strong in compression but weak in tension. Therefore determining the magnitude of the principal tensile stresses developed is of great importance.

2.2 Biological issues

When a breakdown of the bone-cement interface is noted, a fibrous tissue is often found to encapsulate the cement mantle and is therefore placed between the bone and cement. It is considered by some, eg Clarke (1990), that it is the body's reaction against the implant materials that causes the bond to breakdown and the fibrous membrane to develop. It is generally accepted that the body tolerates the materials such as stainless steel, polyethylene and acrylic cement in their intact form, however in particulate form this is not the case. When the hip joint is loaded, mechanical abrasion causes particles of cement and polyethylene to become free and the body treats these particles as foreign bodies and attempts to break them down into less harmful substances. This process is known as phagocytosis. The body contains macrophages which are cells that ingest and then try to 'break down' the foreign wear particles. The macrophages cannot dissolve these wear particles, however, due to their inorganic nature. High levels of enzymes enter the macrophage cells to assist in the attempted 'break down' of the wear particles, however the wear particle is eventually rejected from the macrophage when this attempted 'break down' fails. The macrophages become 'activated' due to the high enzyme level and this leads to events in the surrounding bone tissue which are very destructive such as osteolysis (particle disease), causing destruction of bone tissue.

Another important biological issue is the reaction of bone to stress and strain. Although the exact mechanism is not clear, bone has an ability to remodel due to an excess or a deficit in stress or strain. When areas of bone are subjected to high stresses, osteoblasts or bone forming cells "flock" to the area and both internal remodelling (an increase in the density of bone) and external remodelling (an increase in the cross-sectional area of bone) occur.

Conversely stresses lower than the normal physiological levels lead to thinning of the bones or 'disuse osteoporosis'. This phenomenon is known as Wolff's law, which is actually more of a qualitative observation than a law. It has great relevance in the field of joint replacement surgery as the stress and strain distribution in the bone alters dramatically after procedures such as total hip replacement. High levels of bone remodelling are noted on post-operative radiographs, even after periods as short as six months.

2.3 Interaction between the biological and mechanical issues

The mechanical and biological issues are not separate but are in fact deeply interrelated. For example, a design may include a rough or matt surface prosthesis to transfer load by frictional shear to the cement mantle. Although this type of design may produce a more desirable stress distribution than say a polished stem, the 'rougher' surface will possibly cause greater amounts of wear particles to be generated which should be avoided. Hence a conflict between the biological and mechanical objectives is evident. Another conflict is noted in trying to prevent 'stress-shielding'. When an artificial hip joint is loaded, the load which is normally taken entirely by the femur is shared with the prosthesis hence reducing the amount of stress in the proximal femur. This is known as 'stress-shielding' and due to Wolff's law, resorption of the bone takes place. The thinning of bone decreases the radial support for the cement, increasing likelihood of failure. It is clear then, that it is important to maintain a reasonable level of stress in the proximal femur. In order for load to be passed to the proximal femur however, it must be passed through the cement, and high stresses in the cement mantle may also cause failure. Here again another conflict in objectives is noted.

2.4 Structure of study

In this study, two critical factors were studied.

1)   The magnitude of tensile stresses induced in the cement mantle due to loading.

2)   The magnitude of peak strains present in the proximal femur due to loading.

A method therefore needed to be employed in order to determine the stress distribution present in an artificial hip joint system. A numerical approach was chosen due to the ease of studying parameter variations without the practical difficulties involved with methods such as strain gauge studies. The Finite Element Method (FEM) lends itself well to such an analysis and has been used by many researchers in orthopaedic biomechanics as detailed in Chapter Three. In the present study, a Finite Element model of a total hip replacement of an adult sheep was constructed. A sheep hip was modelled in order to complement a corresponding practical study which was undertaken on live sheep. This study was conducted by the Department of Orthopaedics and Trauma, University of Adelaide (Brumby *et al.*, 1996) and involved the implantation of specially designed cemented hip prostheses with different surface finishes. The sheep were sacrificed after designated time periods and the femurs were studied. Although this present study reports the results of the numerical analysis only, future work will compare the theoretical and practical studies.

Finite Element Analysis (FEA) involves describing a structural system as a set of small components or elements which are linked at a finite number of points or nodes instead of an infinite number of points in a continuum. Within each element there are simple relationships relating stress, strain and displacement. Finite Element Analysis allows calculation of the strain within each element by considering the external loads, restraint conditions and also the overall stiffness characteristics of the system. Once the strains are calculated, constitutive relationships are used to obtain stresses. The greater the number of elements, for a given volume, the more accurate the solution. However for an increase in element density, an increase in computer time is also required to calculate the stress distribution. In order to model a total hip joint replacement system numerically and utilise the Finite Element Method, the following information is required:

- the external loads acting on the structure;

- the structural properties of the materials present in the system;

- the geometry of the system;

- the boundary conditions of the structure, ie how it is restrained;

- the interface conditions between components in the structure;

It is appropriate to briefly describe these characteristics which comprise the finite element model.

2.4.1 Loading

The loads which the hip joint are subjected to are wide ranging and depend on the activity in question. For example, the loading due to two-legged standing is completely different to that of stair climbing due to changes in orientation of body parts and muscle involvement. In this study, the loading due to walking at normal rate was considered and the gait loading of an adult sheep was modelled. It has been shown (Bergmann *et al.* 1984) that the hip joint forces in sheep and humans are similar in orientation, and similar in magnitude considering the smaller geometry of the sheep hip. For this reason the results from this study may be used qualitatively to describe the stress distribution in a human artificial hip joint. Many methods are available to calculate the loading on a hip joint and include 'force-place' studies (measuring the ground reaction force), measuring muscle activity, movement studies, and using instrumented prostheses. These methods are detailed in Chapter Three. The aim was to calculate the **magnitude** and **orientation** of the **resultant load** acting on the prosthesis head by the acetabulum. It is this resultant load which will partly determine the stresses present in the system.

2.4.2 Material properties

There are essentially three materials which compose the femoral component of the total hip replacement system, the metal of the prosthesis, the acrylic bone cement, and the bone itself.

2.4.2.1 The prosthesis

The metallic prosthesis can be made from stainless steel, or alloys such as: titanium, aluminium and vanadium; or chromium, cobalt and molybdenum. The prosthesis modelled in this study was of stainless steel, with Young's modulus of 200×10^3 MPa and Poisson's

ratio of 0.3. Young's modulus is the ratio of stress to strain and Poisson's ratio is the negative ratio of transverse strain to longitudinal strain.

2.4.2.2 The bone cement

Bone cement consists of a solid and liquid component. The liquid component is primarily composed of a monomer known as monomethylmethacrylate (MMA) and the solid powder component contains a polymer, polymethylmethacrylate (PMMA). The components are mixed during surgery and a process of polymerisation occurs which leads to hardening of the cement. Temperatures at a level of $80^{\circ}C$ are given off during the process causing damage to the surrounding bone (thermal necrosis). Air entrainment occurs in the hardening of the cement and blood and tissue debris are also included in the resulting cement mantle. The resulting material is weak, flexible and inhomogeneous, hardly an ideal structural material! The tensile and shear strengths are low although the compressive strength is relatively high. The Young's modulus is two orders of magnitude less than that of steel, approximately 2×10^3 MPa. Bone cement also creeps, ie. under a constant load, there is an increase in strain with time. In this study the cement will be modelled as linear elastic, although the effects of creep will also be considered. The material is also modelled as isotropic (same properties in all directions) and homogeneous (uniform throughout).

2.4.2.3 Bone

As shown in Figure 1.2 there are two classifications of bone, dense stiff cortical bone, and porous flexible spongeous bone. Figure 2.1 shows a segment of the spinal column. The dense hard outer bone is the cortical bone and the spongeous inner bone is known as cancellous or trabecular bone. The individual struts or rods of bone comprising cancellous bone are known as trabeculae. The distinction between very dense cancellous bone and very porous cortical bone is not immediately obvious, however cortical bone is normally defined as having porosity (pecentage of non-solid material per volume) 5 - 30 % and cancellous bone as having porosity 30 - 90 %. The cortical bone makes up the outer shell of long bones such as the femur. The cancellous bone is comprised of similar material to cortical bone but is very porous and consists of a plate and rod arrangement. The cancellous bone is found in the end of long bones ie. the head the neck of femur and acts as a shock absorber due to its high ductility. The individual rods and plates align themselves

along lines of principal stress to safely withstand the loads transmitted through the joint. The ability of cancellous bone to absorb high loads is due to its ability to withstand large distortions or rearrangements of its internal structure before failing, ie cancellous bone requires a high level of work to produce failure. The Young's modulus of cancellous bone varies enormously, although a typical figure may be 1.0×10^3 MPa. Both cortical and cancellous bone are anisotropic and non-linear although in this study all bone is modelled as

trabeculae network
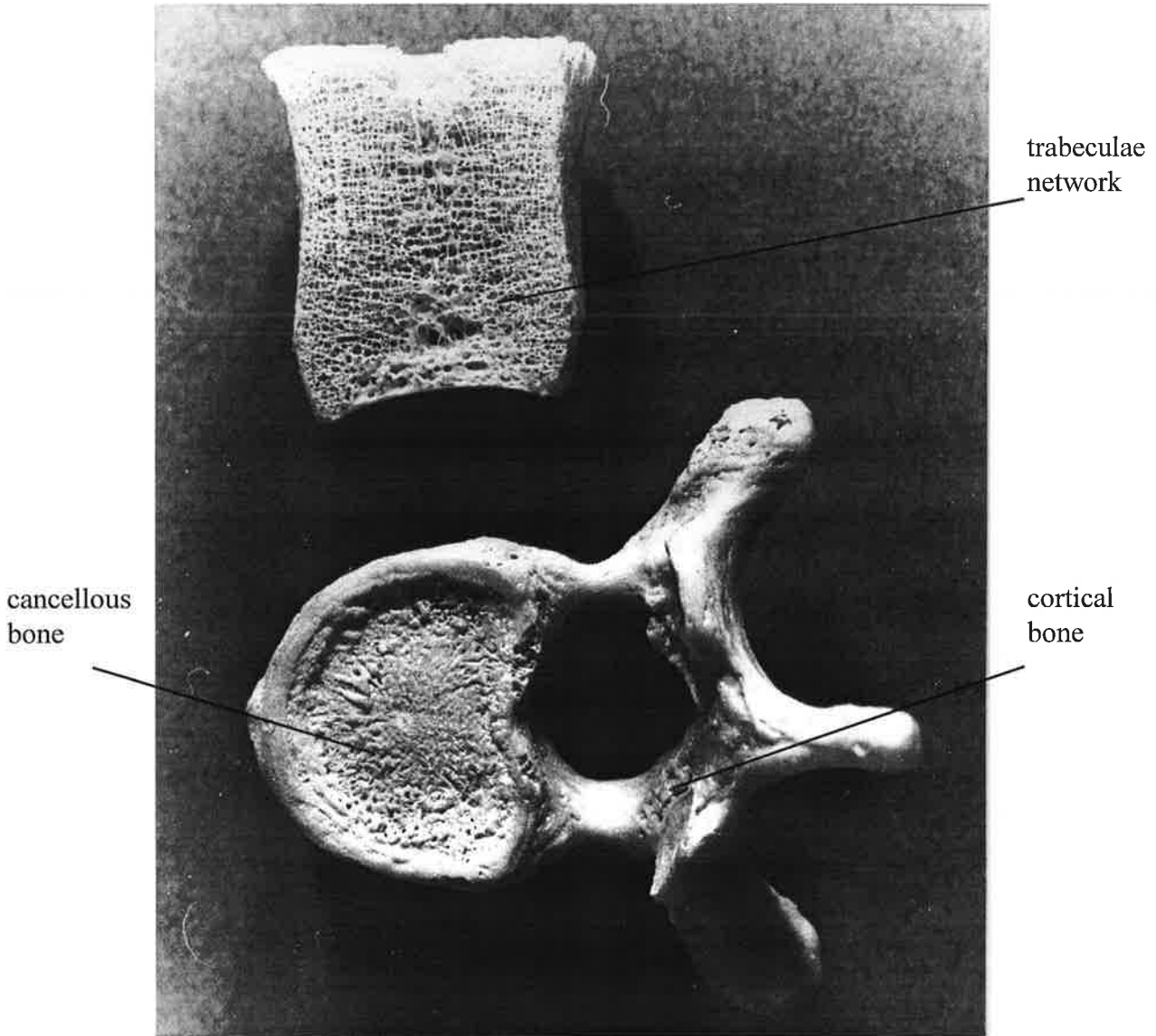
cancellous bone

cortical bone

Figure 2.1: The lower section shows a section of the spinal column with the hardened outer cortical bone and the spongeous inner cancellous bone. The upper section shows a section of the cancellous or trabecular bone. The individual rods and struts are the trabeculae.

homogenous isotropic linear elastic. The stiffness of cortical bone is approximately one order of magnitude lower than that of steel and is approximately 17.0×10^3 MPa.

2.4.3 Geometry

The geometric properties of the bone were taken from CT or Computed Tomographic X-ray scans which provide a cross-section at certain intervals giving a two dimensional image. From these two dimensional images, points were digitally scanned and used to construct the three dimensional structure. The CT scans were performed after the prosthesis had been removed hence the geometry of the prosthesis was also provided by the resulting gap in the cement mantle which appeared on the section. By also using the prosthesis design drawings, the orientation of the prosthesis within the femur could be determined. The determination of cancellous bone as distinct from cortical bone, was difficult but was carried out on the basis of apparent density from the CT scans. An air gap formed by the centraliser under the prosthesis tip was also considered. A distal air-gap is used to encourage subsidence of the prosthesis and engage a taper lock.

2.4.4 Boundary conditions

The femur is supported at the knee by muscle and ligament action. In this study it was assumed that the femur was restrained from translational or rotational movement at a section sufficiently distal from the prosthesis tip as to not unduly affect the stress distribution. This was to prevent sections of bone beyond the fixity, that have only a small influence on the region under investigation, from being modelled, thus saving significant computer time.

2.4.5 Interface conditions

There are two interface conditions which need to be considered, the bone-cement and the stem-cement interface.

2.4.5.1 Bone-cement interface

As has been mentioned, there is often a fibrous membrane which is present, even if only partially, between the cement and the bone. This membrane was not modelled in this study. There is no adhesive bond at the bone-cement interface ie the cement is not a glue, but the bond relies on mechanical interlocking. Although thermal necrosis occurs during curing of the cement, a bond remains present at the bone-cement interface. In this study an intact bond was assumed at the bone-cement interface ie normal, shear, tensile and compressive stresses were transmitted across the interface. This assumption was tested during the study.

2.4.5.2 Stem-cement interface

The mechanical integrity of this interface is suspect with a weak interface strength present at this region. There is presently debate in regards to prosthesis design and the stem-cement interface. Different surface finish conditions include:

1)   A rough or matt surfaced prosthesis with a high coefficient of friction between prosthesis and cement. Stress transfer across the interface is primarily by frictional shear stress and normal stress, with the shear stress component dominating;

2)   A smooth or polish surfaced prosthesis with a low coefficient of friction allowing subsidence of the prosthesis with the creep of the cement. With this design, normal stresses dominate in transfer across the interface, with little longitudinal shear stress;

3)   A chemically precoated prosthesis surface with grooves to produce a bonded stem-cement interface.

This study modelled different interface conditions at the stem-cement boundary and the effect of this interface on the resulting stress distribution.

2.5 Study focus

The main aim of the study was to investigate the biomechanical implications of varying the conditions at the stem-cement interface. One of the main theories put forward from proponents of a polish surfaced prosthesis is that reductions in deleterious tensile hoop

stresses will occur over time due to the viscoelastic properties of the cement. To that end, the creep properties of bone cement were included in the model for investigation. The incidence of potential cracking in the distal region of the cement mantle was also a common feature of many theoretical and clinical studies. In some prosthesis systems an air-gap is present under the prosthesis tip to encourage distal subsidence of the prosthesis within the cement mantle and utilise wedge action. The present study also investigated the effect of this air-gap on the resulting stress distribution within the cement and femur.

A three dimensional study was clearly necessary due to the asymmetric nature of the loading. A double-tapered prosthesis was modelled as it is believed by some authors (Fowler *et al*. 1988) that this design is beneficial for proximal load transfer and torsional resistance. Convergence of the solution was also tested by varying the mesh density.

The output of the model focused on two main areas:

1)   principal tensile stresses in the cement mantle;

2)   distortional strain energy density present in the proximal medial femur.

The study output focused on these two issues because two of the prime objectives of an artificial hip joint design are to minimise tensile cement stresses, but maximise the distortional strain energy density in the proximal femur (to avoid 'stress-shielding').

The next chapter will provide a review of the literature relevant to a numerical investigation of cemented total hip replacement.

Chapter Three

Literature review

3.1 Introduction

In order to carry out a stress distribution study of a total hip replacement (THR), relevant clinical and biomechanical issues must be identified. This is so that the appropriate simplifications can be made when constructing a model, and results can be interpreted in a way which is beneficial to clinicians such as orthopaedic surgeons. Firstly, it is necessary to review appropriate clinical observations which have been made in relation to total hip replacement, as the clinical presentation of a patient with a failed implant is pain and discomfort. Techniques to determine the loading on the joint must also be reviewed as well as the mechanical properties of the materials comprising a THR. Finally biomechanical studies and relevant stress analyses must also be reviewed in order to compare the results of this study with others.

3.2 Clinical observations

Charnley (1964), reviewed the performance of forty eight THRs (Total Hip Replacements) which had been functioning *in vivo* (whilst living) for up to four years. A common feature of all hip prosthesis systems was the significant resorption of the femoral calcar. The femoral calcar in this study refers to the proximal medial region of cortical bone and was identified in Figure 1.2. This indicated that the "normal" pre-operative load transmission to

the proximal femur was being bypassed and load transmission was now occurring distally. Six of the specimens were studied at autopsy, and in five of these specimens a thin line of fibrous tissue was found at the bone-cement interface although the prostheses did not clinically present as "loose". A clinical presentation of "looseness" would have been indicated by pain or discomfort whilst walking.

Weber and Charnley (1975) studied radiographs of 6,649 hips with metal prostheses and observed cement fractures at the tip of the prostheses. Of the reviewed hips, 1.5% had distal fractures in the cement mantle. Of the ninety-nine patients presenting with cement fractures, fifty-eight patients presented with the fracture after six months. Seventy of the ninety-nine hips with fractures showed subsidence based on radiographic (X-ray) evidence after twelve months. Subsidence can be described as distal migration of the prosthesis over time and can sometimes be identified by comparing subsequent radiographs. The authors noted that clinically, cement fracture in its own right, even when associated with subsidence, is not a failure of the system due to "wedge action". "Wedge action" occurs as the prosthesis is loaded axially and moves distally within the medullary canal. Weber and Charnley suggested this process may inevitably lead to crack formation in the cement mantle. This does not mean however, that cement fracture is not an initiating event leading at a later stage to system failure. System failure will not occur until there is a breakdown at the bone-cement interface.

Fornasier and Cameron (1976) studied 5 femoral components at autopsy which were functioning well at the time of death. In each of the hip systems, a fibrous membrane was seen between the prosthesis and cement, which the author suggested will lead to micromotion between the prosthesis and cement. This was believed to be of great concern as micromotions produce the microscopic wear particles which lead to osteolysis (particle disease). It cannot be stated from a study of only five hips, however, that this fibrous membrane is invariably present at the stem-cement interface, and many clinicians now believe this paper is a 'red herring'.

Beckenbaugh and Ilstrup (1978) reviewed 333 total hip athroplasties, four to seven years after operation. It was stated that from radiographic evidence, 24 % of hips were "loose". The definition of "loosening" was equivalent to subsidence and the authors point out that most patients presenting "looseness" are asymptomatic. This definition of looseness, which

implies failure, seems inappropriate as subsidence of the prosthesis within the cement mantle may actually improve the long term conditions for the THR, hence the absence of symptoms in most patients. Many of the "loose" prostheses were a result of poor packing of cement, which decreases the strength of the stem-cement interface. The authors also identified proximal calcar resorption. Oh *et al.* (1978), showed that the bone-cement interface strength was substantially improved and that the incidence of loosening, which clinically and symptomatically presents after a breakdown of the bone-cement interface, could be reduced by introducing an intramedullary plug. This plug is placed distally to the tip of the prosthesis and increases the curing pressure of the cement. The cement plug prevents the cement from flowing too far distally into the femoral cavity.

Gruen *et al.* (1979) shed further light on the problem of "loosening" with a review of 389 hip replacements, of which 19.5 % showed radiographic evidence of mechanical looseness. This "looseness" was defined by either fracture of the cement or a radiolucent gap at the stem-cement or bone-cement interface. 14.4 % involved "looseness" at the stem-cement interface and four modes of failure were described to account for this interface looseness; stem pistoning within cement (3.3 %), cement-embedded stem pistoning with the femur (5.1 %), medial midstem pivot (2.5 %), calcar pivot and bending fatigue (4.0 %).

Harris *et al.* (1982) showed that the incidence of loosening had significantly decreased following the introduction of the distal intramedullary cement plug. Harris *et al.* stated that the cement plug, introduced by Oh *et al.* (1978), decreased the amount of voids in the cement mantle and increased the bone-cement interface strength. Harris *et al.* found only 1.1 % of hips replaced in this study showed definite evidence of loosening at an average of more than three years of follow-up review since time of surgery. The authors' definition of "definite looseness" was defined by a single criterion of definite evidence of migration. Harris *et al.* stated that "Migration may present in the form of a change in the position of the prosthesis or the cement mantle, or both; as the development of a crack in the cement, or as a stem fracture."

It appears very difficult to compare series which study the incidence of "looseness" as definitions of "looseness" vary greatly, and surgical technique and technological advances are also variable factors. It is clear, however, that voids in the cement mantle and a weak bone-cement interface are precursors to a higher incidence of "looseness".

Sutherland *et al.* (1982) reviewed 100 THRs performed during 1970, and the minimum review time was ten years. The authors found a 28 % incidence of migration of the femoral component, leading them to state that "aseptic (non-infective) loosening is the most significant long-term problem that is encountered after total hip replacement." The authors also found a 15 % incidence of proximal femoral resorption in hips which did not present as loose, indicating the prevalence of resorption. Sutherland *et al.* stated that some of the design characteristics of the prosthesis (Muller curved-stem total hip replacements) may have led to the high incidence of looseness. Again, though, this "looseness" is actually distal migration which may occur as a result of creep of the bone cement, and therefore may not be "looseness" at all.

Stauffer (1982) performed a ten-year follow-up study of total hip replacements and determined that 29.9 % of the 231 hips studied were deemed loose. The criteria for "looseness" were very inclusive and were specified as "the appearance of any lucent line between the prosthesis and the polymethylmethacrylate; a complete lucent zone between the cement and bone; or any change in position (angulation or sinking) of the femoral component." Stauffer found a significant correlation between cracking in the cement mantle and looseness and concluded that the "finding of a cement crack is thus an ominous sign of impending loosening or, indeed, indicates that loosening has already occurred." Stauffer found that the most common type of loosening "resulted from large tensile hoop stresses present in the proximal region of the cement mantle which produced a breakdown of the prosthesis-cement interface." The author also found 14 % of the hips reviewed presented resorption of bone in the medial cortex in the region of the femoral calcar.

Paterson *et al.* (1986) reviewed 882 consecutive THRs and found that 8 % were "loose". The authors defined "looseness" as a radiolucent line appearing at the stem-cement boundary on radiographic examination. 24 % of the patients presenting "looseness" showed clinical symptoms, and in 97 % of cases the "looseness" was present two years after surgery. Paterson *et al.* found that the most common mode of failure was a "fracture of the mid-zone cement, with slowly progressive sinking of the metal prosthesis and the distal cement mass, which was itself sometimes fractured."

Fowler *et al.* (1988) reviewed the performance of the Exeter Total Hip Replacement system since its inception in 1970. The Exeter prosthesis is slim, collarless, tapered in two

planes and polished and was designed to subside in the femoral canal in order to take advantage of wedge action. Fowler *et al.* pointed out the inevitability of "subsidence", often associated with "looseness" and therefore failure, due to the creep or time dependent displacement of the bone cement. The review showed very low rates of calcar resorption and occurrence of radiolucent lines at the bone-cement interface. The authors suggested it is inappropriate to link subsidence of the prosthesis within the femoral canal with looseness because designs such as the Exeter are intended to subside, and *improve* long-term stability.

This raises an important point. Many reviewers suggested that an observation of a gap at the stem-cement boundary meant that the prosthesis had become loose during the period following surgery. It is highly likely however, that due to surgical technique, or designs such as the Exeter, there was *never* an intimate bond at the stem-cement interface and that a gap at the interface may actually have been present at the time of surgery. Many reviewers, however, noted a radiolucent gap at the stem-cement interface after radiographic examination and assumed it implied failure. Therefore stating that either distal subsidence of the prosthesis, or the presence of a gap at the stem-cement boundary is grounds for the definition of "having becoming loose", is incorrect, as "never bonded" may be more appropriate.

Maloney *et al.* (1989) tested retrieved autopsy specimens of total hip replacements that had been functioning *in vivo* for durations ranging from 0.5 to 210 months. Maloney *et al.* used strain gauge experiments to demonstrate that there is "marked stress shielding of the proximal medial femoral cortex after insertion of a cemented femoral component."

Clarke (1990) commented on the biological implications of implant design choice. Clarke pointed out that any gross or micro-motion between components of a total hip replacement system will produce particulate wear debris. In the opinion of Clarke, "release of wear particles is the single most important mechanism triggering osteolytic changes around the joint that will eventually and insidiously destroy implant fixation". The body tolerates the intact materials such as metal, polymethylmethacrylate, and polyethylene, but in particulate form, biological reactions occur as the body senses these particles as foreign bodies and attempts to destroy them. This process leads to destruction of bone tissue. It appears that a prosthesis intimately bonded with the cement mantle would prevent motion between the

stem and cement in theory, but *in vivo* such a bond is difficult to achieve, and is even harder to sustain.

Jasty *et al.* (1991) studied 16 femora from autopsy with the aim of establishing the initiating events in the failure of total hip replacement systems. The femora with implanted prostheses were all performing satisfactorily at time of death and had been functioning *in vivo* from two weeks to seventeen years. Jasty *et al.* identified the four critical regions as the stem-cement interface, the cement itself, the cement-bone interface, and the bone. The authors pointed out that many previous studies "cannot define the initial causes of loosening, since clinical radiographs are inadequate to identify the really early changes, and, by the time revision is performed, most of the critical information has been obscured." Jasty *et al.* noted that some debonding of the stem-cement interface was present in every case, and concluded that this debonding occurs early after surgery. As has been stated, it is likely that this "debonding" actually means "never bonded".

Jasty *et al.* noted the presence of fatigue cracks which mainly originated either at the stem-cement boundary or at voids in the cement mantle, and crack widths and lengths were found to be larger with greater *in vivo* use ie more time after surgery. It was concluded that "cement undergoes accumulated fatigue damage *in vivo* well before gross loosening is manifest". Jasty *et al.* noted that these fractures may eventually lead to looseness and production of particular polymethylmethacrylate which leads to osteolysis. Osteolysis may degrade the integrity of the bone-cement interface as reported previously. It was suggested that it is the breakdown of the stem-cement interface which initiates failure and that long-term improvement may occur by increasing the strength of this interface. It should be noted that this is the opposite view of designers of systems such as the Exeter prosthesis, who believe a polished prosthesis surface should be utilised to encourage subsidence.

Three of the main issues identified by reviewing various relevant clinical studies are:

1)   The high incidence of "loosening".

2)   The high incidence of crack formation in the cement mantle.

3)   The high incidence of calcar resorption.

As has been seen, the definition of "looseness" is extremely varied and depends often on the clinician performing the review. Some reviewers regard loosening as a breakdown of the stem-cement interface or even any distal migration of the prosthesis stem. Although these factors, along with cement crack formation may ultimately lead to "loosening", they are more likely to be initiating events. It seems more appropriate to define "loosening" as a breakdown of the bone-cement interface as this crucial interface transfers the load through to the distal femur. The present study investigated various conditions at the stem-cement interface and compared the effect of the changing environments.

3.3 Loading

The loading on the hip joint is of prime importance as the magnitude and orientation of the applied load will partly determine the resulting stress distribution. The determination of this loading pattern is difficult due to the joint itself being surrounded by living tissue and direct measurement requires an invasive technique. Non-invasive techniques are available but do not *directly* measure the applied force, but instead rely on analytical determination.

Inman (1947) provided insight into the loads which act on the femoral head. Inman conducted his study in two dimensions and analysed forces acting in the frontal or sagittal plane. Inman made the important finding that "the direction of the reacting force through the head of the femur is constant and, therefore, independent of the position of the pelvis". Inman also confirmed that the line of action of the resultant force corresponded to the orientation of the medial trabeculae of the femoral neck. The author concluded that in one-legged stance the resulting force acting on the femoral head is approximately 2.4 to 2.6 times the body weight, and acts at an angle of approximately 165 to 170 degrees from the vertical.

Rydell (1966) used instrumented prostheses to directly measure the forces obtained whilst loading the hip joint under various activities such as running, walking standing etc. The instrumented prosthesis contained built in strain gauges and were implanted in two human subjects. Rydell noted that the results were only valid for the prosthetic hip due to possible alterations in muscle and ligament activity in the post-operative state.

The strain gauges were placed in the neck of the prosthesis permitting the prosthesis to act as a force transducer. The resultant force acting on the head of the prosthetic hip could be calculated from the three orthogonal force components measured whilst the patient undertook the various activities. The subjects produced maximum forces of 1.80 times body-weight and 2.0 times body-weight respectively, whilst walking at 1.3 metres per second and 1.4 metres per second respectively. The second subject produced a maximum force of 4.3 times body-weight whilst running. The line of action was also determined during the various prescribed activities.

Paul (1971) described a method in which the resultant force acting on the hip joint was calculated by observing movements of the leg-segments (hip to knee and knee to ankle) and measuring the ground-to-foot force produced during these movements. Photographs were taken during a walking cycle to produce a three-dimensional configuration of the two leg segments whilst a force-plate dynamometer recorded the ground-to-foot force. From this information, the moments and force transmitted between the segments were calculated. The author stated there were 22 muscles acting at the hip and 14 muscles and 6 ligaments at the knee, and in order to simplify calculations, these muscles and ligaments were divided into groups based on anatomical position and function. The line of action and location of origin of the muscle forces were known and by isolating the leg segments as free bodies and drawing force vector diagrams, the magnitudes of these muscle forces could be determined. An explicit solution could not be obtained at the hip joint, hence limit curves were produced. The resultant force was slightly higher than the force calculated in Rydell's (1966) study due to the increased walking speed of the subjects, however the results compared favourably.

Crowninshield *et al.* (1978) used a similar, yet more comprehensive technique in order to determine the resultant force acting on the hip joint. Similarly to Paul (1971), the pelvis and lower extremity were modelled as separate rigid links. Light-emitting diodes were attached to each section and photographs taken during various phases of gait. A piezoelectric force platform was used to record ground-to-foot forces corresponding to the kinematic data collected by photography. From this information, forces and moments were calculated at the various joints of the lower extremity. Various equilibrium equations were then established considering muscle location and line of action. In this study 27 muscles were considered at the hip joint alone. Due to the indeterminate nature of the solution, an

optimisation technique was presented. The objective function was to minimise the sum of the individual stresses produced in each muscle. The solution provided hip joint contact forces which were of interest. During normal gait an average resultant force of 4.3 times body weight was calculated.

Lanyon *et al.* (1981) similarly to Rydell (1966), used instrumented prostheses to directly measure strains produced whilst walking. Lanyon *et al.* used sheep in their study, noting that similar biological and mechanical changes occur post-operatively in sheep to those of humans. The authors used a back calculation method to determine the force acting on the prosthetic head. The maximum strains during gait were recorded, and then by assuming elastic properties of bone and measuring geometric properties of the composite structure, the load acting on the prosthetic head to produce the recorded strains, was determined. The study was carried out *in vivo,* hence both joint and muscle forces contributed to the recorded strain measurements. In the back calculation, however, a single force and its line of action were determined, and this force was assumed to act directly on the prosthesis head. The resulting force as a percentage of body weight varied for the four sheep (57.5 %, 62.9 %, 88.0 %, 82.0 %). The differences between these results and those calculated in previous studies are simply explained by the obvious differences in gait between quadrupeds and bipeds. The line of action was also determined, and was found to be similar to that found in humans.

Bergmann *et al.* (1984), as previously stated, justified the use of sheep and dogs for joint replacement studies by noting that load orientations in the animals were similar to those reported for man. Instrumented prostheses were implanted in sheep and dogs and results were taken at various times post-operatively and for various speeds. For the sheep studies, the maximum peak resultant force measured during a gait cycle was equivalent to 110 % body weight, however other sheep produced peak forces of approximately 65 % body weight. The results generally agreed with Lanyon *et al.* (1981) and considering the obvious differences in gait between quadrupeds and bipeds, the results indicate the suitability of using sheep in biomechanical analyses involving hip prostheses.

Davy *et al.* (1988) used a telemeterized total hip prosthesis to directly measure the forces acting on the prosthetic hip. The instrumented femoral prosthesis contained a three axis load-cell which provided information of the forces acting in three perpendicular directions.

The resultant force and its line of action were then determined. The patient tested produced peak resultant forces, during gait at approximate 0.5 meter per second, of 2.5 to 2.8 times body weight.

Bergmann *et al.* (1992) again used instrumented prostheses to measure the three-dimensional joint forces produced whilst walking, and ascending and descending stairs. Bergmann *et al.* noted that torsion is a significant factor in prosthesis design due to the large out of plane forces acting on the prosthetic head, especially in activities such as stair-climbing. The median peak hip joint force increased dramatically during stair-climbing. For the three prosthetic joints, median peak forces during stair-climbing were approximately 3.3, 4.2 and 3.3 times body weight respectively compared with median peak forces during walking of approximately 2.2, 3.2 and 1.8 times body weight respectively.

3.4 Material properties

The materials which comprise the femoral component of an artificial hip joint are the bone, the bone cement and the prosthesis material. The mechanical properties of these materials must be known in order to numerically model the system. The mechanical properties which are of interest are the Young's Modulus and Poisson's ratio for the materials as well as the viscoelastic properties of the bone cement.

3.4.1 Cortical bone

Reilly and Burstein (1974) presented an excellent review of the mechanical properties of cortical bone. It was pointed out that up to 1974, the data presented for the mechanical properties of bone varied enormously due to the variety of experimental methods, approaches, and goals. It was also pointed out that variations in results have occurred due to the testing of whole bones compared with testing of bone matter itself as a structural material. The review of Reilly and Burstein presented the elastic constants, viscoelastic parameters, plastic parameters, and strength properties of cortical bone, as found in the literature.

It was stated that the objective of any mechanical test on bone must be clearly established as it is a composite anisotropic structure which is at various levels of organisation down to

the molecular level. For example, at one extreme, single osteons, the fundamental building matter of whole bones such as the femur can be tested, or at the other extreme, the whole bone itself can be tested. The defined objective in most tests was to investigate cortical bone as a "material", one level below that of whole bone, with a cross-sectional area of between four and twenty square millimetres. Another limitation noted by the authors in comparing data was the state of the bone being tested, ie whether dry, wet, embalmed or rewetted, as the hydration state of the bone affects the mechanical behaviour of bone, and bone is certainly not "dry" *in vivo*.

In order to determine how many parameters are required to define the elastic properties of a material, its state of isotropy must be known. As was stated in Chapter Two, a material is isotropic if it behaves mechanically in the same fashion regardless of the direction in which testing is performed. An isotropic material requires only two parameters to define its elastic behaviour, Young's Modulus (E) and Poisson's ratio (ν). Young's modulus is defined as the ratio of stress to strain and Poisson's ratio is the negative of the ratio of transverse strain to longitudinal strain in the direction of uniaxial loading. An anisotropic material behaves differently in every direction and requires twenty one independent parameters. Bone, however, can be defined as transversely isotropic which means it behaves differently in the longitudinal and transverse orientations, but the behaviour in the transverse plane in any direction is the same. Five elastic parameters define a transversely isotropic material, Young's Modulus and Poisson's ratio in both directions, as well as the shear modulus (G) which relates angular distortion (shear strain) to shear stress. Reilly and Burstein presented a summary of data from the literature in relation to these parameters. Most authors calculated the Young's Modulus in the longitudinal direction ie the loading direction parallel to the bone axis, but values for the other constants were presented.

The authors pointed out that many of the results were inappropriate due to the experimental technique, hydration state, and perhaps most importantly, strain rate. Strain rate is of importance because bone is viscoelastic in nature. A viscoelastic material will increase its strain over time when a constant load is applied. Hence, appropriate tests to determine elastic parameters should have a loading rate within "physiological" limits, ie similar to which bone may experience in every day activity. Three results were presented as being satisfactory due to the use of an extensometer, and a satisfactory loading rate; McElhaney *et al.* (1964), using compression and 0.1 per second strain rate, E = 24.1 GPa; Simkin and

Robin (1973), using tension and low strain rate, E = 23.8 GPa ; and Burstein *et al.* (1972) using tension and 0.1 per second strain rate, E = 24.5 GPa. These results were for wet bone done with loading direction parallel to the bone long axis. Poisson's ratio values varied enormously from 0.08 to 0.482 depending on direction and other factors.

The viscoelastic nature of bone was also identified, and by referring to the study of McElhaney and Byars (1965), showed the ultimate compressive stress and Young's Modulus increased with increasing strain rate whilst the maximum strain decreased. The authors also provided a review of plastic and strength properties of cortical bone, as well as fatigue and crack initiation properties, but as the present study assumed cortical bone is subject to loading within the elastic range, this information will not be reviewed.

Bonfield and Datta (1974), using wet compact bone specimens determined the Young's Modulus of longitudinal bovine tibia. The strain rate was very low, 3×10^{-4} per second, and a capacitance strain gauge was used. The specimens were tested in tension and the average Young's Modulus was determined to be 27.3 GPa.

Reilly *et al.* (1974) tested human and bovine specimens of cortical bone and showed that there was no significant difference in the modulus of elasticity determined by a tension or a compression test. The specimens were tested wet with the use of an extensometer and the strain rate was 0.05 per second. The average value for the Young's Modulus of human femur was 17.1 GPa and for bovine femur 26.4 GPa.

Reilly and Burstein (1975) tested human and bovine specimens extracted from the middle third of long human and bovine bones in order to verify the existence of an isotropic plane perpendicular to the long axis of bone. Specimens were tested in tension and compression at strain rates of 0.02 to 0.05 per second. The specimens were tested wet and an extensometer was used to record strains. Specimens were tested at various orientations parallel to the longitudinal axis, perpendicular and at various intermediate angles. The determination of the shear modulus was carried out by the use of torsion tests.

Reilly and Burstein determined the five elastic constants necessary to define transverse isotropy by testing longitudinal and transverse specimens and determining the Young's Modulus and Poisson's ratio in each direction. It was found that in the transverse plain

(perpendicular to the long axis of bone), that the Young's Modulus did not significantly vary with direction, and this also applied to the Poisson's ratio. Finally, transverse isotropy was verified, by applying a transformation equation to determine the Young's Modulus at a particular angle to the transverse plain, theoretically and these results were compared with experimental results from samples cut at the same angle. Good correlation was noted when the values were compared, hence a transverse isotropic model of cortical bone can be assumed. If E_l, v_l, G_l represent the longitudinal properties and E, v represent transverse properties the following average results were presented; bovine: $E_l = 22.6$ GPa, $E = 10.2$ GPa, $G_l = 3.6$ GPa, $v_l = 0.36$, $v = 0.51$, human: $E_l = 17.0$ GPa, $E = 11.5$ GPa, $G_l = 3.28$ GPa, $v_l = 0.46$, $v = 0.58$. The authors suggested the Poisson's ratio values (greater than 0.5 would indicate an increase in volume under loading) are extremely high because "the 'material' is really a structure with a high degree of kinematic deformation."

Lanyon *et al.* (1979) used bending tests to determine the Young's Modulus of cortical bone from the sheep radius, a bone located in the sheep leg. Both compression and tension faces were used to provide data and care was taken to remain within elastic limits at the extreme fibres. The specimens were tested wet, and a four point bending test was employed to ensure that pure bending (ie no shear), was present at the location of the strain gauges. A measured mean value for the longitudinal modulus of sheep bone was 18.2 GPa.

Schaffler and Burr (1988) carried out determinations of Young's Modulus for cortical bone from 2-3 year old steers (desexed male bulls). The aim of this work was to determine if there was a relationship between porosity, density and Young's Modulus. The specimens were tested wet in uniaxial tension at strain rates of 0.01 per second and 0.03 per second. It was found that compact or cortical bone stiffness is proportional to apparent bone density to the 7.4 power. Apparent density = true density multiplied by (1 - porosity). An important difference was noted between this relationship and that described for cancellous/trabecular bone. Cortical bone is sometimes defined as having porosity less than 15 % and trabecular bone as having porosity greater than approximately 70 %. Some authors believed one mathematical relationship between morphological properties (density, porosity etc.) and stiffness could describe the entire continuum of bone porosity values. It will be shown however (Section 3.4.2), that for cancellous bone, stiffness is proportional to the apparent density cubed. Schaffler and Burr stated that both cancellous and cortical bone are fundamentally composed of the same substance, lamellar bone. Within cortical and

cancellous bone the organisation of the lamellar is fundamentally different. The cortical bone is essentially a solid material with little internal void space whilst cancellous bone contains mostly spaces separated by interconnected plates and rods of lamellar bone. The mean longitudinal stiffness of cortical bone was 21.8 GPa. The authors concluded that cortical and cancellous bone should be treated as separate engineering materials, due to their different structural orientations.

Keller *et al.* (1990) used four point bending tests to determine the Young's Modulus for adult cortical bone. Specimens were taken from the femur and were tested wet at strain rates of approximately 0.05 per second. The authors noted a correlation between stiffness and apparent density. The mean elastic modulus was 12.1 GPa, but it must be noted that porosity was generally high (40 %) for tested specimens. The authors also concluded that extrapolation of the relationship between stiffness and apparent density for cortical bone to provide a relationship between the apparent density and stiffness for cancellous bone provides inaccurate results. This is similar to the findings of Schaffler and Burr (1988) who showed that cortical and cancellous bone should be treated as different structural materials.

3.4.2 Cancellous bone

Pugh *et al.* (1973) developed a quantitative model for cancellous bone by approximating the geometry with a hypothetical network of compact bone. The authors assumed that the material which comprises cancellous bone is identical to that of cortical bone ie the individual rods and plates making up cancellous bone have the same material properties as cortical bone. Pugh *et al.* set up a simplified structural model comprising of sheets and rods and applied the finite element method to observe the behaviour of this trabecular network under load. It was noted that the macroscopic stiffness of cancellous bone is important in determining the "shock absorber" capabilities of the material. The authors' model suggested an overall stiffness of 10^5 pounds per square inch (equivalent to 690 MPa). The authors also suggested that "the intertrabecular soft tissue is probably of no importance to the mechanical properties". Pugh *et al.* reassessed the statement of equality of stiffness of the material making up cancellous and cortical bone and concluded that the "compact bone which constitute the trabeculae is probably not as stiff as cortical bone". The global stiffness of cancellous bone was found to be totally dependent on the arrangement and spatial orientation of the individual rods and plates.

Carter and Hayes (1977) pointed out that the porosity of cancellous or trabecular bone can vary from 30 % to more than 40 % depending on anatomical location. The porosity of cancellous bone is approximately proportional to the apparent density, the apparent density being defined as the mineralised tissue per total tissue volume. It is the amount of mineralised tissue which dictates the strength and stiffness of bone. The authors stated that whole bones can be modelled as composite structures consisting of both a solid and fluid phase; the solid phase being the mineralised bone tissue, and the fluid phase being composed of blood vessels, blood, red and yellow marrow, nerve tissues, miscellaneous cells, and interstitial fluid. Carter and Hayes drew a structural analogy between cancellous bone and materials such as open-celled rigid plastic foams and porous concrete, in which the apparent density is the governing factor determining material properties such as strength and stiffness. The authors also identified the anisotropic nature of cancellous bone.

Specimens of cancellous bone from human tibial plateaux and bovine femoral condyles (the distal end regions of the femur; see Figure 1.3) were tested wet with strain rates varying from 0.001 to 10 per second. Tests were carried out in uniaxial compression in the longitudinal direction of the whole bone and also with and without marrow. It was found that for testing with marrow, the viscous flow of marrow out of the pores did not cause any significant increase in stiffness or strength. It was found that with increasing strain rate the stiffness increased, in fact Young's modulus was found to be proportional to the strain rate raised to the 0.05 power. It was also found that stiffness of cancellous bone was proportional to the cube of apparent density. Mean values of stiffness were 56.6 MPa, 75.5 MPa, 81.5 MPa, 81.2 MPa and 83.7 MPa for strain rates of 0.001, 0.01, 0.1, 1 and 10 per second respectively.

Brown and Ferguson, Jr. (1980) determined the Young's modulus for cancellous bone from proximal human femurs. Uniaxial compression tests were performed at low strain rates (0.0001 to 0.01 per second). Stiffness contours were mapped throughout the proximal region of the femur, and regions of high stiffness were found to correlate with regions of high density as seen from radiographic examination. The average Young's modulus for loading in the superior-inferior, medial-lateral and anterior-posterior directions were 3.39 GPa, 2.60 GPa and 1.97 GPa respectively. The authors also presented average values of Young's modulus obtained from other studies; Brown and Ferguson, Jr. (1978) in the same directions, 3.34 GPa, 2.24 GPa and 2.51 GPa respectively; Townsend *et al.* (1975) in the

same directions, 3.91 GPa, 3.44 GPa, 3.00 GPa respectively; and Schoenfeld *et al.* (1974) from the femoral head parallel to the neck axis, 3.45 GPa.

Williams and Lewis (1982) used experimental and finite element methods to determine the anisotropic properties of cancellous bone. Specimens were taken from the proximal tibial epiphysis and tested in compression at a strain rate of 0.005 per second. Stiffness measurements were made in three orthogonal directions. The results in the longitudinal direction were far lower than the previously mentioned studies, excluding Carter and Hayes (1977), with values for Young's modulus ranging from 100-500 MPa. A large degree of anisotropy was evident with values of stiffness in the transverse plane being approximately 50 MPa.

Martens *et al.* (1983) determined the mechanical characteristics of cancellous bone at the upper femoral region. Specimens were tested wet under compression at high strain rates along three orthogonal axes and anisotropy was noted to be present. The values for Young's modulus varied extensively and depended on the direction of loading, anatomical location and the subject from which the bone specimen was taken. The typical range varied approximately from 200 MPa - 2000 MPa. A power relation was *not* observed between stiffness and bulk density (dry weight of the specimen divided by total sample volume). It was suggested that density does not fully account for the wide variation in mechanical properties of cancellous bone, and that the microstructure must also play a role.

Gibson (1985) pointed out that cancellous bone is a cellular structure and applied stress analysis theory which had previously been used to evaluate other cellular materials. Gibson identified four different types of cancellous bone. When an area is subject to high stress, the trabeculae are dense and form closed cell, plate-like structures whereas for porous regions the trabeculae form open cell rod-like structures. Furthermore if the stress pattern applied to an area is complex, the trabeculae also form complex patterns and are asymmetric, however if the loading is predominantly uniaxial, the trabeculae form symmetric patterns. Hence four different structural arrangements are possible. If the rod or plate elements have a high length to thickness ratio, failure is by elastic buckling, but if the ratio (slenderness ratio) is low, the rods or plates will yield plastically. The behaviour is also governed by the elastic modulus of the material which compose the rods and plates. This material was presumed to be the same mineralised material of which cortical bone

was composed. This model correlates very well with the data of Carter and Hayes (1977), as well as other studies. Studies by Ku *et al.* (1987) and Mente and Lewis (1987) indicated however that the stiffness of the fundamental matter which composes the plates and rods of cancellous bone is between 0.2 - 0.5 that of values reported for cortical bone in the literature.

It is seen from these studies that bone is indeed a very complex structural material. It is non-homogeneous, anisotropic and viscoelastic and its mechanical properties also depend on the state of hydration. The mechanical properties also vary dramatically depending on the anatomical location and the porosity of the bone. Obviously, an assumed mechanical behaviour of bone must be used in a numerical model, which is representative of its true behaviour.

3.4.3 Bone cement

In Chapter One, it was stated that in terms of the mechanical behaviour of bone cements, the physical properties which are of interest in this study are the stiffness, Poisson's ratio and viscoelastic properties. The review of the literature will therefore focus on these properties although in many of the papers reviewed, exothermic and chemical properties were also presented.

Lautenschlager *et al.* (1974) pointed out the variation of strength of commercial bone cements with curing pressure. It was pointed out that PMMA (polymethylmethacrylate) is twice as strong in compression as tension. The authors performed compression and diametral tension tests at a strain rate of 0.02 per minute and noted that pressure curing substantially increased both compressive and tensile strengths.

Haas *et al.* (1975) performed a number of tests on commercial polymethylmethacrylate. Compression and diametral tension tests were used to provide strength and stiffness information. The average Young's moduli were found to range from 2.69 - 3.28 GPa. The average tensile strength was approximately 30 MPa whilst the compressive strength was approximately 92 MPa. The porosity of PMMA was also identified and found to range from 1 to 10 %. PMMA was also found to exhibit volume contraction of up to 5 % on setting.

Bayne *et al.* (1975) showed that curing commercial PMMA at elevated pressures produced higher strengths in tension and compression due to the decreased porosity of the set PMMA. Tensile strength increased from 13.2 MPa to 23.7 MPa and compressive strength from 76.5 MPa to 83.9 MPa, following an increase of curing pressure from atmospheric to 27.6 MPa. The authors pointed out that due to the practicalities of hip replacement surgery, these curing pressures could never be obtained, but any increase in the curing pressure would be advantageous.

Treharne and Brown (1975) performed room temperature compression creep and recovery tests on several commercially available bone cements to determine the factors which influence the viscoelastic properties of bone cements. It was found that decreasing the porosity of the bone cements increased their resistance to creep.

Lautenschlager *et al.* (1976) showed that impregnating bone cement with small doses of antibiotic does not affect the compressive and tensile strengths of commercial PMMA, however large doses (10 grams of antibiotic powder added to 60 grams of PMMA) caused significant decreases (48 % and 33 %) in both compressive and tensile strengths.

Pilliar *et al.* (1976) performed tests on both normal and carbon fibre-reinforced PMMA bone cements. The Young's modulus for these two materials were found to be 2.76 GPa and 5.52 GPa respectively for uniaxial tension tests, and the ultimate tensile strength was 24 MPa and 38 MPa respectively. The strain rate was 5×10^{-3} per second. The fatigue resistance of the bone cement was significantly improved with carbon fibre-reinforcement.

Holm (1977) used bending tests to determine the Young's modulus and flexural strength of some commonly used acrylic bone cements. Holm noted the effect of continuing polymerisation and showed that the stiffness of all bone cements increased with time. Mean values for the Young's modulus of three cements tested after eight hours of curing were 2.44 GPa, 2.38 GPa and 2.22 GPa and after three weeks were 2.67 GPa, 2.41 GPa and 2.46 GPa. The author also showed that the stiffness decreased with the addition of blood and antibiotics. Flexural strength also increased with time. For the three cements, test values after 8 hours were 57.3 MPa, 52.0 MPa and 61.4 MPa and after 3 weeks, 61.2 MPa, 56.4 MPa and 68.4 MPa. Holm also noted that the cured product is extremely inhomogenous and there are large variations in flexural strengths.

Kusy (1978) performed uniaxial tension tests on various commercially available cements at a strain rate of 0.1 per minute to determine the Young's modulus and ultimate tensile strength. Kusy noted large differences in both Young's modulus and ultimate tensile strength after conditioning the specimens in distilled water at 37°C for 10 months. Testing in air at room temperature without conditioning produced stiffness's of approximately 2.51 GPa and ultimate tensile strength of 42.7 MPa whereas testing after 10 months conditioning at 37°C produced values of 1.96 GPa and 22.7 MPa respectively. Kusy identified porosity and residual stresses obtained due to shrinkage as defect causing.

Holm (1980), performed experiments to determine the viscoelastic properties of acrylic bone cements. A compromise was made between a creep and a relaxation test. The experiments were carried out in distilled water at 38°C and specimens were initially in tension in a "U" shaped spring. The spring slowly regained its original shape hence producing a slowly decreasing load. Holm used this method in order to get an estimate of the time factor involved when the cement is anchored to the bone where the stress will decrease as the cement creeps. Holm expressed the total cement strain as:

$$\varepsilon_{total} = \varepsilon_o + \varepsilon_{cr},$$

where ε_{total} is the total strain,

ε_o the elastic strain and

ε_{cr} is the time dependent or creep strain;

ε_{total} was further expressed as $\varepsilon_{total} = \varepsilon_o + mt^n$,

where m is a constant dependent on the stress and temperature and n is a material dependent constant but independent of stress.

The determination of these constants defined the viscoelastic behaviour of bone cements. In Holm's experiments n ranged from 0.5 - 0.8, and m ranged from 0.1 - 0.7. Factors which were shown to increase the rate of creep were temperature, humidity and the immersion in water.

Saha and Pal (1984), conducted an extensive review of the mechanical properties of bone cement as presented in the literature. The static properties such as tensile and compressive ultimate strength, Young's Modulus, elastic limit, flexural strength and shear strength are sensitive to method of testing, test temperature, environment, method of specimen preparation, and strain or loading rate. A relevant summary of the authors' review is presented below:

Lee *et al.* (1977) determined the tensile strength of surgical Simplex bone cement (a common brand name), in saline solution at 37°C by performing diametral compression tests and found it to be 25 MPa. Taitsman and Saha (1977), used uniaxial tension tests and found the ultimate tensile strength to be 27.6 MPa, whilst Wright and Trent (1979) using similar methods found the tensile strength to be 30.8 MPa. Sih and Berman (1980), using tensile tests with an environment simulating *in vivo* conditions that are found in total hip replacement surgery, found tensile strength to vary between 21.7 and 34.8 MPa and Young's modulus between 3.1 and 5.1 GPa. Compressive strength variations were in the range from 64-103 MPa. Young's modulus in compression ranged from 2.14 GPa to 3.1 GPa.

Saha and Pal (1984) pointed out that bone cement is similar to concrete in that it is weak in tension and shear but strong in compression. Lee *et al.* (1977) determined the shear strength of simplex cement to be 41 MPa (direct shear) and 37 MPa (torsional shear). Wilde and Greenwald (1974) found shear strength to vary between 37.8 MPa and 40.6 MPa and Astleford *et al.* (1975) reported shear strength of 21.1 MPa however the testing method may have been suspect, with bending stresses contributing to failure. Greenwald *et al.* (1977) found the shear strength to be in the range of 41 MPa and Saha and Warman (1979) found the shear strength of surgical Simplex-P (a common brand name) to be 30 MPa.

Saha and Pal (1984) also reviewed the viscoelastic properties of bone cements. From the relaxation studies of Pal and Saha (1982) and Saha *et al.* (1981), the following equation was developed:

$$\sigma_t = 18.907e^{-0.2856t} \text{ MPa},$$

where σ_t is the stress present after time t in hours, assuming an initial stress of 18.907 MPa.

Due to the viscoelastic nature of bone-cements, Saha and Pal pointed out that with increasing strain rate, the stiffness and ultimate strengths in various loading modes will increase; for example Astleford *et al.* (1975) reported a 50 % increase in direct shear strength when strain rate was increased from 0.001 per second to 0.1 per second.

McKellop *et al.* (1988) quantified the viscoelastic creep properties of PMMA surgical cement. The authors measured the elastic and creep extensions of specimens loaded for ten thousand seconds at five constant tensile stresses over the range 5.6 to 21.5. Equations were developed using a five-parameter equation representing two Kelvin elements in series and a three-parameter power law model. It was concluded that "the behaviour of surgical PMMA is highly linear viscoelastic, such that a set of parameters determined from a single creep test at a given stress can be used to accurately predict the creep at other stress levels". This discovery was important as *one* equation relating creep strain to instantaneous stress and time could be used to describe the viscoelastic properties of commercial bone cement.

McKellop *et al.* (1989) then developed a non-linear creep model for commercial bone cement which accounted for loading at a constant stress rate. The non-linear model developed was of a double-exponential form and was found to provide a good fit for specimens tested under constant stress and time-dependent stress.

Bone cements have been shown to be inhomogeneous with voids present and its mechanical behaviour dependant on temperature, hydration state, and humidity. It is also highly viscoelastic and the time-dependant properties also depend on environmental conditions. Reasonably strong agreement was found between authors in terms of the strength and stiffness of commercial bone cements. As was the case with the mechanical properties of bone, simplified mechanical properties of bone cement must be used if a numerical model is to be employed.

3.5 Relevant biomechanical analyses

Charnley (1960) described the use of "cold-curing" acrylic cement in total hip replacement surgery. Charnley pointed out that there is no direct adhesion between the cement and bone, and that the cement acts as a "filler" or "grout" between the prosthesis and bone. The cement acts as a cast largely increasing the area of bone to which the stress is transferred. The author suggested that the cement need only resist compression and that the tensile strength properties of bone cement were not of great importance. This proposition in hindsight is incorrect as large tensile hoop stresses are invariably present in the cement mantle.

Charnley (1965a) showed that the inclusion of acrylic cement reduced relative movement between the prosthesis and bone by a factor of 200. Prostheses were inserted with and without cement in cadaver femurs extracted after autopsy. Compression loads were then placed on the head of the prostheses and the distal migration of the stem of the prosthesis was measured. The use of cement dispensed the need for an interference fit between the prosthesis and bone and virtually eliminated the relative slip.

Charnley (1965b) used simple geometric models to demonstrate the biomechanical advantage of using acrylic cement as an intermediary between prosthesis and bone. Without the use of cement Charnley demonstrated that significant mechanical "fretting" occurred between the prosthesis and bone when a smooth prosthesis was used and showed that load transmission is restricted to isolated areas of the proximal and distal femur. With a "rough" surfaced prosthesis, Charnley pointed out that load transmission is by longitudinal shear resistance of the cortices of the femur and trabeculae. The smooth surfaced prosthesis, however, relies on the "hoop" or circumferential resistance of the femoral cortices. Charnley demonstrated that the introduction of acrylic cement significantly reduces fretting and also the magnitude of longitudinal shear stress being passed through to the femur.

Martens *et al.* (1974) embedded prostheses with attached strain gauges into acrylic cement and applied various compressive loads to the head of the prostheses. The line of action of the applied load was varied to account for variation in alignment between the axis of the prosthetic stem and the femoral axis, ie different rotations of the prosthesis within the

cement mantle. The authors had noted that when fatigue failures of the prosthetic stem were studied, there was a high incidence of the tip being near the lateral femoral cortex (a varus position). Hence the varus/valgus orientation of the prosthetic stem was thought to be an important factor in stem fracture. A valgus orientation would mean the tip of the prosthesis would be near the medial femoral cortex. It was found that the applied loads representing the *in vivo* situation of a prosthesis orientated in a varus position caused significantly higher bending stresses in the lateral midstem area of the prosthetic stem, where clinically, stem fractures had been noted.

Markolf and Amstutz (1976) used strain gauge experiments to determine the stresses present in three different types of prostheses, varying orientation and acrylic fixation. Failure of prosthesis stems had been due to high tensile stresses imposed laterally on the stems. Both lateral (cantilever) and vertical (axial) loads were placed on prostheses which were set in acrylic cement. Stresses were highest in the lateral mid-point of the stem from cantilever loading and for the longitudinal loading stresses increased moving from a valgus to a varus position. Tests were also performed on prostheses not securely "potted" in the PMMA but in a loose condition. This mode of fixation led to very high tensile stresses being produced in the prosthetic stem which were significantly higher than the "tight" condition.

Andriacchi *et al.* (1976) used a two dimensional (2D) finite element analysis (FEA) to study factors influencing fatigue failure of a collared prosthetic stem. The region of interest was the lateral surface of the stem in the middle third of the prosthesis. Constant strain, planer elements were used and linear elastic behaviour was assumed, with full bonds assumed at all interfaces. A strain gauge model was also tested and there was reasonable agreement between experimental and computer predicted results. The authors found the tensile stresses in the stem to be highest in the mid-third of the stem, agreeing with clinical observations and the stem in varus position produced highest stresses in this region. The region of calcar support was also studied and a decrease in calcar stiffness caused increased stresses in the prosthetic stem.

Beaumont and Plumpton (1977) performed pull-out tests on steel specimens embedded in bone cement. A shear lag analysis was used to determine the interfacial shear strength of the stem-cement system and found it to be 18 MPa. It was also showed that trapped blood

reduces the interfacial strength. Beaumont and Plumpton pointed out that shear stresses acting at the interface *in vivo* reach close to the level of 18 MPa.

Svensson *et al.* (1977) used a 2D finite element analysis to calculate the stress distribution in the femur with an implanted Charnley prosthesis. Spanning "side-plate" elements were used to account for the out-of-plane thicknesses of the cortical bone sections which vary with position distally down the shaft. All materials were assumed linear elastic and validity of the model was justified by comparing results with Brockhurst (1975), who performed stress-coating experiments. The authors acknowledged that hoop stresses, which are of great importance, cannot be calculated with the 2D model. Svensson *et al.* reported good qualitative agreement with the stress-coating experiments of Brockhurst, however the results of Brockhurst were of a higher magnitude. Svensson *et al.* explained this as being due to differences in stiffness between the numerical and experimental analyses and also the 2D modelling approach. It was suggested that the stress values in bone should be increased by 40 % to be realistic. The important point was raised that the bond between metal and bone cement may be of limited interest as so called "failure" at this interface may be completely "normal" as there is very little adhesion at this interface. This again argues the case that stem-cement debonding may actually mean "never bonded". Svensson *et al.* varied the stiffness's of bone and prosthesis and pointed out that a decrease in the stiffness of cement decreases the stresses in the cement but raises them in the prosthesis. This issue had importance at the time of writing due to the high incidence of prosthesis stem failure. The authors also performed an analysis allowing slip between the stem and cement and concluded that in terms of the cement stresses, the distribution altered considerably.

Oh and Harris (1978) measured femur strains *in vitro* by "potting" intact and prosthetic femurs in bone cement and applied loads simulating one-legged stance. The main result that was noted was a large decrease in strain at the proximal part of the femur and a large increase at the level of the tip after insertion of the prosthesis. This process known as "stress-shielding" is reported to be linked to problems such as loosening and failure of the prosthetic stem. An important assumption was that strain gauges were placed in line with principal stresses because rosette strain gauges were not used. It was suggested that the large decrease in stress at the proximal femur will lead to disuse atrophy which is a "thinning" of bone due to decreased strain energy per volume at a given region.

Yettram and Wright (1979) used 2D finite element analyses to determine the normal and shear stress distributions at the stem-cement and cement-bone interfaces. The authors varied the stiffnesses of bone, cement and prosthesis and found that the more flexible the cement, the more uniform the stress distributions and that normal stresses proximally were compressive on both the medial and lateral sides.

Huiskes (1980) provided an excellent review on the clinical and biomechanical factors involved in analysing failure of a total hip replacement system. He pointed out the difficulty in mathematically modelling the hip joint due to a variety of factors such as material and geometric irregularities and complicated mechanical interfaces.

Huiskes constructed a simplified model of an intramedullary fixation structure which assumed linear elastic material properties, full bonds at both interfaces and a constant cross-section. The model was used for an axisymmetric finite element study and used linear stress triangular elements. The author also carried out strain gauge experiments on cadaver femurs with inserted prostheses and there was good qualitative agreement between the numerical and experimental results. Equivalent stresses were calculated in the numerical model based on a maximal deformation energy criteria.

It was found that the equivalent stresses in the prosthesis and bone were virtually equivalent to the axial stresses, hence these materials behave in accordance with beam theory, whereas the cement characterisation was truly three dimensional. The highest stresses which were found in the cement occurred near the stem-cement interface, with the radial stress being the largest component. Huiskes observed the proximal-distal bending stress distribution and proposed the use of beam-on-elastic-foundation theory to explain the behaviour of the composite system. Good agreement was found between results obtained from using beam-on-elastic-foundation theory and finite element analysis.

The author also commented on the differences between 2D and three dimensional (3D) finite element models. Huiskes pointed out that 2D models which did not have spanning elements, such as Andriacchi *et al.* (1975), connecting the medial and lateral cortices, result in sandwich construction, and the resulting model is quite inappropriate. It was suggested that the only suitable 2D models are those which include spanning "side-plate" elements linking the cortices. Huiskes further concluded that although his model included 3D

behaviour, it only provided "first-order" approximations of the intramedullary fixation system mechanical behaviour.

Huiskes also used a 2D model with spanning elements to compare the stress distribution of the total hip system assuming both fixed and loose stems. It was found that the longitudinal shear stress in the cement at the stem-cement interface decreased markedly with a "loose" stem. A loose stem was modelled numerically by disallowing tensile stress to be transferred between adjacent cement and prosthesis elements, he also found a large increase in the normal cement stress at the bone-cement interface with the loose stem. Essential parameters of the total hip system were identified and it was shown how the variation of these parameters affected the resulting stress distribution. The essential parameters identified included stem length, and stiffness's of the three structural materials, cement, bone and metal.

The author then provided design guidelines based on these parameters. It was proposed that proximally, the stem should be thick and stiff to reduce cement stresses in this region. Here is seen the fundamental paradox, however. A flexible and thin proximal stem will increase the stresses in the bone hence decreasing the risk of disuse atrophy, but to transfer the stress between the prosthesis and bone it must be passed through the intermediate layer of cement. In other words, more "natural" or physiological stress levels in the proximal femur will be at the expense of high proximal cement stresses. Huiskes pointed out that "iso-elastic" prostheses with Young's modulus similar to that of bone, increase cement and interface stresses by 200 %. Therefore it is seen that, as in many other engineering systems, there are conflicting design objectives.

Cook *et al.* (1980) pointed out that disuse atrophy and proximal cortical thinning can increase the demand placed on the cement interface, and will certainly increase tensile hoop stresses in the cement mantle due to the decreased restraint of bone. A 2D finite element analysis without spanning elements was employed to show that decreasing the stiffness of the prosthesis increases stresses in the proximal femur to a more "natural" anatomical state. The authors claimed reasonable quantitative agreement between this work and the strain gauge experiments of Oh and Harris (1978), measuring strains at the outer surface of the cortex.

Jacob and Huggler (1980) used a strain gauge study to determine the stress distribution of the femur with and without an inserted prosthesis. As with other authors, Jacob and Huggler noted on implanting a prosthesis that the stresses in the bone altered considerably as compared with the physiological condition, with "stress-shielding" occurring at the proximal femur. The authors pointed out that the moment acting in the frontal plane transmitted by the prosthesis is essentially resisted by a couple acting transversely at the distal and proximal ends of the stem, thus transferring high stress concentrations to the cement at these points.

Keller *et al.* (1980) used uniaxial tension tests to determine the strength of the stem-cement interface. The load at which the cement "pulled away" from cylindrical metal stub specimens was divided by the contact area to determine the tensile bond strength of the stem-cement interface for "rough" and polished surfaces. Bond strengths for stainless steel ranged from 6.5 - 11.7 MPa for "rough" surfaces. It can be seen from these experiments that although it had been previously stated that there was no adhesive bond between the metal and cement, this author claimed that tensile stresses, to a certain level, can actually be transferred from the prosthesis to cement. The bond strength significantly decreased, however, when tested in saline solution at 37°C. It is doubtful however if the "tensile" strength of the bond was actually being tested, and whether cohesive and shear effects were contributing to failure.

Crowninshield *et al.* (1980a) used 3D finite element analysis to determine how variations in the cross-sectional properties of hip prostheses affects stress distributions in total hip systems. It was found that the proximal regions of cement were critical, and that prostheses with broad anterior-posterior dimensions laterally result in larger areas of cement in compression and less in tension. The authors pointed out that bone cement is three times stronger in compression than tension and suggested a beneficial prosthetic system would be one which does not rely on a bond between metal and cement. This is due to the fact that compression can be passed from prosthesis to cement without a bond being present. If a bond is assumed, its subsequent breakdown which often occurs clinically, or is never present will dramatically alter the stress distribution to one for which the system was not designed.

Hampton *et al.* (1980) also used a 3D finite element analysis to determine bending and shear stresses in a Charnley prosthesis. Although a coarse mesh was used, verification with strain gauge models was claimed as far as predicting stresses on the prosthesis surface was concerned. The authors raised a very pertinent point when it was stated "in attempting to validate models of this nature experimentally, the study should be designed to measure the specific parameters for which the model has been designed for. Thus, it would not be prudent to employ validity of cement and bone stresses based on analytical results of models in which only stress calculations in the femoral stem were validated." It was pointed out that the cement does not transmit the "bending" stress from the prosthesis due to the large difference in elastic modulus and identifies a stress pattern in line with Huiskes' beam-on-elastic-foundation model, ie pure bending theory does not predict the stresses correctly in the cement mantle. This can be explained by the fact that with elastic bending theory plane sections must remain plane and, due to the two-order-of-magnitude difference in stiffness between prosthesis and cement, plane sections do not remain plane in the stem-cement interaction. It was also put forward that subsidence of the prosthesis does not necessarily define failure which is clinically presented as loosening at the bone-cement interface.

Crowninshield *et al.* (1980b) used a 3D finite element analysis to study the effect of varying parameters such as material stiffness and stem length on the stress distribution throughout the total hip system. As has been seen in previous studies, increasing the stiffness of the stem increased cement stresses distally and reduced them proximally whilst decreasing the prosthesis stiffness caused the converse effect. Increasing the cement modulus increased the cement stresses, whilst reducing the stem length, or decreasing the cross-sectional size of the stem, increased the cement stresses. The authors noted that collarless prostheses produce much larger tensile hoop stresses in the proximal calcar than longitudinal compressive stresses which exist in the "natural" or intact state. Crowninshield *et al.* stated that tension cannot be transmitted across the stem-cement boundary. However the work of Keller *et al.* (1980) suggested this may not be the case though his study may not have represented the clinical situation. It can be concluded that *the weakest link in the total hip system is the cement and one of the primary objectives must be to minimise stresses in the cement.* Crowninshield *et al.* identified the design

conflict that the transferral of stresses to the proximal femur implies high stresses in the cement at that region.

Raab *et al*. (1981) identified the stem-cement interface as a crucial region in the transfer of load from the prosthesis to the femur and attempted to mechanically characterise the interface. The authors pointed out the difficulty of testing the tensile strength of the bond as specimens usually fail outside the bond, ie cohesively and suggested this was the case in the work of Keller *et al*. (1980). Raab *et al*. used both theoretical (axisymmetric FEM study) and experimental analyses to characterise the interface. The finite element study showed high concentrations of normal and shear stresses at the interface which decreased both longitudinally and radially. The magnitude of normal and shear stresses were very similar although the restraining effects of bone were not modelled. It was suggested that in spite of 'shear' loading, tensile failure is likely due to the brittle nature of the observed failure. The authors presented values for the quasistatic interface strengths of various prosthetic materials bonded to cement. A large decrease in interface strength was identified when the stem-cement bond strength was tested in saline solution after sixty days. The author also studied contact angles of bone cement on prosthesis. A contact angle in interface strength studies provides an indication of the strength of an interface. A very low contact angle would indicate "minimum interface flows and maximum interaction area and therefore superior bonds", however contact angles for bone cement on metal were found to be at least 50°, indicating weak strength. It was concluded that the stem-cement interface performs poorly and should not be relied on to transfer anatomical loads without failure. The authors further stated that failure of this interface may increase stresses in the cement mantle and hence the bone-cement interface leading to failure of the system as a whole.

Sih *et al*. (1981) used a strain energy density criterion to identify potential failure sites in the cement mantle. The authors only used a 2D finite element model however, without spanning elements, and thus it did not represent the clinical situation. It was stated that areas of potential failure identified in his work do not necessarily correlate with clinically observed failures and states that a more realistic modelling approach to the cement properties was probably necessary.

Ling *et al*. (1981) reviewed the clinical performance of the Exeter prosthesis, a flexible collarless prosthesis and made the important observation that the prosthesis could subside

within the medullary canal and not produce adverse symptoms. This concept had been previously stated, ie distal movement of the femoral stem within the cement does not mean failure and the resulting wedge action may actually stabilise the system, a well established engineering concept. It was postulated that subsidence was accommodated by the creep of the bone cement

Lanyon *et al.* (1981) recorded *in vivo* strain measurements from femoral bone and the prosthesis following total hip replacement. The authors used sheep in the study and pointed out that sheep femur undergo similar radiographic changes postoperatively to humans. The strains were recorded whilst the subjects were walking at one metre per second and significant decreases in the proximal principal compressive strain on the medial side were noted. Similar large decreases in both principal tensile and compressive strains on the lateral side of the femur were also detected. The study revealed that theoretical calculations based on bonding of the stem-cement interface assumption do not correctly predict the strains (and stresses) which actually occur *in vivo*. Lanyon *et al.* concluded that despite a clinically firm fixation, micromovement between stem and cement must be occurring "even within a few days of implantation". Again this pointed to the fact that there may never have been an intimate bond at the stem-cement interface. Lanyon *et al.* also noted that strains within the proximal calcar actually decreased with time leading to extensive calcar resorption which is noted clinically. Maintaining a reasonable level of stress in the proximal calcar may be crucial to prevent loosening and hence failure of the total system.

Skinner *et al.* (1982) used a 2D finite element study to confirm that the use of a cement plug placed distally to the prosthesis tip in the medullary canal reduces stresses in the femoral canal at the level of the tip. This agreed with the experimental work of Oh *et al.* (1978).

Krause *et al.* (1982) performed experiments to determine the shear and tensile strengths of the bone-cement interface. For pressure injected cement samples the tensile strength of the bond ranged from 6.4 to 8.5 MPa, and the shear strength ranged from 25.2 to 42.0 MPa. Kusleika and Stupp (1983) similarly studied the tensile strength of bone-cement interface and found the mean strength to be in the order of 7.5 MPa.

Crowninshield and Tolbert (1983) used foil strain gauges encapsulated within PMMA to measure strains in the cement mantle *in vitro* for both fixed and loose bonds at the stem-cement interface. Significant increases were noted in the proximal strains within the cement mantle when a loose bond was assumed, whereas little difference was noted for the distal strains. These results agreed qualitatively with previous numerical studies, although the percentage increase in stresses with loosening was less. Because rosette strain gauges were not used, the distal cement stress changes may not have been detected if the orientation of the stresses was not aligned with the direction of the strain gauge.

Huiskes and Chao (1983) provided a comprehensive review of finite element analysis as applied to orthopaedic biomechanics. The authors pointed out the importance of both the *validity* and *accuracy* of a finite element model. The validity is concerned with how well the computer model mimics the actual situation, ie loading, material properties, support conditions etc. The accuracy is concerned with the mathematical precision of the solution and may be checked with a convergence test ie increasing the mesh density should cause the solution to converge to a particular value. The validity must be checked by experimental means. It must be stated that prior to 1983 software and hardware requirements, compared with availability, were such that fully 3D and non-linear studies were very difficult to perform with reasonable accuracy. In a similar light, many of the analyses lacked suitable validity, often due to the lack of experimental evidence available, but more often due to high computer expense (the run time of the solution extracted). For example, anisotropy and interface modelling, even if characterised in the literature, were difficult to model with any accuracy.

Huiskes and Chao pointed out the extreme difficulty in comparing results from finite element analyses quantitatively "due to vast differences in mesh density, geometry, material properties and loading." The authors also remarked that the *objectives* of the finite element study must be clearly defined as compromises must be made in terms of the validity. For example, if stresses at the stem-cement interface were of interest, special contact elements may need to be used and a fine mesh at the interface is needed, however the mesh could be far coarser elsewhere. On the other hand, if broad qualitative trends only are required, the accuracy is not of great importance, however the validity of the modelled parameter (ie, stem length) is important. It was concluded that "rarely is an absolute

solution either needed or possible because of many unknown conditions inherent to the biological system".

The conflict between validity and accuracy was also noted and it was stated that sacrificing accuracy for the sake of a true anatomical model may be unnecessary and produce misleading results. A statement of the assumptions used in a model was also stated as being of prime importance. It was also stated, as had been previously, that stresses predicted from the finite element model which agree with experimental tests at a particular location (ie. outside the bone), does not mean stresses at other locations (ie. inside cement mantle) are correct, although many authors have claimed this. The authors also remarked that mesh density, element type, and total degrees of freedom should be presented in any FEM study so that the reader has a "feel" for the accuracy of the solution and comparisons with other models can be made.

Rohlmann *et al.* (1983) compared strain gauge experiments with finite element output to study the stress distribution of the prosthetic femur. The author found good agreement with results obtained from the femoral surface, as has been seen in previous studies, however results obtained from the distal prosthesis stem did not correlate as well. The authors suggested this may be due to micromotions at the stem-cement interface. The finite element model assumed a fixed stem-cement interface. The asymmetric nature of the stress distribution in the cement mantle was demonstrated especially between the medial and lateral sides. High shear stresses were identified in the proximal third of the cement mantle and also low stresses in the proximal femoral cortices which may lead to disuse atrophy.

Lewis *et al.* (1984) used 3D finite element and strain gauge analysis to determine the influence of prosthetic stem stiffness and of a calcar collar on stresses in a total hip replacement system. A collar is used in some prosthesis designs to impart load directly onto the medial calcar. The assumption of perfect collar-calcar contact in the finite element model led to large increase in the longitudinal compressive stresses in the femoral cortices however the validity of this assumption *in vivo* is very dubious with several reports of collar-calcar debonding, even though at the time of surgery the bond appeared to be quite solid. The authors' results showed that a proximal increase in cement stresses is noted with a more flexible stem (lower stiffness). Conversely, a decrease in distal cement stresses was

noted with the more flexible stem. The more compliant stem also had the advantageous effect of increasing stresses in the proximal femoral cortices.

Ahmed *et al.* (1984) used "push-out" tests to determine the critical strain energy rate of the stem-cement interface. The critical strain energy rate is an important variable in describing the strength of the interface. The higher the critical strain energy rate, G_c, the stronger the interface parameter. This parameter G_c was found to decrease after immersion in saline after sixty days leaving a weak bond, confirming the results of previous authors. The authors noted a significant increase in bond strength when stems were precoated with PMMA.

Weightman *et al.* (1987) suggested that the use of a bone cement with low stiffness, low creep resistance and high ductility used with a suitably shaped femoral component could dramatically improve the stress transfer to the proximal femur. As has been previously stated, the implantation of a femoral prosthesis "reverses" the anatomical stress distribution ie post-implantation stresses are "shielded" proximally and are passed, in a concentrated manner through the bone cement to the distal femur. Weightman *et al.* performed experiments to show that subsidence of various prostheses due to an applied load significantly increased before any cracking of the cement mantle due to the use of the low modulus cement. It must be noted however that the authors presented results as penetration to fracture and **NOT** load to fracture. It is obvious that for a less stiff and greater ductility cement that penetration will increase dramatically for the same applied load. The system must however be able to sustain the load placed upon it regardless of the amount of ductility, hence actual loads producing these deformations is an important consideration and are not presented for the simplified tests. Again, here the conflict was noted between increasing stresses in the proximal femur and decreasing stresses in proximal cement. Weightman *et al.* did point out that due to the lower modulus of the cement, cement stresses will decrease, however the proposed new bone cement had only 50 % static strength of traditional PMMA. Finite element or strain gauge verification would seem appropriate to verify the stress distribution. It was pointed out that maximum benefit was obtained, with the use of the more compliant cement, when a proximal wedge is employed in the design of the femoral component. A proximal wedge is represented by a large angle between the lines of the prosthesis stem and prosthesis neck. It was noted that subsidence

with the use of the wedge increases longitudinal compressive stresses in the proximal femur.

Huiskes *et al.* (1987) used a 2D finite element model with spanning elements combined with a bone-remodelling theory to predict the effect of stress-shielding after implantation of a femoral prosthesis. A value for the average homeostatic strain energy density at the outer bone surface was presented for the pre-operative state. The authors then incorporated into the model the theory that after implantation it is the object of bone to remodel in such a way that the strain energy density is normalised to the pre-implantation level.

Both internal and external remodelling theories were used to predict remodelling. The internal remodelling involved altering the stiffnesses of individual elements in the finite element model in order to normalise the strain energy density. The external remodelling involved changing the position of the nodes at the outer surface of the finite element model again to normalise the strain energy density. The external remodelling was far more dramatic than the internal and significant geometric changes were noted, especially resorption of the bone in the proximal cortices as well as distal hypertrophy. These results agreed with clinical observations of "stress shielding" and also strain gauge experiments which predicted decreased stresses in the proximal cortices and increases at the level of the tip. The authors also noted that medial calcar "stress-shielding" was minimised by using stems of low moduli. A significant finding was that when the interface between the prosthesis and cement was assumed loose, *less* "stress-shielding" was noted, ie load transfer was more "anatomical" than an assumed bonded stem-cement interface.

Brown *et al.* (1988) used a 3D anatomical finite element model to assess the effect of a fibrous membrane between bone and cement on the resulting stress distribution. The presence of a membrane is similar to modelling a loose interface between cement and bone due to the very low elastic modulus of the fibrous membrane (1.4 - 69.0 MPa). The upper bound represented a modulus equal to that of the adjacent cancellous bone and represented the fixed case. The fibrous membrane had been observed in many clinical observations and the results of Brown *et al.* showed that stresses in the proximal lateral femur were increased with the presence of a compliant membrane, encouraging hypertrophy at this region.

Fowler *et al.* (1988) reviewed the *in vivo* performance of the Exeter total hip replacement over the previous seventeen years. The authors reported very good clinical performance with a low rate of loosening compared to other studies. As has been previously established the Exeter prosthesis has a polished stem, no collar, and has a double taper. The design of the prosthesis is such that distal subsidence of the stem is encouraged. The authors reported that it is not appropriate to define "loosening" as distal movement of the prosthetic stem between subsequent radiographic examinations, as distal movement is in fact necessary to engage the wedge action of the system, and stabilise movement of the prosthesis within the cement mantle, especially under torsional loading.

The authors identified the viscoelastic nature of the cement and stated that the polished stem allows the stem to subside with the creep of the cement. It was proposed that the subsidence increases the stresses in the proximal cortices, and reduces disuse atrophy. In terms of cement stresses, the authors pointed out that with a polished stem, normal compressive stresses increase, which can be tolerated due to high cement compressive strength, and longitudinal shear stresses decrease. It is not stated however, that subsidence will greatly increase tensile hoop stresses in the cement, although the low incidence of observed cement fractures suggested this may not be a problem, due to stress relaxation over time.

Maloney *et al.* (1989) performed a biomechanical investigation of cemented total hip replacements retrieved at autopsy after years of *in vivo* service. Strain gauges were employed to show that even after years of service, there were still low stress levels in the proximal medial cortex and high distal levels of stress, although these levels were "more normalised" than the immediate post-operative state. It was concluded that localised strain energy density is not the only factor in determining bone remodelling, as the strain levels had not normalised in some cases after seventeen years *in vivo* service.

Weinans *et al.* (1990) used a 2D finite element model with side plates to assess the effect of a fibrous membrane interdisposed between cement and bone on the stress distribution of the proximal femur. The authors showed that the presence of the membrane, which is often present in follow up radiographs after THR significantly increased stress concentrations in the bone cement which may lead to total failure of the THR system.

Huiskes (1990) compared the stress distributions of cemented, press-fit, and ingrown femoral stems by using 2D finite element models with side plates. Similar patterns were found with the cemented and ingrown implants but a markedly different stress distribution was noted with the non-cemented press-fit implant. Huiskes noted greater stress-shielding with the ingrown stem than the cemented due to the increased rigidity of the canal-filling ingrown prosthesis. The author suggested that for cemented stems the stiffer CoCrMo alloy should be used in preference to titanium stems as titanium stems will increase cement stresses at the interfaces and in the cement mantle itself. Huiskes' model assumed a fixed interface at the stem-cement interface. It was proposed that a loose interface with a titanium stem will also increase stresses however these stresses will be mainly compressive which cement can tolerate. There will also be an increase, however, in tensile hoop stresses, and if these stresses are excessive the titanium implant would not be appropriate as the benefits of stress-transfer to the proximal cortices would not be realised. The stress-distribution of the press-fit stem is different from the other two types because the load is transferred directly to the bone as normal stresses and the absence of tensile and shear stress transmission due to the lack of any bond.

Lee (1990) commented on the biomechanical differences between stems which produced fixed cement interfaces and stems which produced sliding interfaces. The author emphasised the importance of designing a system "that puts acceptable stress/strain conditions onto the host bone and encourages it to model into new bone". It was also pointed out that the critical failure region is the bone-cement interface and that this bond must remain intact for clinical function to continue satisfactorily. It was proposed that a polished stem will produce increased hoop stresses in the bone cement, although, he predicted these stresses will relax with time due to the viscoelastic nature of the cement. Shear stress at the bone-cement interface will be significantly reduced with a polished stem due to the stress transmission being passed as normal instead of shear due to the low friction.

Miles (1990) similarly compared the stress regime resulting from the use of smooth and rough stem surfaces. Miles embedded strain gauges in cement surrounded by an aluminium sleeve and inserted a tapered steel cylinder. The surfaces of the steel cylinders were either smooth with a low coefficient of friction, or rough, with a high coefficient of friction. As predicted the smooth stems produced significantly higher normal compressive stresses due

to the absence of shear transmission. The tensile hoop stresses developed in the cement mantle for the polished stem were higher than for the bonded stem but not significantly higher. This is because hoop or circumferential stresses depend on the degree of radial support, which *in vivo* is bone, not aluminium. This experiment used aluminium hence actual comparisons between magnitudes of developed hoop stresses may not be appropriate.

Mann *et al*. (1990) used push-through pin tests and finite element analyses to determine the friction coefficient of the stem-cement interface. Mann simulated thermal contraction of the cement by assuming a thermal reduction from 85°C to 25°C. Load displacement graphs were plotted from the experimental data and the numerical results were found to best agree with experimental when the friction coefficient was 0.35. The experiments were performed in air and due to the "wet" environment *in vivo*, it is envisaged that the coefficient may be lower. It is also unknown whether the prosthesis had a "smooth" or "rough" surface.

Harrigan and Harris (1991a) used a 3D anatomically accurate finite element model to show that the presence of a calcar collar reduces stresses in the bone cement. The authors modelled the THR system with a fixed collar, a "slipping" collar which could move laterally relative to the calcar and no collar. The presence of a fixed calcar-collar bond was found to reduce peak principal stresses proximally by 66 %. Again, however, the sustainability of such a bond *in vivo* is highly questionable.

Harrigan and Harris (1991b) used a similar 3D finite element model to study the effect of debonding at the tip of a femoral prosthesis. This study was relevant due to the plethora of debonded tips seen clinically. It was found that although the magnitude of the peak principal stress did not alter significantly, relatively large tensile stresses developed just proximally to the tip which the authors suggested may lead to further debonding. Estok *et al*. (1991) similarly studied stress concentrations at the tip of a prosthesis and found the presence of high compressive and tensile stresses. It was found that peak stresses could be reduced with a smaller tip section.

Harrigan and Harris (1991c) used a non-linear 3D anatomically accurate finite element model to assess the effects of debonding at the stem-cement interface. The author looked at partial debonding by simulating regions of looseness at the stem-cement interface where

elements adjacent to the "region of looseness" were able to slide with zero friction over each other. Harrigan and Harris applied simulated stair-climbing loads and observed the resulting stress distribution when debonding was assumed to occur down to a horizontal plane which was either 35, 62.5 or 82.5 mm below the prosthesis collar. Complete debonding was also modelled with gait loading. A large increase in peak principal cement stresses was noted with debonding. The criteria which was cited as important in terms of failure are maximum principal cement stresses, maximum stresses on a cement pore, and maximum tangential stresses at the stem-cement interface. For partial debonding, increases in all stress criteria were substantial with stair-climbing when compared to the bonded case. An increase was also noted with gait loading. With the assumption of a fully loose prosthesis, an extremely large increase in the magnitude of the distal maximum principal cement stress was noted, although the stress was compressive (fixed bond - 6.5 MPa in tension, loose bond - 34.9 MPa compression). The authors suggested that the magnitudes of tensile stress found in this study indicate fatigue failure of the cement will occur *in vivo* with a loose interface.

Mann *et al.* (1991) modelled Coulomb friction at the stem-cement interface in a 3D "anatomical" finite element model. Similarly to other studies, the authors found a large increase (400 %) in the magnitude of peak tensile stresses in the cement mantle with the slipping interface when compared to the fully bonded. The peak stress (8.4 MPa - tension) was found in the proximal-medial region and was a circumferential or hoop stress. It was suggested that a tensile stress of this magnitude may approach the fatigue limit of bone cement.

Harrigan *et al.* (1991) used an anatomically accurate 3D finite element model to suggest failure initiation regions for the cemented THR system. All interfaces were assumed bonded and magnitudes of tensile and shear stresses were obtained from the model near the stem-cement interface. The authors concluded that "the most likely region for initial failure is at the cement-metal interface." It was noted that stresses occurring at the prosthesis tip during gait loading are sufficient to debond the stem-cement interface, and pointed out that clinically many failures have been noted in this area.

Bugbee *et al.* (1992) measured the shear strength of the bone-cement interface at various locations and found the interface strength to be weakest distally and strongest proximally.

It was noted that high stress concentrations in the cement mantle are found distally and that these stresses must be passed through to the bone at an area where the bond strength is low, further suggesting that the distal region is a zone of weakness.

Mann *et al.* (1992a) used experimental and finite element models to determine the characteristics of the stem-cement interface. The authors assumed non-linear behaviour of the interface and calculated the critical parameters required to predict the behaviour of the interface. Mann *et al.* calculated the tensile strength of the interface from experiments and then determined the shear strength and coefficient of friction from correlating push-through-stem tests with finite element models. It was found that a "smooth" interface could be modelled assuming no tensile or shear strength and a coefficient of friction of 0.3, whereas a "rough" interface achieved by plasma-spraying could be modelled assuming a tensile strength of 15 MPa, shear strength of 45 MPa and a post-failure friction coefficient of 3.0.

Mann *et al.* (1992b) suggested that the use of the plasma-sprayed stem with significantly increased stem-cement bond strength could reduce the chance of failure as stresses may be less in the proximal cement mantle with a "tight" bond. The authors used a 3D finite element model to assess the effects of different degrees of bonding, ranging from fully loose, to partially bonded to full bonding. It was found that the maximum principal stress in the cement mantle decreased as the degree of bonding increased however the normal tensile stresses across the bone-cement interface increased.

Estok and Orr (1992) used a simplified 3D finite element model with a very high mesh density to map the strain distribution in the cement mantle after insertion of a femoral prosthesis. The authors assumed fully bonded interfaces and modelled both gait loading and stair-climbing. A high cement stress concentration was found to occur near the tip of the prosthesis providing further evidence of possible failures at this location.

Lu *et al.* (1992) used a simplified 3D finite element model with cantilever loading to assess the effect of the stem-cement bond strength on stresses in the cement mantle. Non-linear Coulomb friction interface elements were used with varying tensile strengths so that when this strength was exceeded, debonding at this region occurred. The authors found that when zero tensile strength of the interface was assumed the peak principal stress in the cement

were lower than when a full "tight" bond was assumed. Principal cement stresses were found to be a minimum when partial debonding was assumed.

Helmke *et al.* (1992) verified the weakness of the stem-cement interface by observing the level of porosity. Helmke found that "significant porosity is present at the cement/stem interfaces of femoral prostheses." Air entrainment was suggested as the course of this porosity. Porosity means that there are significant voids in the cement mantle, particularly near the stem-cement interface. It was suggested that if a "fixed" bond is required at this interface, mechanical interlocking will be far more effective than trying to achieve adhesion.

Lu *et al.* (1993) used a similar finite element model to their 1992 study to study the energy release rate of a debonded stem. Different values for the strength of stem-cement bond was assumed and it was suggested that debonding at one location would not lead to complete debonding. The energy release rate was calculated by dividing the strain energy produced by debonding, by the incremental debonded area. It was found that for successive increments of debonding, the energy release rate remained below the critical value which would lead to unstable separation. These results held true for even the weakest assumed bond strengths. It was concluded that minor debonding is possible "without precipitating catastrophic failure of the remaining stem-cement interface, and without marked increase in the maximum principal stresses in the cement."

McKellop *et al.* (1994) used a 3D finite element model with simplified geometry to assess the effects of creep on stresses in the cement mantle. The authors assumed three different stem-cement interface conditions; full bonding, sliding without friction, and sliding with friction coefficient of 0.22. A simulated cyclic load was also applied. It was found that the creep of the bone cement did not significantly affect the stresses within the cement mantle and that the assumed bonding condition was far more influential. McKellop *et al.* found that for the loose interface without friction both maximum tensile and compressive cement stresses were higher than for the fully bonded interface.

Lu and McKellop (1995) showed with the use of a 3D finite element model that, due to the restraining effects of the bone, the effects of creep were not overly significant. The authors studied the long term effects of cement creep by considering load/unload cycles

representing daytime activity and nightime rest. It was found that for the bonded and frictionless interface conditions, there was no long-term accumulation of creep, ie the creep recovered during the period of rest. The frictional interface did not recover, however, with residual stresses presenting as much as 29 % of the maximum. The amount of subsidence predicted by the author (0.5 mm) did not correspond with clinical observations (2 mm subsidence) however the authors explained this could be due to remodelling of the femoral cortex *in vivo*. A relatively simplified geometry and loading were also used in this study.

Saligrama *et al.* (1996) predicted high levels of tensile stress relaxation in the cement mantle when the same three interface conditions as McKellop *et al.* (1994) were considered. A 3D finite element model predicted that for the three interface conditions of bonded, friction coefficient 0.22, and frictionless, reductions in peak tensile cement stresses were reduced by 40 % (from 31 MPa), 33 % (from 8.4 MPa) and 18 % (magnitude not given) for the respective conditions. The magnitude of these stresses were far higher than those predicted from other studies. A double tapered prosthesis was also modelled in the study of Saligrama *et al.* It is a fundamental property of viscoelastic bone cement that the higher the level of stress, the greater the creep, a creep strain is a function of stress. It is therefore not surprising that larger degrees of relaxation were noted in the study of Saligrama *et al.*

3.6 Summary

The literature review sheds light on the complexity of the problem of failure of a cemented total hip replacement system. The incidence of aseptic loosening is high and the exact mechanism of the breakdown is unknown and multi-factorial. Definitions of loosening vary and controversy remains over the extent of either a predominantly biological or mechanical cause.

There are two key factors which have been identified as being crucial to the long term mechanical survival of total hip replacement; the incidence of cement cracking and calcar stress shielding. Both of these issues can be studied by utilising a numerical simulation such as the Finite Element Method.

One controversy which persists among clinicians and designers is the role of the stem-cement interface. The interface is difficult to characterise mechanically *in vivo* and it is unclear whether a bonded or sliding interface is more beneficial in the long term to prevent loosening at the bone-cement interface. This study aimed to explain the biomechanical rationale of different stem-cement interface conditions, and the role of cement creep in the long term sustainability of cemented total hip replacement.

Chapter Four

The finite element model

4.1 Introduction

This chapter concerns itself with the development of the finite element model. Firstly, the finite element method will be detailed in relation to both linear and non-linear analyses. A general description of the model used in this study will then be presented. The physical properties of the model will then be detailed followed by the application of these properties to the finite element model. The various analyses performed in this study will also be specified, as well as details of model validity and accuracy. In this study, a commercially available software program, the LUSAS/MYSTRO system (LUSAS user manual 1990) was used for all analyses.

4.2 The finite element method

4.2.1 Basic concepts

In any material continuum there is an infinite number of points at which a state of stress and strain is present. The stress and strain distribution is continuous throughout the material. For simple geometric arrangements, with known material properties, boundary, and loading conditions, the basic laws of stress analysis allow the state of stress and strain to be determined at any point within the continuum (Timoshenko and Young 1965). For

systems which contain complex geometric arrangements, non-uniform material properties or complex loading and boundary condition arrangements, a simple determination of the stress and strain distribution is not possible. The complex system must be modelled as containing a finite number of small volumes or elements which each have a simple geometric shape. Each element's behaviour is governed by a constitutive relationship which relates stresses and strains.

The Finite Element Method is thus an approximation of the true continuum behaviour. The greater the number of elements, the more accurate the model will be in predicting the state of stress and strain in the continuum. The elements are connected by nodes at the element boundary and it is the displacement of these nodes which must be determined. Again, the true number of interconnections between any 'finite element' isolated by some imaginary boundaries and the neighbouring elements are infinite (Zienkiewicz and Taylor 1971), however in a finite element model the number of interconnection points is finite. The accuracy of the model will also be improved by increasing the number of interconnection points between elements. Either increasing the number of elements or the number of nodes per element will increase the computational expense of the problem. This is because the number of nodes governs the number of equations which are needed to produce a stress or strain distribution. Once the nodal displacements are calculated, integration is performed to determine the resultant stresses and strains within each element.

The process to determine the nodal displacements will now be outlined for both linear and non-linear models. The concepts outlined will be both basic and general and a more detailed analysis is beyond the scope of this work. The reader is referred to texts such as (Zienkiewicz and Taylor 1971), for a more detailed discussion.

4.2.2 Linear analysis

A linear finite element analysis is conducted when all the physical properties making up the model are linear in nature. These properties include: a linear relationship between stress and strain for all materials comprising the system; static loading; bonded or fixed interface relationships (eg at the stem-cement interface); and linear boundary conditions.

The nodal displacements for the system under consideration are determined by the following steps.

1)   **Identify the problem**: The external forces acting on the system are related to the overall stiffness of the system and the global displacement of the nodes. In matrix form:

$$[F] = [K^e] [\delta^e] \qquad \qquad \text{Eq. (4.1)}$$

where $[F]$ is the external force matrix, which is known, $[K^e]$ is the element stiffness matrix and $[\delta^e]$ is the displacement matrix. Therefore to solve for $[\delta^e]$, $[K^e]$ must be determined.

Determination of $[K^e]$.

2)   The first step is to relate general displacement of any point within an element to its nodal displacement.

$$[f] = [N] [\delta^e] \qquad \qquad \text{Eq. (4.2)}$$

where, $[f]$ is a column vector representing the displacements at any point within the

element, $[\delta^e]$ is the nodal displacement vector, and $[N]$ contains components which are in general a function of position.

3)   A matrix $[B]$ is now considered which relates strain at any point within the element to the nodal displacement

$$[\varepsilon] = [B] [\delta^e] \qquad \qquad \text{Eq. (4.3)}$$

Where $[\varepsilon]$ is a column vector representing the strain at any point within an element, $[B]$ is a matrix simply derived from $[N]$ which relates internal strains to external nodal displacement.

4)   A **constitutive** relationship is then specified, relating strains to stresses

$$[\sigma] = [D] [\varepsilon] \qquad \qquad \text{Eq. (4.4)}$$

Where $[\sigma]$ is a column vector representing the stress at any point within the element, $[D]$ is a matrix which relates stresses to strains derived from fundamental stress-strain relationships.

6)   The principle of **virtual work** is then employed:

This principle requires that for an arbitrary or virtual nodal displacement, the work done by the nodal forces to produce the virtual displacement is equal to the sum of the products of the individual force components and corresponding displacements. Another way of stating the principle is that the external work done on the system must be equal to the internal work, for a virtual displacement

Using this principle the following relationship can be derived:

$$[K^e] = \int [B]^T [D] [B] \, d(vol.) \qquad\qquad \text{Eq. (4.5)}$$

Where d(vol.) is the incremental volume. $[B]$ and $[D]$ are known hence by integrating over the volume, $[K^e]$ can be determined. The nodal displacements are then calculated from Equation 4.1.

7)   **Evaluate stresses**:

Stresses within an element can then be obtained by:

$$\sigma = [D] [B] [\delta^e] \qquad\qquad \text{Eq. (4.6)}$$

The steps outlined above are performed on the computer in a linear fashion, ie. all relationships are linear in nature. Therefore non-linear material properties, boundary conditions or geometric conditions require an incremental-iterative approach.

4.2.3 Non-linear analysis

In this study, slipping interface conditions and the modelling of time dependent strain in the bone cement require a **non-linear** approach. In a non-linear system, the relationship between the applied force matrix and the nodal displacement matrix (Equation 4.1) is no

longer linear, as the global stiffness matrix is not constant. Consider Figure 4.1, which shows a non-linear relationship between load and displacement. The total load is applied in steps or increments. For each increment of load, an iterative process is performed until a specified convergence criterion is reached. The stiffness matrix $[K^e]$ does not remain constant in creep studies, and for sliding interfaces, small displacement theory no longer holds, hence a tangent modulus approach to specify $[K^e]$ was adopted. This approach is summarised below for a particular load increment, referring to Figure 4.1.
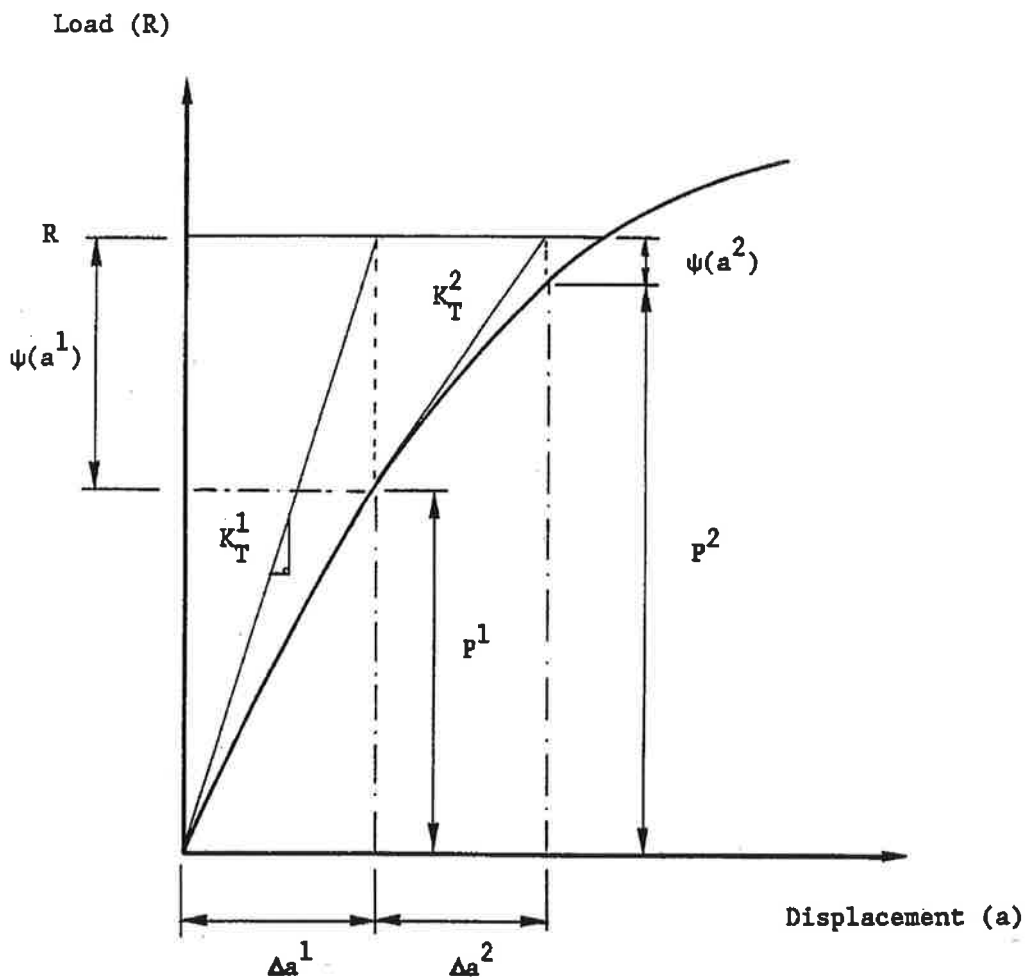
Figure 4.1: Non-linear Force-Displacement diagram. *After LUSAS user manual (1990).*

For a given load increment R, if a significant degree of non-linearity occurs during the load step, the stresses integrated through the volume of the structure will not satisfy equilibrium with external forces, leaving a residual force vector $\psi(a^1)$ where the superscript refers to iteration 1. A correction procedure is then needed to restore equilibrium. $\psi(a^1)$ is subtracted

from R at the point where the tangent modulus K_T^1 intersects the line Load = R (Figure 4.1). The next iteration is then performed by assuming a stiffness of K_T^2 and subtracting the residual force vector $\psi(a^2)$, to obtain the next location on the curve. This process continues until a specified convergence criteria has been satisfied. This criteria can be in the form of stating that the ratio of the residual to the total force must be below a certain value ie. 0.01. Other convergence criteria may be specified. ie the residual work as a percentage of the total work must be below a certain value. Once convergence has been obtained the next increment of load is added and this continues until the entire load is applied. The choice of load increment is problem dependent and is highly influenced by the degree of non-linearity.

The above description is known as the Newton-Raphson procedure and was used in this study, although other methods of non-linear analysis are available. For sliding interface conditions the load was incremented in force steps and for the creep models, time steps were applied until the total response time was reached.

4.3 Model properties

4.3.1 General description

In order to construct a finite element model the following information is needed:

- System geometry

- Loading

- Material Properties

- Boundary Conditions

-Interface Conditions

As was stated in Chapter Two, a sheep hip joint was modelled in this study as it has been noted that similar post-operative changes occur in the sheep femur when compared to the human femur and the orientation of the femur load is also similar (Bergmann *et al.* 1984).

The actual values used to define the model properties are now detailed.

4.3.2 System geometry

The geometry used to construct the finite element mesh was obtained in the following manner. A cemented prosthesis was inserted into the left femoral canal of a 65 kg live Merino adult sheep. The sheep was then sacrificed and the prosthesis removed leaving the cement mantle intact. CT scans of the femur were then taken. In this study, two dimensional sections were obtained at 10 mm intervals along the femur, from the knee level to the most proximal section of the femur. A typical CT scan section of the sheep femur is shown in Figure 4.2.

bone cement

gap caused by air entrainment

gap caused by prosthesis

cortical bone
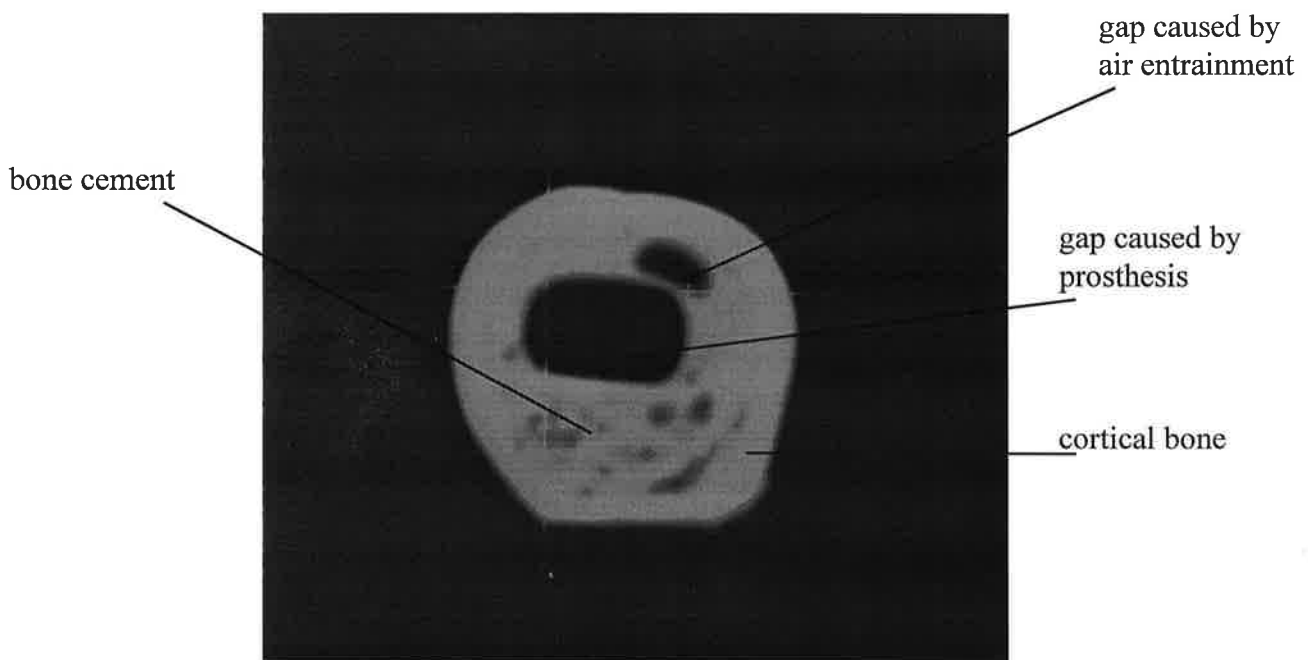
Figure 4.2: A typical CT scan section of a sheep femur.

It was initially hoped to construct a full anatomical model, however convergence problems for the non-linear analyses and excessive computer time (Section 4.5.4) disallowed the use of this model due to the number of nodes required. Hence, a quasi-anatomical model was

produced, which represented the main geometric features of a sheep cemented total hip replacement. The final three dimensional finite element model was constructed by joining two dimensional planer sections, obtained from the CT scans taken from the sheep femur. For the quasi-anatomical model, the three dimensional geometry was obtained by joining six distinct sections which are representative of the main geometric features of the prosthetic femur. The six sections are shown in Figure 4.3 with level numbers for reference. The reference axes orientation are also shown. The z-axis is in the direction of the line of femur and the xy plane contains the two dimensional sections. Coordinate (0,0,0) is the centre of Level 0. The x-axis is in the lateral-medial direction with the positive axis directed laterally. The y-axis is in the anterior-posterior direction with the positive axis directed anteriorly. The z-axis is in the distal-proximal direction with the positive axis directed proximally.

Level 0: (z = 0)

This is the most distal part of the model and contains only cortical bone. The section at Level 0 is shown in Figure 4.4. The entire femur was not modelled and Level 0 represents the "cut-off" section. This section is approximately 50 mm proximal to the bottom of the femur (femoral condyles), and is the base reference level for the model. It was reasonable to use a "cut-off" section as the stresses in the very distal section of the femur were not of interest in this study. At Level 0, the section was restrained from moving (see Section 4.3.5) whereas *in vivo* restraint occurs at the knee. Restraint at Level 0 did not unduly influence the peak stresses in the cement mantle, (see Section 5.8.2). Referring to Figure 4.4, the outer diameter of the bone is 21 mm and the inner diameter 14 mm. The thickness of the cortical shell at this level was therefore 3.5 mm. The section was composed of eight surfaces and it was these surfaces which were used to construct the 3D volumes.

PROXIMAL

Level 5

Level 4

Level 3

MEDIAL   LATERAL

Level 2

Level 1

DISTAL   Level 0
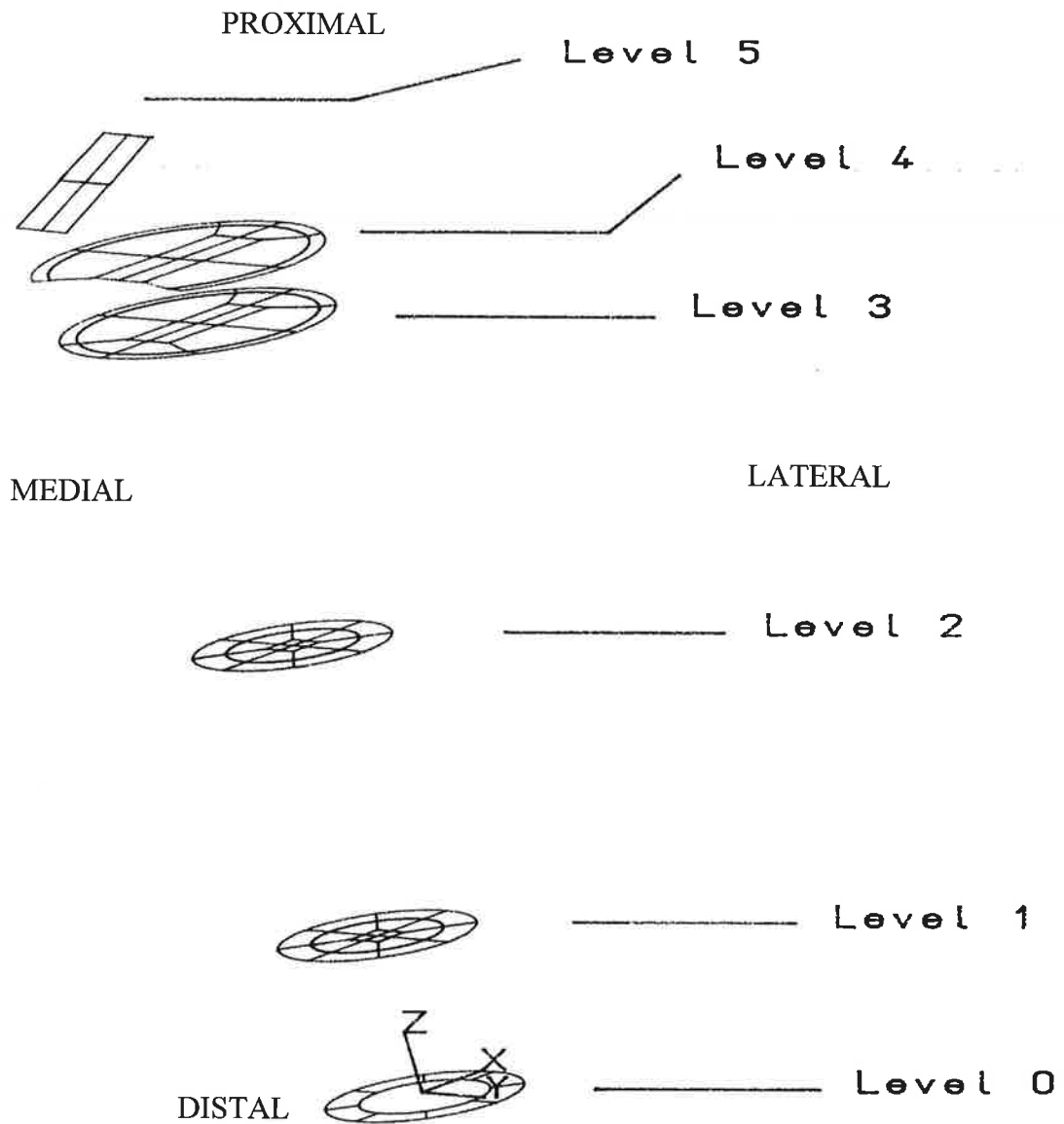
Figure 4.3: The two dimensional sections used to construct the three dimensional model

Level 1: (z = 25 mm)

At a level 25 mm proximal to the base level a second section was defined. This section was distinct because it contained the base of the cement mantle. This section is shown in Figure 4.5. It was assumed that the bone geometry was the same as for Level 0 ie. outer diameter = 21 mm, inner diameter = 14 mm. At this section, twelve cement surfaces were also defined.
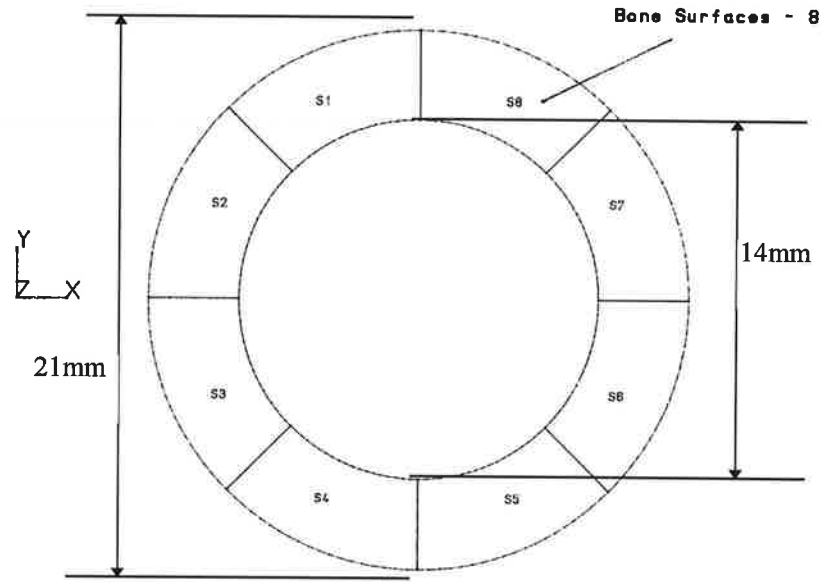
Figure 4.4: The two dimensional sections defined at Level 0
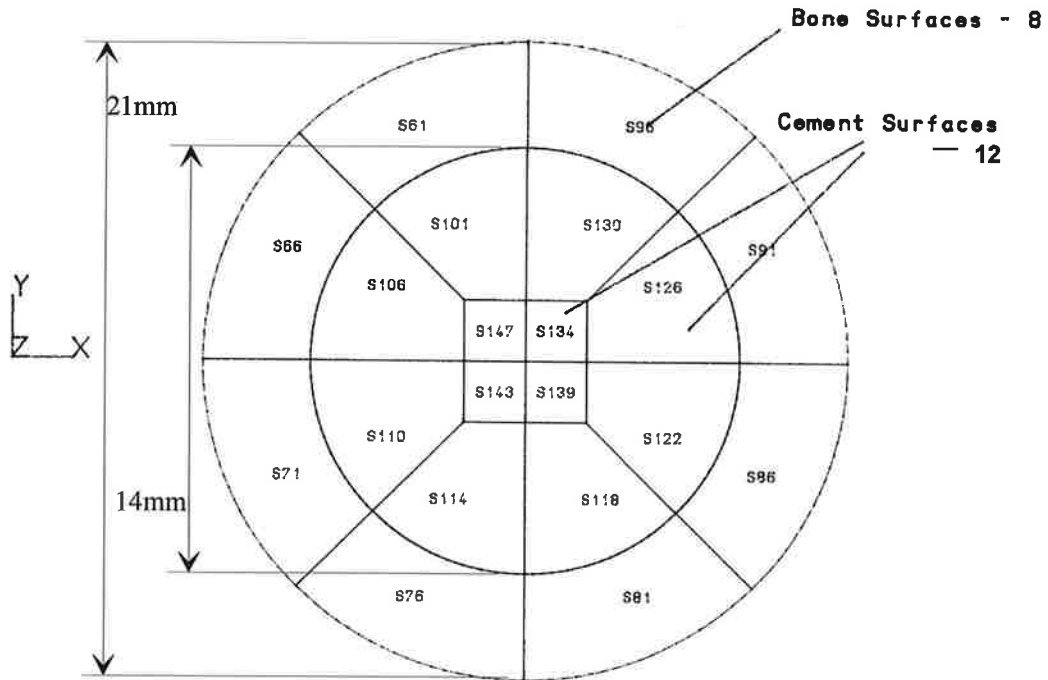
Figure 4.5: The two dimensional sections defined at Level 1.

68

Volumes: Level 0 - Level 1

Eight volumes of cortical bone were created by joining the bone sections from Level 0 and Level 1. These volumes are shown in Figure 4.6. The surfaces at different levels were joined by straight lines.
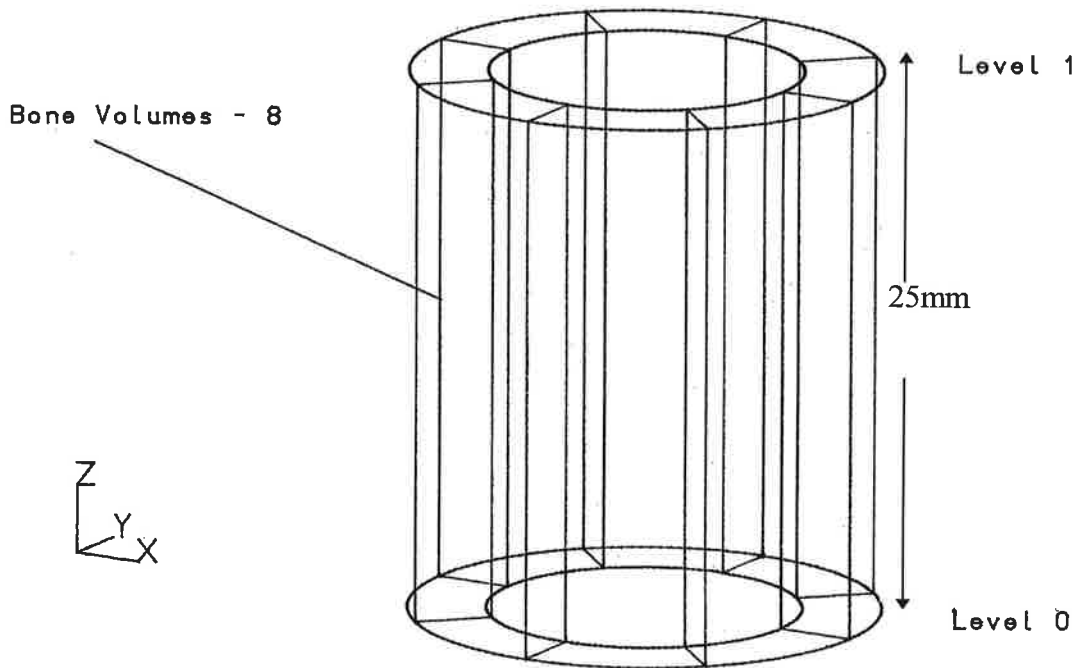
Figure 4.6: Cortical bone volumes defined from joining Levels 0 and 1

Level 2: (z = 70 mm)

At this level the base or tip of the prosthesis was situated. The section at Level 2 is shown in Figure 4.7. The inner and outer diameter of bone was taken to be the same as for Levels 0 and 1. The prosthesis was taken as rectangular in section with the tip having dimensions 4 x 4 mm. Figure 4.7 shows the inner four prosthesis surfaces, eight cement surfaces and eight bone surfaces.
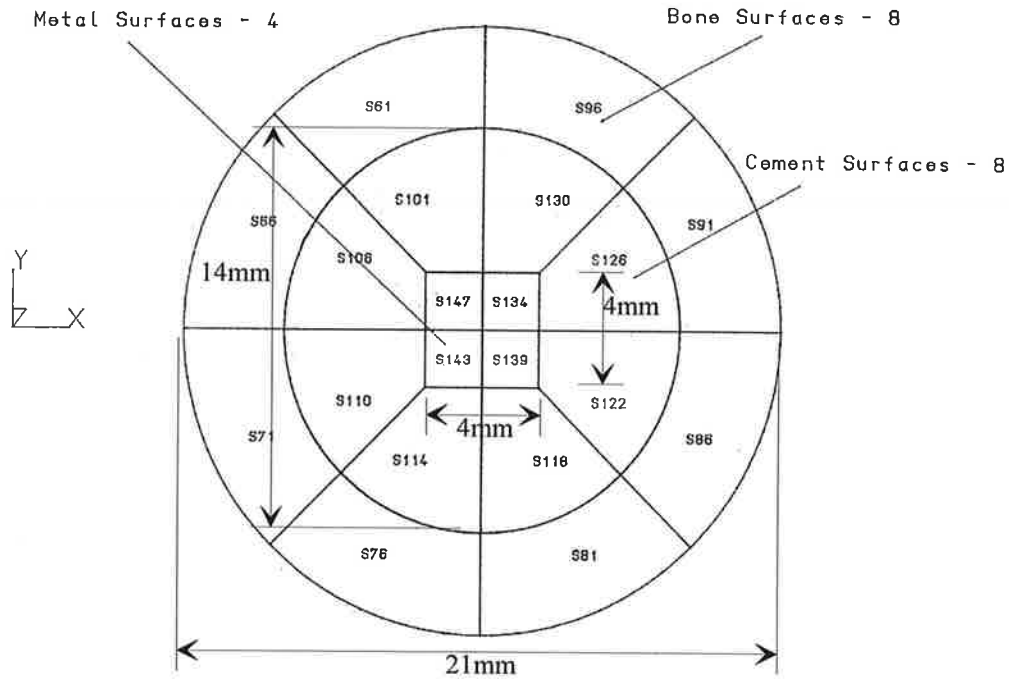
Figure 4.7: The two dimensional sections defined at Level 2

Volumes: Level 1 - Level 2

Eight volumes of cortical bone were formed and twelve volumes of cement by joining surfaces from Level 1 and Level 2.

Level 3: (z = 120 mm)

At this level the thickness of cortical bone decreased and the diameter of the section increased. Inner bone diameter = 22 mm, outer diameter = 25.5 mm, therefore the thickness of cortical bone at this level was 1.75 mm. The prosthesis has sectional dimensions 15 x 6 mm at this level. The sectional details are shown in Figure 4.8. This level also represented the uppermost level for two medial bone sections and two cement sections.
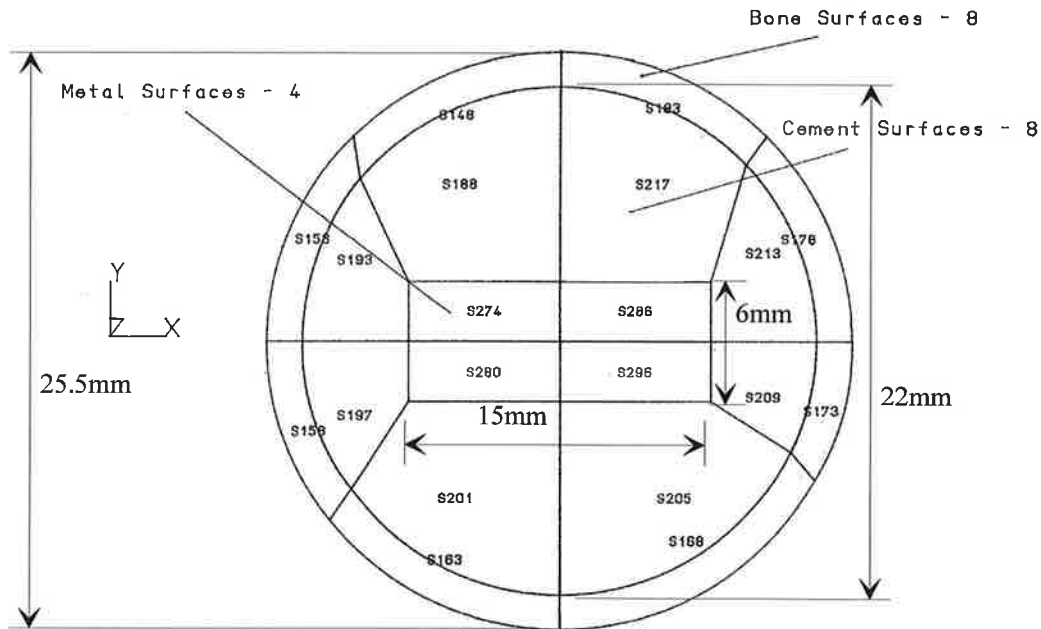
Figure 4.8: The two dimensional sections defined at Level 3

Volumes: Level 2 - Level 3

Eight volumes of cortical bone, eight volumes of cement, and four volumes of prosthesis were defined by joining surfaces from Level 2 and Level 3. The volumes were formed by connecting the surfaces with straight lines. The expansion of medullary canal was therefore modelled as linear, as was the thinning of the cortical shell. The resulting structure was a tapered steel rectangular section inside an expanding bony cylinder interdisposed with cement.

Level 4: (z = 130 mm)

The section at Level 4 is shown in Figure 4.9. The circular section was not complete due to the discontinuity of the two bone and cement sections at Level 3. This was to model the line of amputation through the neck of femur. In reality the line of cut will leave an exposed bone surface at approximately 45 to the femoral axis, as shown in Figure 1.3. In this study however a "step" was modelled. This was necessary for continuity of the intersecting volumes. This "step" is shown in Figure 4.10. The inner diameter of bone at this section was 23.6 mm and the outer diameter was 27.1 mm with the thickness of

cortical shell the same as for Level 3, ie. 1.75 mm. The prosthesis has sectional dimensions 18 x 7.2 mm. Level 4 also signified the upper end of the bone and cement sections.
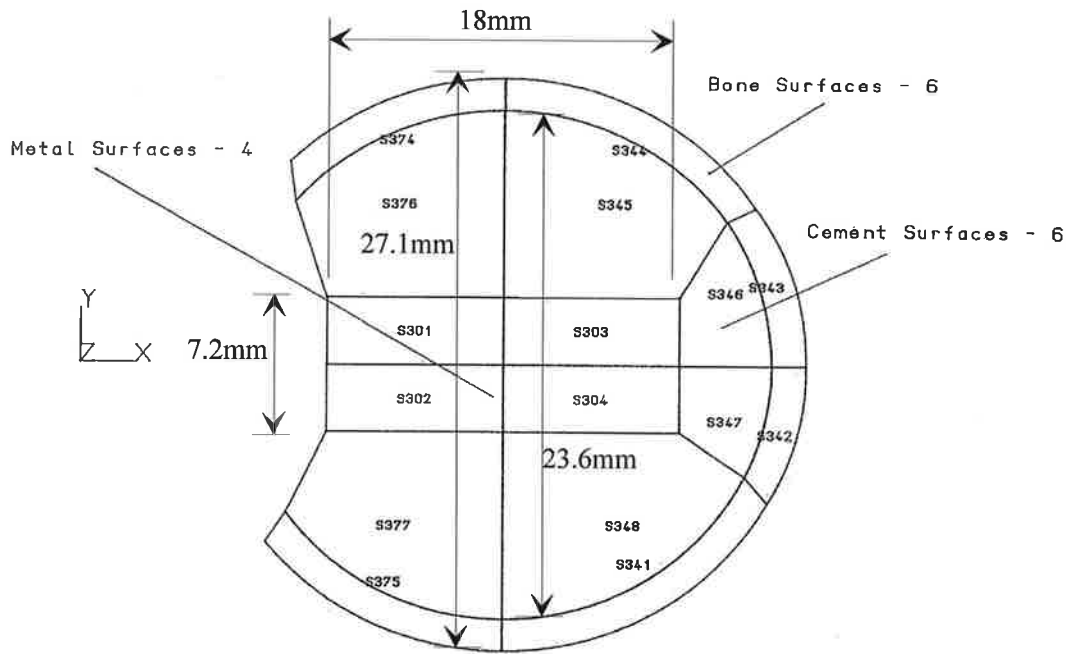
Figure 4.9: The two dimensional surfaces defined at Level 4

Volumes: Level 3 - Level 4

Six volumes of cortical bone, six volumes of cement, and four volumes of prosthesis were formed by joining the surfaces of Level 3 and Level 4. These volumes are displayed in Figure 4.10.
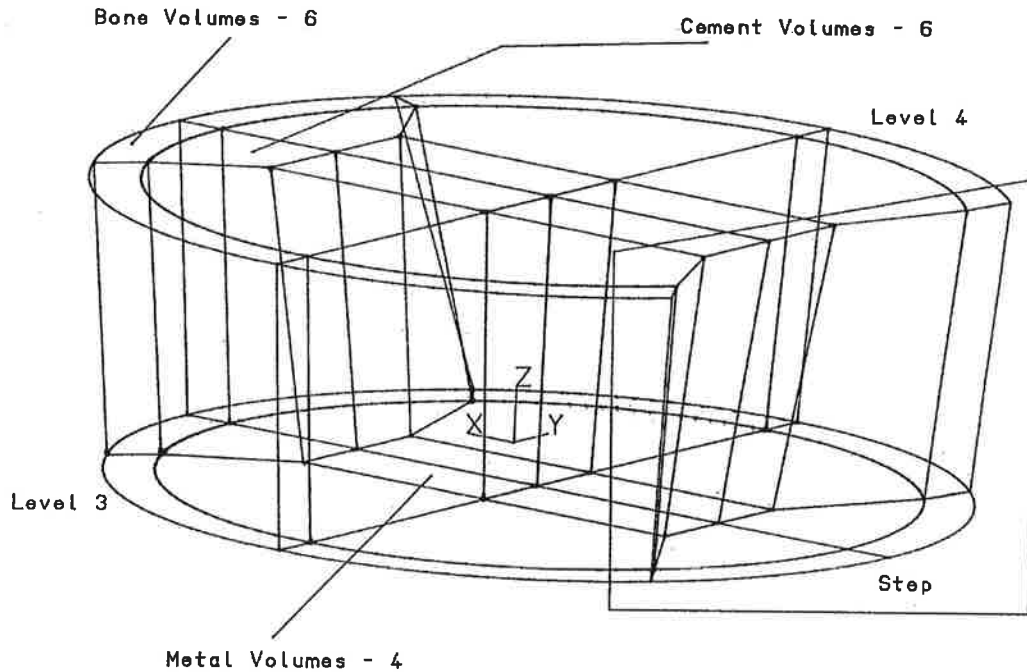
Figure 4.10: Volumes defined by joining Levels 3 and 4. Note the "step" present to model the line of amputation.

Level 5: (z = 143 mm)

This level contains four prosthesis surfaces only. *In vivo* the prosthesis forms a "ball" section to fit into the acetabulum. In this study the stresses in the prosthesis itself were not of interest and a simplification was made in the region of the prosthesis outside the femur. The surfaces were defined at Level 5 to contain a point approximately coincident with the centre of the prosthesis head, and it is through this point that the load was applied. The Level 5 surfaces were formed by sweeping the Level 4 prosthesis surfaces through an angle of 27° in the xz plane, centre (-33,0,120). The dimensions of this surface were the same as for Level 4, ie. 18 x 7.2 mm. Sectional details are shown in Figure 4.11.

Volumes: Level 4 to Level 5

Four volumes of prosthesis were formed by sweeping the Level 4 prosthesis surfaces to create a "neck" of the prosthesis. These volumes are shown in Figure 4.12.
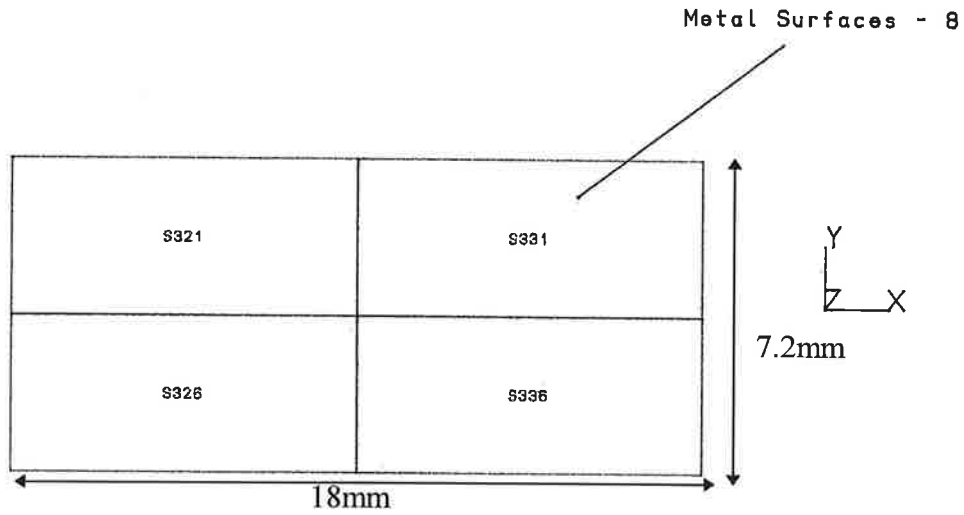
Figure 4.11: The two dimensional surfaces defined at Level 5

Overall Geometry:

The completed model with all volumes constructed is shown in Figure 4.13. It is restated that this is a quasi-anatomical, simplified model of a true cemented THR system.
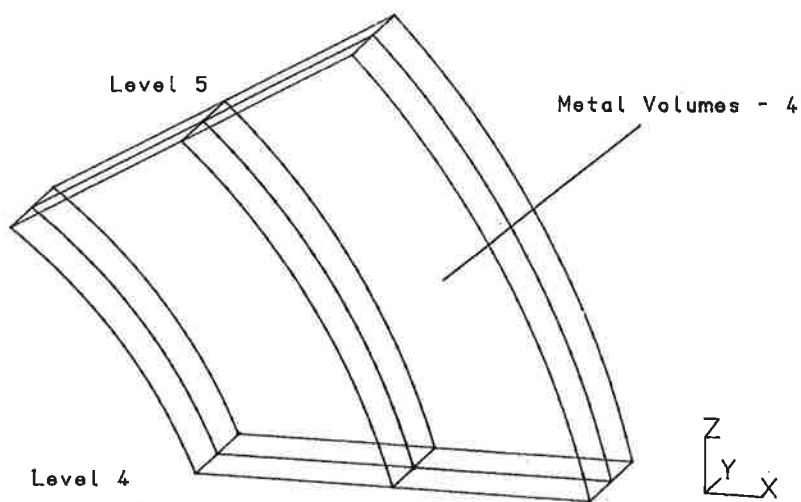
Figure 4.12: Volumes of prosthesis between levels 4 and 5
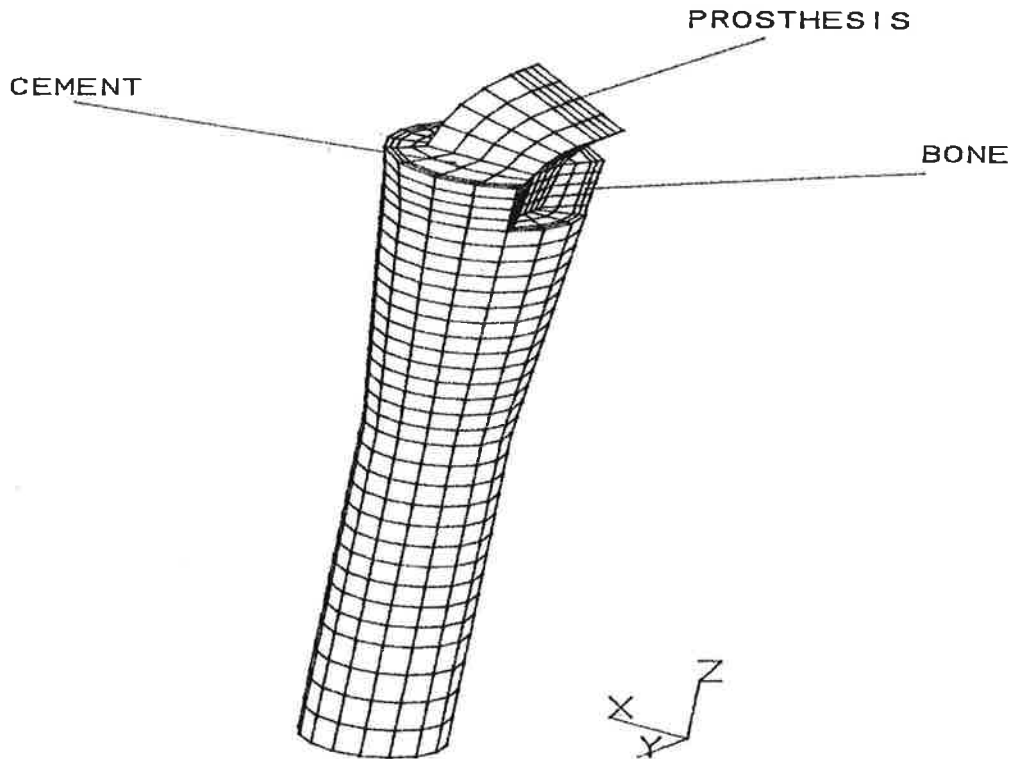
Figure 4.13: Full geometric view of system geometry

The prosthesis stem itself however was quite representative of actual dimensions with sectional properties taken from design drawings, which show the rectangular section and the double taper of stem. The true prosthesis does not contain sharp corners, ie it is not a true rectangular section, however in the present work, it was modelled as a rectangular section. The mesh density required to accurately model the small radii of the prosthesis section "corners" would have led to unreasonable computer expense. The head or ball of the prosthesis was not modelled because it was not in the region of interest. Design drawings of the prosthesis are shown in Figure 4.14. It is restated here that qualitative trends were of greatest importance in this study, and it is the comparison of models with parameter variation which was of greater interest than quantitative data. Bearing this in mind, the geometric simplifications appear reasonable.

(a) xz plane   (b) yz plane
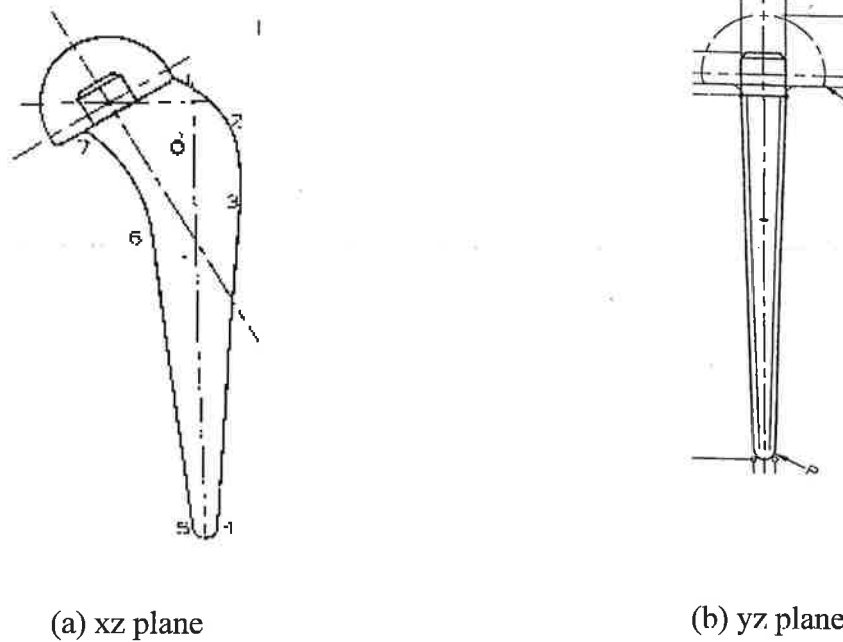
Figure 4.14: Prosthesis design drawings in the xz and yz planes. Not to scale.

4.3.3 Loading

4.3.3.1 Derivation of the resultant load

As stated in the introduction, the loading which acts on the prosthesis head was defined by a resultant force with **magnitude** and **direction**. It was also seen in the literature review that a variety of methods can be adopted to determine this resultant load. For this work, the load was determined using the methods of Lanyon *et al.* (1981). The loads determined in this study were for sheep walking at 1 ms^{-1}.

The mass of the sheep used in this study was 65 kg. Based on the study of Lanyon *et al.*, the load representative of this mass is:

$$R = 460 \text{ N}, \alpha_1 = 35^\circ, \alpha_2 = 20^\circ$$

Where, R is the resultant force, α_1 and α_2 are defined by referring to Figure 4.15. The line of action is taken to act through the centre of the prosthesis head.
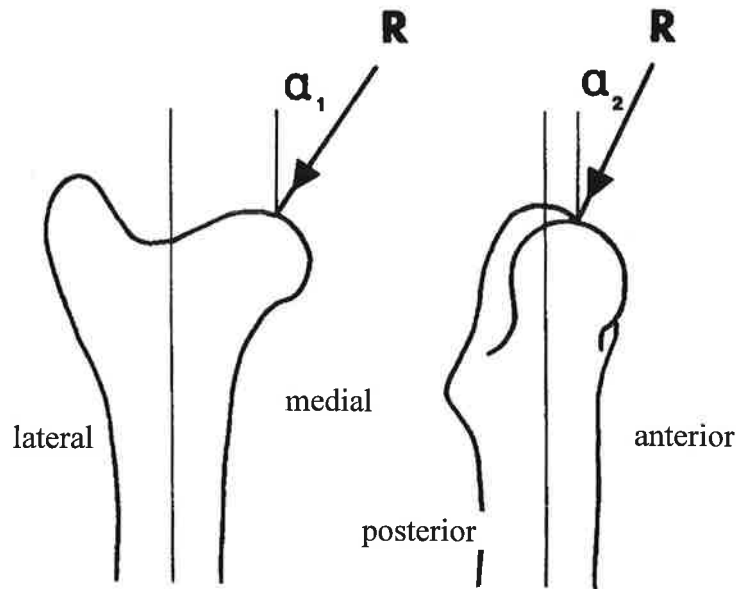
Figure 4.15: Tracings of the proximal end of a sheep's femur in the anteroposterior and lateral projections, showing the directions of the resultant force, R, on the femoral head measured as the angles between the resultant force and the long axis of the femur in the frontal (α_1) and the sagittal (α_2) planes.(After Lanyon *et al.* 1981). Note: In the present study the frontal plane is the xz plane and the sagittal plane is the yz plane.

In order to apply this resultant force, R, in the finite element model, the resultant, R, had to be broken into three orthogonal x, y, and z components. The derivation of these components is shown below.

A force cube is drawn containing the resultant force R, Figure 4.16.
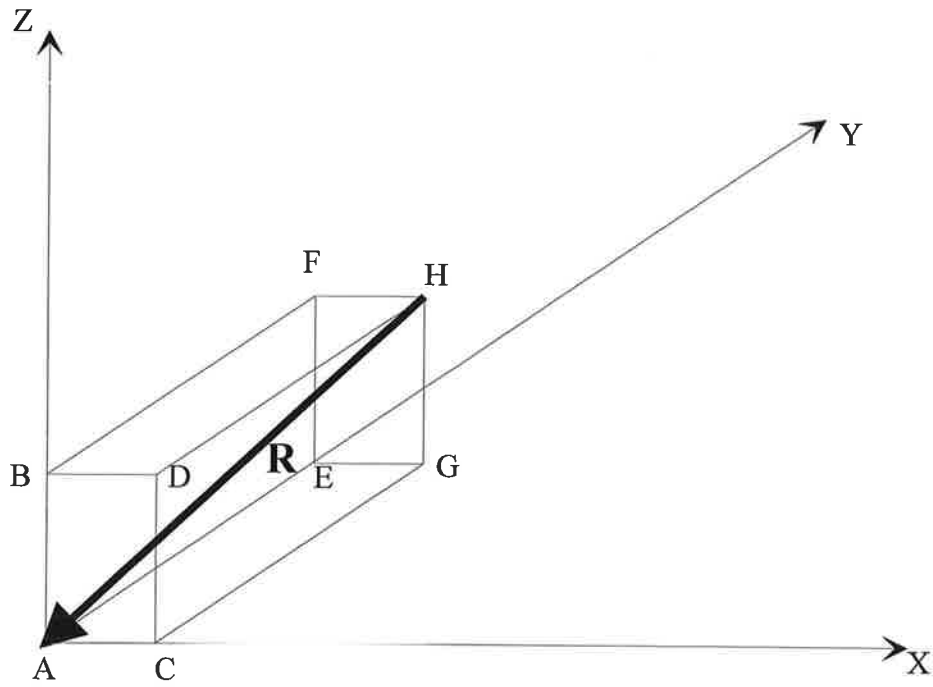
Figure 4.16: A force cube for the resultant hip joint force R

Projections of R onto the xz and yz planes are then considered in Figures 4.17 and 4.18:
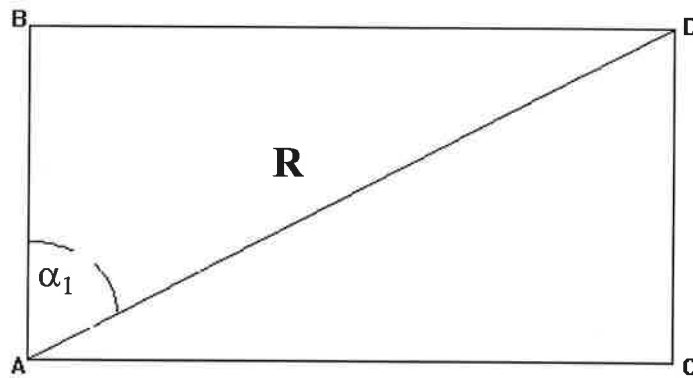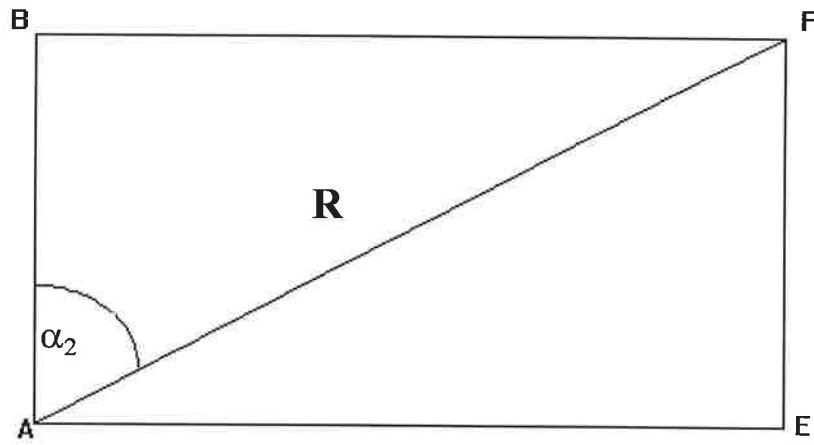

Figure 4.17: Projection of R onto xz plane

Figure 4.18: Projection of R onto the yz plane

The angle $\angle ABD$ is equal to $35°$ and the angle $\angle BAF$ is equal to $20°$.

Now, $$AD\cos\alpha_1 = AF\cos\alpha_2$$ Eq. (4.7)
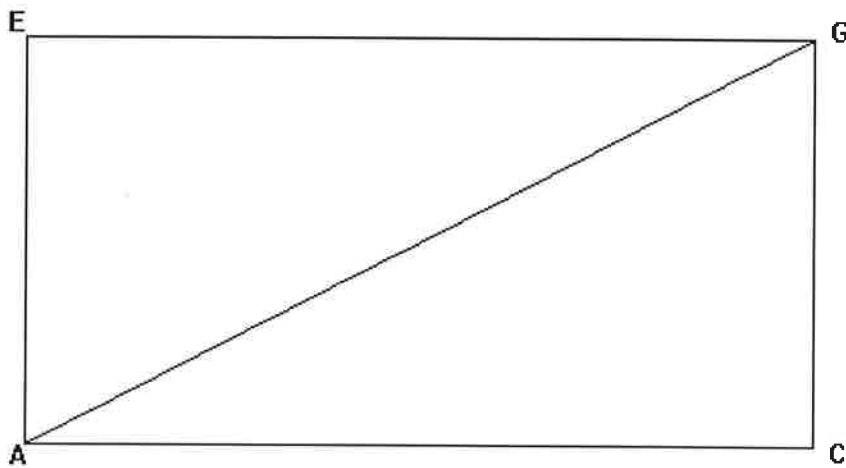
Next the xy plane is considered in Figure 4.19.

Figure 4.19: The xy plane of the force cube

$$AG = \sqrt{AE^2 + EG^2}$$ Eq. (4.8)

Now, $AE = AF\sin\alpha_2$ and $EG = BD = AD\sin\alpha_1$.

therefore

$$AG = \sqrt{\left(AD\sin\alpha_1\right)^2 + \left(AF\sin\alpha_2\right)^2}$$

Eq. (4.9)

Now, consider the triangle $\triangle AGH$ in Figure 4.20:
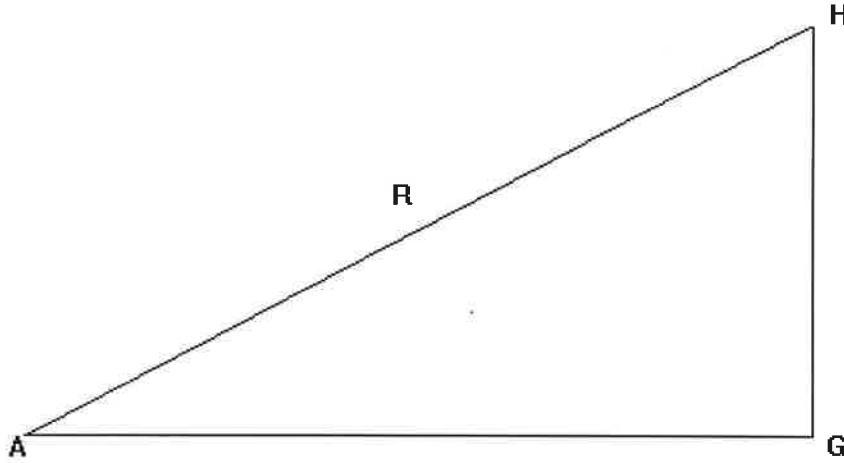
Figure 4.20: The force triangle $\triangle AGH$.

Now, $R = \sqrt{AG^2 + GH^2}$

Eq. (4.10)

Where $GH = AD\cos\alpha_1$

Combining Equations 4.9 and 4.10 and considering **R = 460 N, $\alpha_1 = 35^0$, $\alpha_2 = 20^0$**

$$212 \times 10^3 = \left(AD^2 \times 0.33\right) + \left(AF^2 \times 0.117\right) + \left(AD^2 \times 0.671\right)$$

Now, $AD = \left(0.940 \, / \, 0.819\right) \times AF$ from Eq. 4.7

Therefore   AD = 441.0 N and AF = 384.2 N

Now,   BD = $AD\sin\alpha_1$, AB = $AF\cos\alpha_2$, BF = $AF\sin\alpha_2$

Therefore   BD = 253.1 N,   AB = 361.2 N   BF = 131.4 N.

In terms of anatomical directions,

In the femoral or axial direction, **Fz = -361.2 N**

In the posterior direction, **Fy = 131.4 N**

In the lateral direction, **Fx = 253.1 N**

Note the signs of these component forces. The positive direction of the three system axes are shown in Figure 4.21, along with the loading point location, which is located at coordinate   **(-14, 0, 143).**
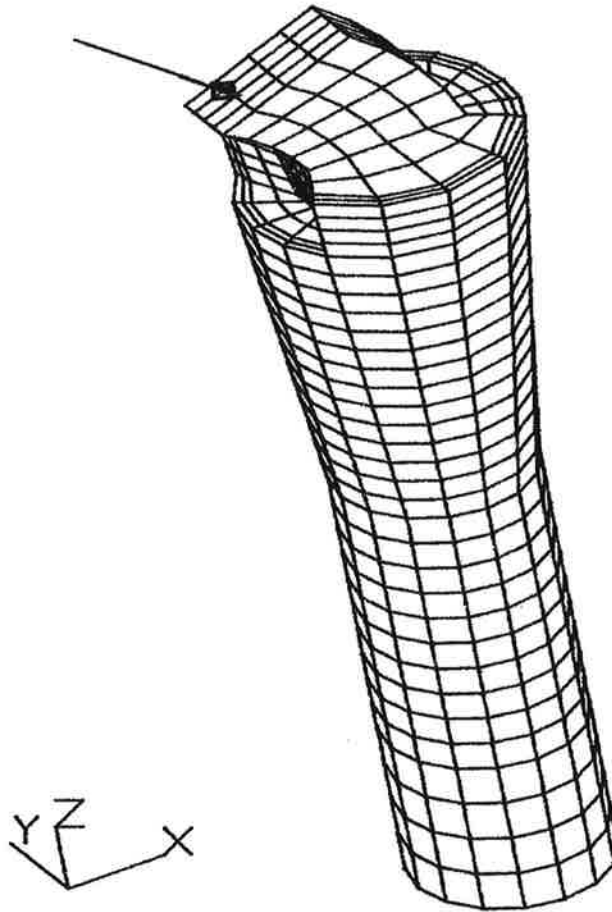

Figure 4.21: The resultant load orientation and location. The axes shown are in the positive direction.

Two loading configurations were modelled.

1. Instantaneous static loading.

2. Loading with creep properties of the bone cement included.

4.3.3.2 Time dependent loading

For time dependant or creep loading, the applied loading pattern as a function of time must be considered. Bergmann *et al.* (1984) showed by measuring applied hip joint forces *in vivo,* that the applied loading pattern during gait is cyclic. It can be shown (McKellop *et al.* 1994), that the total strain (elastic and creep) produced by a number of cyclic load cycles over a certain time period, is equivalent to the strain caused by a constant load applied for the equivalent time, plus the elastic strain due to the remainder of the load applied instantaneously at the end of the loading period.

By observing the cyclic load pattern of sheep walking at 2.5 km/h^{-1}, Bergmann *et al.* (1984) noted a sinusoidal pattern. For this pattern to be simulated, half the peak load is applied until the creep response is obtained (in this study the loading time was four hours), then the remainder of the load is applied instantaneously (McKellop *et al.* 1994).

It must be noted that the application of a single load at one node in the model is a simplification. In reality, the abductor muscles, such as the gluteus medius and gluteus maximus (attachment to femur shown in Figure 1.3) and other muscles will act during gait, altering the resultant stress distribution. *The force applied in this study was a resultant of all forces acting on the femur applied at one location.* However, since this study aimed to compare general trends due to parameter variation, the assumption of applying a resultant load at one point was valid.

4.3.4 Material properties

4.3.4.1 The prosthesis

The prosthesis material was stainless steel with the following mechanical properties.

Young's modulus, $E = 200 \times 10^3$ MPa

Poisson's Ration, $\nu = 0.3$

4.3.4.2 The bone cement

One of the parameter variations considered in this study was the inclusion of creep of the bone cement, therefore both elastic and viscoelastic properties had to be specified. From the literature review, and the following values were chosen, based on the work of Saha and Pal (1984).

Young's modulus, $E = 2.1 \times 10^3$ MPa

Poisson's Ratio, $\nu = 0.3$

The creep strain is a function of uniaxial stress and time. A power law, which has been shown to adequately describe the viscoelastic behaviour of bone cement, was used to define the creep strain (McKellop *et al.* 1989):

$$\varepsilon_{cr} = \frac{\sigma^{1.55} t^{0.10}}{45,997} \qquad \text{Eq. (4.11)}$$

Where, ε_{cr} is the creep strain

σ is the instantaneous uniaxial stress, with units MPa.

t is time, with units seconds.

The bone cement is assumed to be homogeneous and isotropic.

4.3.4.3 The bone

It was initially hoped to include both cancellous and cortical bone in a full anatomical model, however as has been previously stated convergence difficulties required that a quasi-anatomical model be used. In the sheep femur there is far less cancellous bone than

for the human femur and in the present simplified model only cortical bone was considered. It is the cortical bone which is of interest in resorption of the proximal calcar. Various measurements of the Young's modulus of cortical bone are presented in Table 4.1 below.

Table 4.1: Mechanical properties of cortical bone

Author	E (GPa)	Comments
McElhaney *et al.* (1964)	24.1	Compression test strain rate = 0.1/sec
Simkin and Robin (1973)	23.8	tension test low strain rate
Burstein *et al.* (1972)	24.5	tension test 0.1/sec
Reilly and Burstein (1975)	17.0	tension and compression 0.02-0.05/sec
Bonfield and Datta (1974)	27.3	bovine bone, tension, strain gauge used. strain rate = 3×10^{-4}/sec
Reilly *et al.* (1974)	17.1	tension and compression strain rate = 0.05/sec
Lanyon *et al.* (1979)	18.2	four point bending test, sheep
Schaffler and Burr (1988)	21.8	steer, tension 0.01, 0.03/sec
Keller *et al.* (1990)	12.1	4 point bending, 0.05/sec, high porosity

A thorough review of the mechanical properties of cortical bone used in other finite element models (as reviewed in Chapter Three) was also carried out.

The mechanical properties of cortical bone used in this study were based on Reilly and Burstein (1975) who tested cortical bone under physiological conditions. The values used were:

Young's modulus, $E = 17.0 \times 10^3$ MPa

Poisson's Ration, $\nu = 0.3$

Although Lanyon *et al.* (1979) tested sheep bone which may seem more appropriate for this study, it is doubtful whether a four point bending test would provide sufficiently accurate results.

4.3.5 Boundary conditions

It was the stress and strain distribution in the proximal femur and in the cement mantle which were of interest in this study. Therefore it was unnecessary to model the entire femur as this would lead to excessive computation time and an excess of unwanted results. The femur was modelled down to Level 0 and at this level displacements of all points were restrained in all directions (x, y, z). The hypothesis that restraining the femur at this level instead of at knee level would not unduly affect the critical stresses was verified. A linear analysis was conducted with the femur restrained at knee level (Section 5.8.2), and it was found that the difference in the critical cement stresses was minimal (no change proximally, and 0.7 % increase distally) between the knee restraint analysis and an analysis conducted with restraint at Level 0.

4.3.6 Interface conditions

As was seen in Section 4.3.2, the three structural materials form two interfaces, a bone-cement interface and a stem-cement interface.

4.3.6.1 Bone-cement interface

The bone-cement interface is critical in correctly transferring load from the prosthesis to the bone. It is the breakdown of this interface which ultimately presents as failure in a Total Hip Replacement system, although, initiating events may occur elsewhere (Jasty *et al.* 1991). It was assumed that this bond was fully intact due to mechanical interlocking between bone cavities and the cured cement, ie. the strain is uniform across the interface. There will be stress discontinuity across the interface, however due to the large difference

in stiffness (one order of magnitude) between cement and bone. In tests of the bone-cement interface strength (Kusleika and Stupp 1983) the bond strength (7.5 MPa in tension) was not exceeded by cement stress levels found in this study hence the assumption of an intact bone-cement interface was valid.

4.3.6.2 Stem-cement interface

Three separate conditions were modelled at this interface:

1)   Fully bonded: It has been stated that the bone cement is not an adhesive or glue that will "stick" to the prosthesis, and any bond that is present is due to mechanical interlocking. A prosthesis with machined grooves or one that is precoated with cement could allow a full bond initially, although the long term integrity of this bond *in vivo* is doubtful. A fully bonded interface was modelled in an identical fashion to the bone-cement interface, ie strain continuity is assumed across the interface and all shear and bending stresses are transferred across the interface without "slip".

2)   Frictional interface: If the prosthesis has a polished or even a rough surface the prosthesis will slip with friction in the cement mantle. There will now be strain discontinuity at the interface and stress transfer from the prosthesis to the cement occurs by way of normal stresses and frictional shear stresses. The coefficient of friction for the stem-cement interface *in vivo* is unclear however a coefficient of friction of 0.22 was assumed in this study to compare results with two similar studies in which this coefficient was also used (McKellop *et al.* 1994; Saligrama *et al.* 1996). This friction coefficient is representative of a polished prosthesis interface.

3)   Frictionless interface: If the prosthesis has a highly polished surface, sliding will occur without significant friction. For a frictionless interface no frictional shear stress is transferred and load transfer is perpendicular to the interface only, ie. by normal load transfer. A coefficient of friction of 0.0 was used to represent the frictionless interface.

4.4 Construction of the finite element model

After the model properties were defined, they were assigned to the model. It was shown that the model consists of volumes of the different materials. To each of these volumes, a mesh density and appropriate model parameters were assigned. The mesh density is the number of elements per volume.

4.4.1 The finite element mesh

Each volume was assigned an element type and an element density. The finite element model was three dimensional and as such, hexahedral elements were used. Various hexahedral elements are available from the LUSAS finite element library (LUSAS user manual 1990). The choice was between an eight node, constant strain element; an eight node modified strain element and a twenty node linear strain element. These elements are shown in Figure 4.22. The twenty node linear strain element provides a more accurate solution for the same number of elements as the strain varies linearly across the element. The expense or computer time is increased, however, due to the increased number of nodes. Three equations are required for each node and the greater the number of nodes, the more simultaneous equations which are required to invert the global stiffness matrix (Equation 4.1). The use of sliding interfaces in the LUSAS/MYSTRO programme precluded the use of the twenty node linear strain element and the eight node modified strain element was chosen. This modified element provides a more accurate solution than the standard constant strain element for only a small increase in computer time (Simo and Rifai 1990).

An element density was also prescribed. One of the governing factors in determining element density is the aspect ratio. Large length ratios of adjacent sides of an element should be avoided as the solution can be distorted. In this study, for the twelve standard analyses, a total of 2825 nodes for the linear analyses and 3126 nodes for the non-linear analyses were used. The averaged element density for the entire system was 45.5 elements/cm^3.
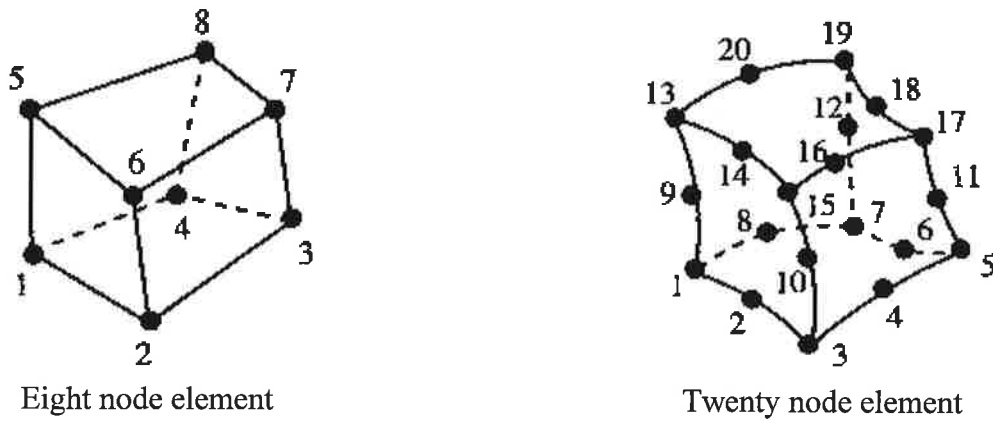
Eight node element   Twenty node element

Figure 4.22: The eight and twenty node element available in the LUSAS finite element library. After LUSAS user manual 1990.

4.4.2 Assigning the model properties

The various model parameters such as mechanical properties, loading, boundary and interface conditions were assigned to the elements comprising the finite element mesh.

4.4.2.1 Material properties

The mechanical properties outlined in Section 4.3.4 were assigned to the appropriate volumes defined in Section 4.3.2. Viscoelastic properties of the bone cement were only assigned to the cement volumes in the time dependent analyses.

4.4.2.2 Loading

The derived resultant load prescribed in Section 4.3.3.1 was applied at a node with the coordinates (-14,0,143). For the time dependent analyses one half of this load was applied for four hours and then the remainder of the load was applied instantaneously. It was noted from a previous study (McKellop *et al.* 1994) that the majority of cement stress relaxation had occurred in the first four hours and the analyses were terminated after this time to

minimise computer analysis time (Section 4.5.4). The effect of extended creep was also considered.

For the non-linear analyses, the load was applied in increments using an automatic procedure. The load was applied in increments, with the magnitude of a subsequent load step being dependent on the convergence history of the previous load step. For example, if the second load step converged quickly ie. in four iterations, the third load step was increased in magnitude. If the load step did not converge quickly, ie twenty iterations, the third load step was reduced in magnitude to account for the higher degree of non-linearity. This procedure led to a more efficient acquisition of the solution.

4.4.2.3 Boundary conditions

It was stated in Section 4.3.5 that the femur was restrained at Level 0. This boundary condition was applied to the model by assigning a condition of zero displacement in the x, y, and z directions for all the nodes which were located at Level 0 (ie z = 0).

4.4.2.4 Interface conditions

The bone-cement interface required only one set of nodes to define its continuous strain behaviour. For the case of a fully bonded stem-cement interface, only one set of nodes was defined at the interface which linked the cement and prosthesis. The strain was therefore continuous across the interface. For the sliding interfaces, however, two sets of nodes must be assigned to the stem-cement interface. One set of nodes belonged to the cement elements and the other set of nodes belongs to the adjacent stem elements. The nodes were geometrically coincident representing the condition of initial contact. The sliding behaviour of the stem-cement interface was modelled by assigning slidelines. A slideline governs the mechanical behaviour of the interface and allows equations to be set up between the coincident nodes defining their interrelationship under applied load. (LUSAS user manual 1990). The coefficient of friction was also assigned to the slideline. For the coefficient of friction of 0.22, load transfer across the interface was by both normal forces and frictional shear, and for the zero coefficient of friction load transfer was by normal forces only.

4.4.2.5 The distal air-gap

It was noted in the literature review that some designers encourage distal subsidence of the prosthesis to utilise wedge action. It is believed that this distal subsidence can be further facilitated by the employment of an air-gap underneath the prosthesis tip, thus removing the bearing resistance of the distal bone cement. An air-gap was modelled in the present study by assigning all elements contained within a 4x4x20 mm volume underneath the prosthesis tip (Level 2) a very low stiffness (10 MPa). A plastic centraliser is used to create this air-gap in the cement mantle.

4.5 The analyses

4.5.1 The twelve standard analyses

Twelve separate analyses were considered in order to study the parameter variation. The model descriptions are summarised in Table 4.2, with Case numbers provided for reference:

Table 4.2: The twelve analysis conditions used in the study

Case No.	Fully Bonded Stem-Cement Interface	Frictionless Stem-Cement Interface	Frictional Stem-Cement Interface	Inclusion of a distal air-gap	Inclusion of cement creep
1	X				
2		X			
3			X		
4	X			X	
5		X		X	
6			X	X	
7	X				X
8		X			X
9			X		X
10	X			X	X
11		X		X	X
12			X	X	X

The twelve analyses were all variations on one basic geometric model. The parameters which were varied were: the stem-cement interface condition; the bearing condition under the prosthesis tip; and the inclusion of time dependent cement properties.

4.5.2 Convergence criteria

For the non-linear analyses, a convergence criteria was specified in the LUSAS data file. The parameters used to specify convergence are defined as follows:

LUSAS parameter *dlnorm*; the limit for the sum of the squares of the iterative displacements as a percentage of the sum of the squares of the total displacements. Only translational degrees of freedom are considered.

LUSAS parameter *rlnorm*; the limit for the sum of the squares of all residual forces as a percentage of the sum of the squares of all external forces, including reactions. Only translational degrees of freedom are considered.

The initial choice of convergence criteria for a particular increment of load was as follows:

$$dlnorm = 0.1 \qquad rlnorm = 0.1$$

It became evident however that these conditions would not produce convergence within a reasonable time frame. The convergence criteria was then altered to:

$$dlnorm = 1.0 \qquad rlnorm = 1.0$$

This led to a reasonable analysis time without an overly "slack" convergence criteria. Considering the assumptions used to construct the finite element model, a 1.0 % round-off error was certainly not unreasonable.

4.5.3 Validity and accuracy of the solution

The accuracy and validity of the solution were also tested for Cases 1 and 11. For Case 1 the number of nodes was varied, to observe the convergence of the solution. The femur was also assumed to be restrained at a further distal location in one analysis to assess the effects

of distal restraint on cement stresses. For Case 11 the effects of extended cement creep were also considered.

The number of nodes used in the model for Case 1 was varied to see if the peak tensile cement stresses altered with an increase in nodes. The number of nodes was varied from 421, to 2825 to 10,570. The peak stresses should converge to a single value if the model is sufficiently accurate.

To test the validity of restraining the femur at a level proximal to the knee, the femur was assumed to extend distally another 50 mm from Level 0 and was restrained at that level (z = -50 mm). This level corresponded to the base of the true anatomical femur and an analysis was conducted for this condition of realistic restraint.

Finally, for Case 11, the long term effects of cement creep were considered in one analysis, by specifying the loading time as six months. This analysis was performed to test the hypothesis proposed by McKellop *et al.* (1994) that the majority of stress relaxation will take place in the first four hours.

4.5.4 Computer hardware and analysis time

All analyses were performed on a UNIX based SunSparc20 computer. The processor contained sixty-four Megabytes of RAM (Random Access Memory) and had a clock speed of one hundred and thirty-three Megahertz. Up to two Gigabytes of hard disk space was available for the computations. An initial attempt to create a full anatomical model, with approximately fifty (depending on section characteristics) points per 2D section led to an analysis time of five hours for one linear run. A non-linear analysis was attempted with slack convergence criteria (dlnorm and rlnorm = 5.0 %), however it was terminated after four weeks run time, after failing to converge. Clearly, a super computer was necessary, however the software was not compatible with the available parallel processor.

The simplified anatomical model took one hour to run for a linear analysis. The non-linear sliding analyses without creep took approximately two weeks, with the convergence critria of dlnorm and rlnorm = 1.0 %. The non-linear analyses with creep took approximately three weeks with the loading time of four hours. Simultaneous analyses were attempted

however the demands on memory were too great and all analyses were performed separately. This made parameter variation very difficult as the results of one analysis had to be studied before another one could begin. With a two to three week run time, this was quite a time consuming process! Realistically, projects of this type must be performed on a computer with parallel processing capabilities.

The results of all the specified analyses are presented in Chapter 5, Finite element output.

Chapter Five

Finite element output

5.1 Introduction

The finite element output contained an extremely large amount of data including displacements, stresses, and strains calculated within each element. Due to the large number of elements used in constructing this model the output files generated from the analyses were cumbersome. A decision had to be made to determine which data were appropriate for addressing the defined problem. An appropriate format also had be chosen to analyse and display the relevant data.

From the literature review it was revealed that two key aspects of the finite element output which required attention were the peak tensile cement stresses, and the strain levels in the medial calcar. The output relating to these phenomena is presented both graphically and numerically. Firstly the output relating to peak tensile stresses in the cement will be detailed, followed by the strain data relating to levels in the medial calcar. A comparison of the results with other studies is presented and the biomechanical interrelationship between cement stresses and calcar strains is discussed. The convergence behaviour and model validity test results are also presented.

5.2 Cement stresses

5.2.1 Output format

Before detailing the appropriate output concerning the stresses within the cement mantle the objectives of the study should be restated. Cement crack formation was noted in a significant number of studies reviewed in Chapter Three. It is suspected that these cracks may propagate through to the bone-cement interface and ultimately lead to failure of the prosthesis system. Therefore a failure criterion must be identified to predict the stress environment under which crack propagation will occur. The failure criterion for a particular material depends on its mechanical characteristics. For example, ductile materials such as mild steel have a failure criterion dependent on the Von mises or equivalent uniaxial stress levels and soils require a Mohr-Coulomb failure criterion, which involves a combination of shear and normal stresses to predict failure. It was shown in the literature review that bone cement or polymethylmethacrylate (PMMA) is a material which is relatively strong in compression but is weak in shear and tension. Weak, brittle materials such as PMMA fail when the level of *tensile principal stress* exceeds a certain value characteristic of the material.

This tensile capacity can be determined by experimental means. The principal stress is the largest value of normal stress occurring at a point within the continuum. When a cemented total hip replacement is loaded, a stress distribution can be obtained throughout the cement mantle. The region of cement which is most vulnerable to failure is where the *maximum tensile principal stress* occurs. Hence in this study, one of the main aims was to identify the magnitude and location of the maximum principal tensile stress within the cement mantle. Comparisons can be made between different designs, subject to this criterion of maximum principal tensile stress.

For each of the twelve analyses, the magnitude and location of these peak tensile stresses will be presented. In all analyses, peak tensile stress concentrations were noted both proximally and distally. Clinical studies (Jasty *et al.*, 1991; Stauffer, 1982) and other *in vitro* and numerical studies (Sih *et al.* 1981; Crowninshield and Tolbert, 1983; Harrigan and Harris, 1991a; Harrigan and Harris, 1991b; Mann *et al.*, 1991) have also noted stress

concentrations both proximally and distally. A proximal location in this study refers to any level above z = 100 mm. A distal location refers to any level below z = 80 mm. Therefore results will be provided for both the proximal and distal maximum principal tensile stresses. A graphical summary of the cement stresses is presented in Section 5.2.3.

The stresses are calculated at the Gauss points within each element. The Gauss points are specific locations within the element where the integrations to determine stresses and strains are performed (Zienkiewicz and Taylor 1971). Figure 5.1 isolates the finite element mesh of the cement mantle with the levels in the femoral or z-axis of both the proximal and distal peak tensile principal stresses. The Case numbers refer to the analysis conditions which were specified in Table 4.2. The cement stresses are presented in Table 5.1 and the location of these peak tensile stresses in the xy plane are then presented in Figures 5.2 through 5.9.

proximal

distal

medial ← → lateral

z = 128mm
Cases 1,4,7,10
All bonded interfaces

z = 118mm
Cases 2,3,5,6,8,9,11,12
All sliding interfaces

z = 70mm
Cases 2,3,5,6,8,9,11,12
All sliding interfaces

z = 26mm
Cases 1,4,7,10
All bonded interfaces
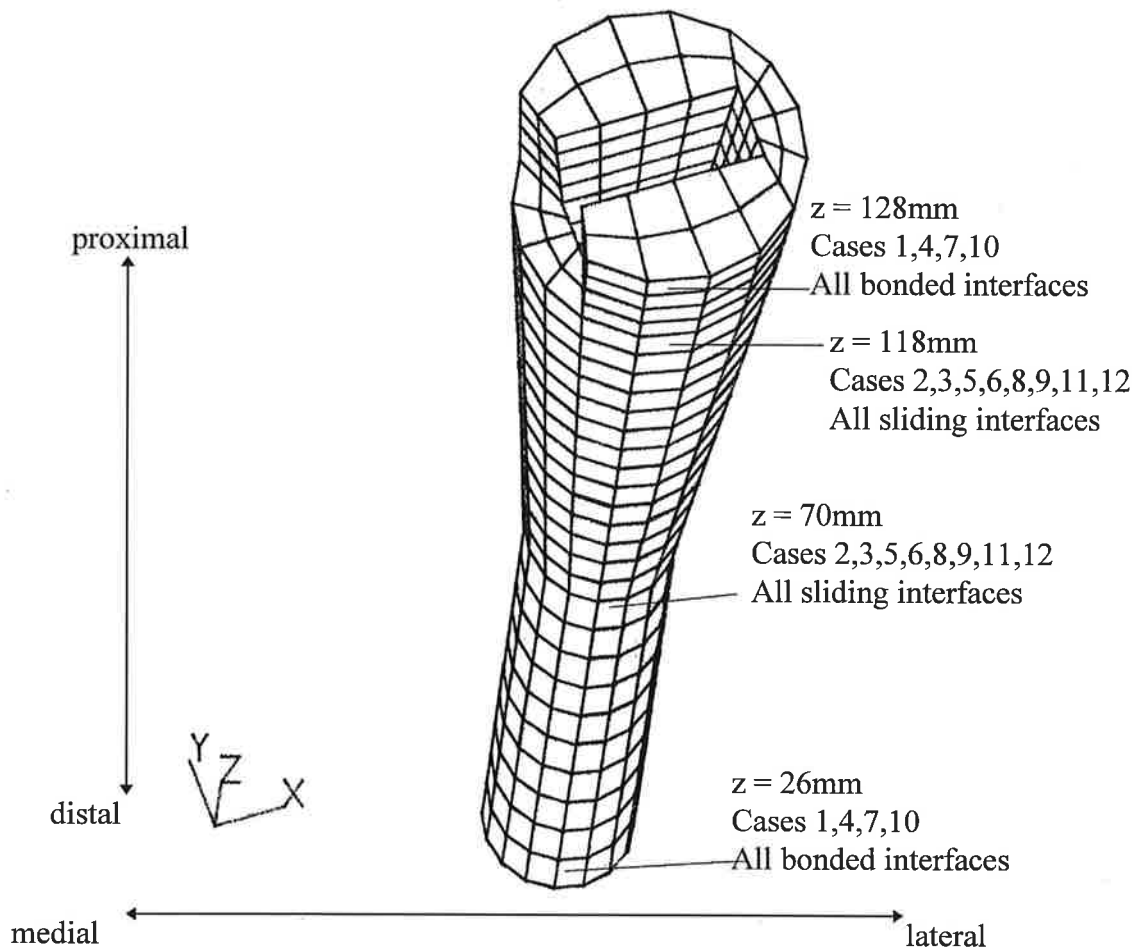
Figure 5.1: Cement mantle showing levels of maximum principal tensile stress.

5.2.2 Cement stress output

Table 5.1: The magnitude and location of peak tensile cement stresses

Case Number	Peak Tensile Principal Stress (MPa)		Peak stress location	
	Proximal	Distal	z-axis location (mm)	xy position defined in Figure
1 (b,ng,e).	1.99 R		128	5.2
		2.89 LB	26	5.3
2 (f,ng,e)	6.27 H		118	5.2
		4.04 H	71	5.3
3 (c,ng,e)	4.70 H		118	5.2
		3.28 H	71	5.3
4 (b,g,e)	1.99 R		128	5.4
		2.89 LB	26	5.5
5 (f,g,e)	6.42 II		118	5.4
		6.20 H	71	5.5
6 (c,g,e)	4.84 H		118	5.4
		3.17 H	71	5.5
7 (b,ng,v)	1.97 R		128	5.6
		2.83 LB	26	5.7
8 (f,ng,v)	6.16 H		118	5.6
		4.04 H	71	5.7
9 (c,ng,v)	4.70 H		118	5.6
		3.28 H	71	5.7
10 (b,g,v)	1.97 R		128	5.8
		2.83 LB	26	5.9
11 (f,g,v)	6.31 H		118	5.8
		5.91 H	71	5.9
12 (c,g,v)	4.69 H		118	5.8
		2.95 H	71	5.9

b - bonded, f - frictionless, c - Coulomb friction, ng - no distal air-gap, g - distal air-gap, e - elastic cement conditions, v - viscoelastic cement conditions, H - hoop stress, LB - longitudinal bending stress, R - radial stress.
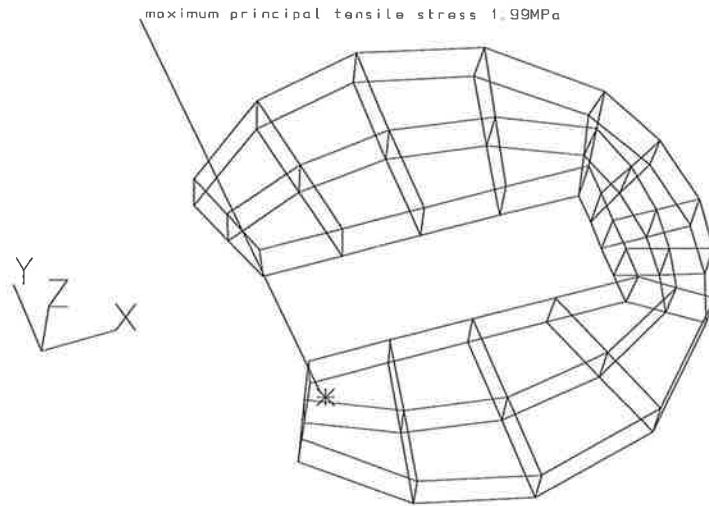
(a) Case 1: z = 128 mm, Bonded.
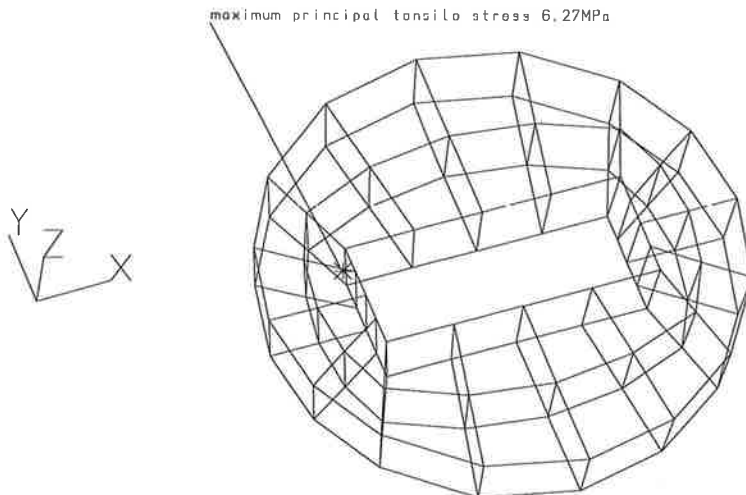
(b) Case 2: z = 118 mm, Frictionless.
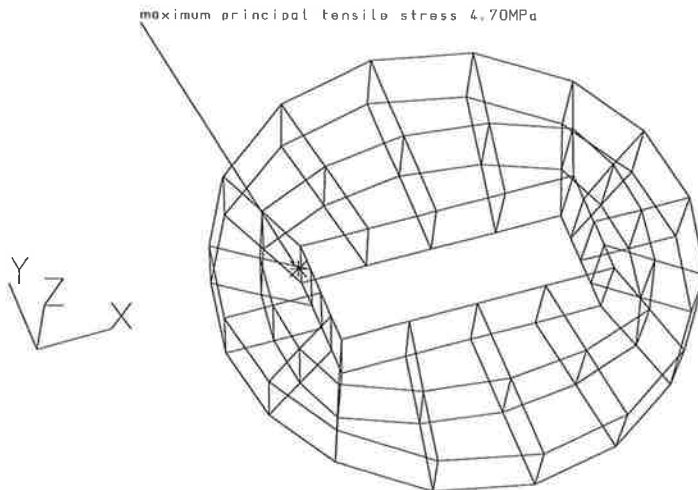
(c) Case 3: z = 118 mm, Coulomb friction.

Figure 5.2: Location in xy plane of proximal maximum principal tensile cement stress for Cases 1, 2 and 3. No air-gap, elastic cement conditions.
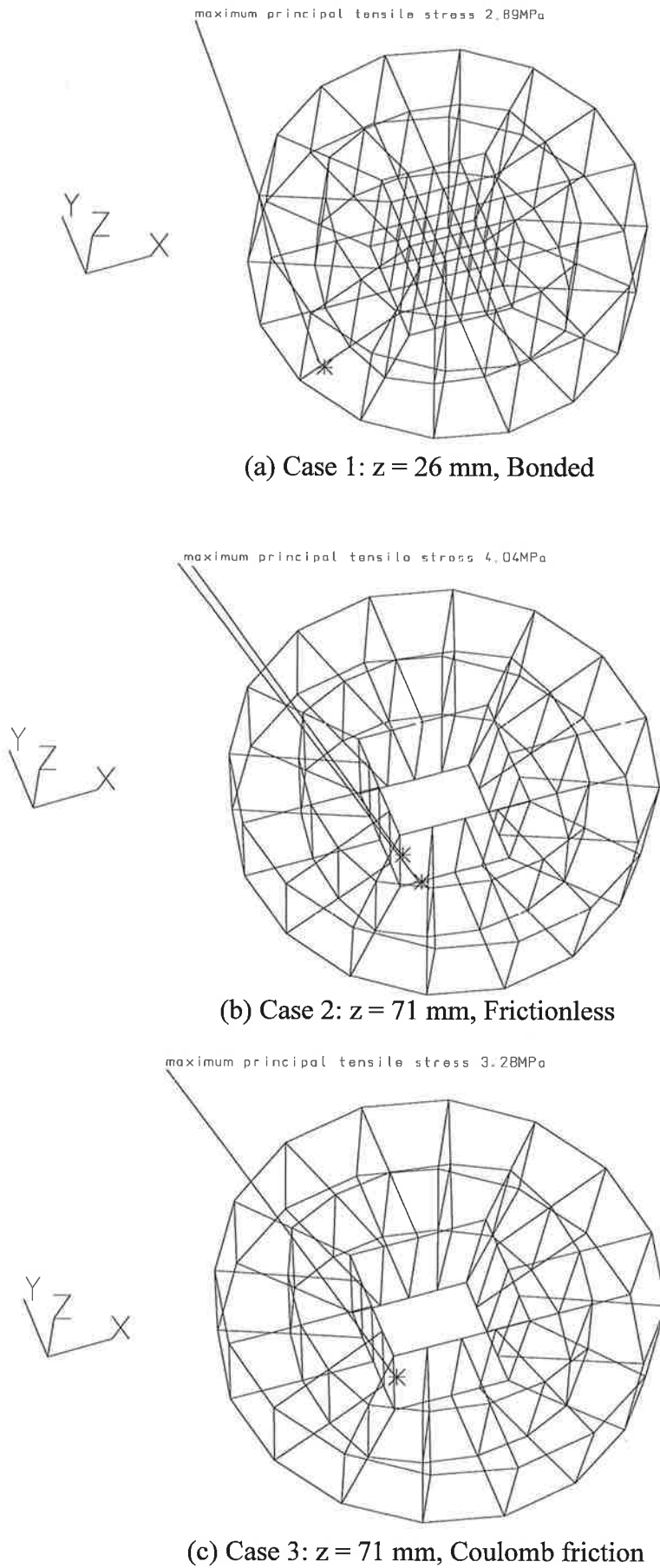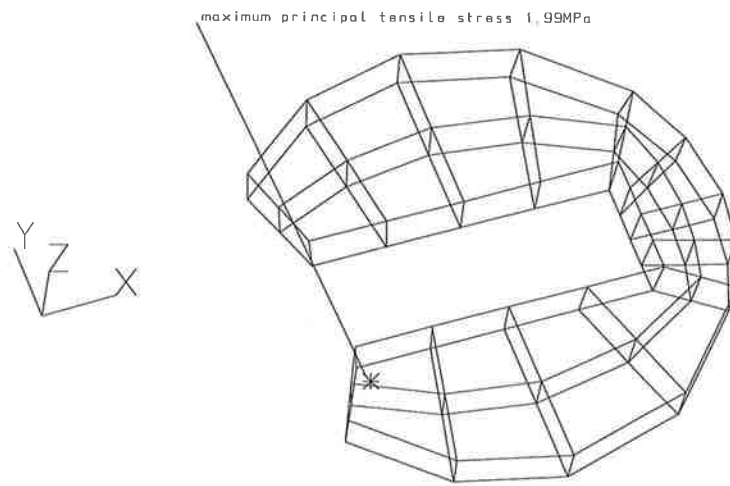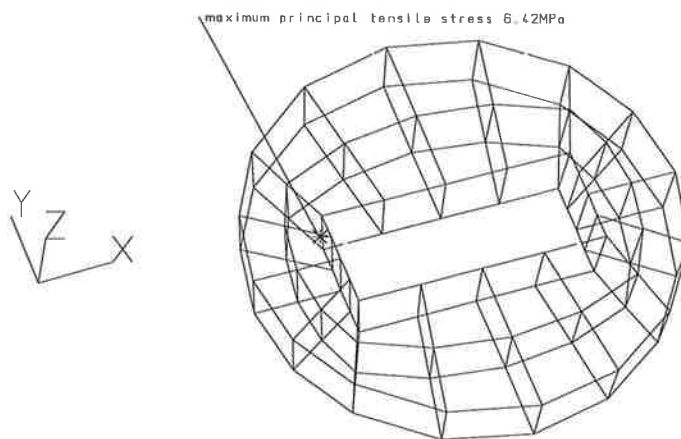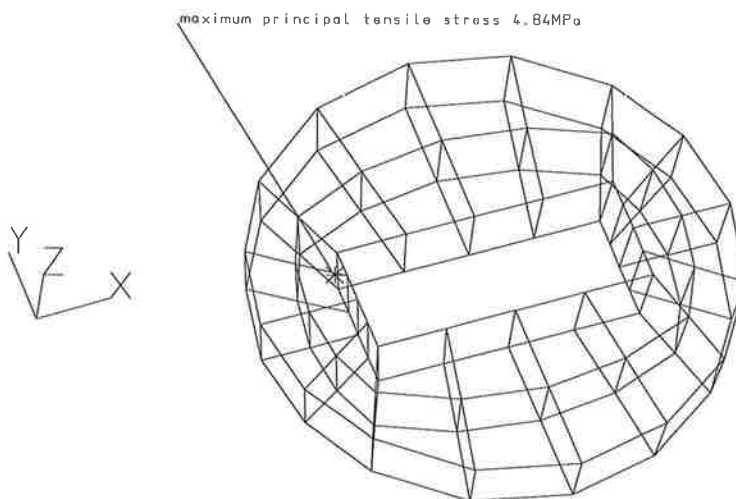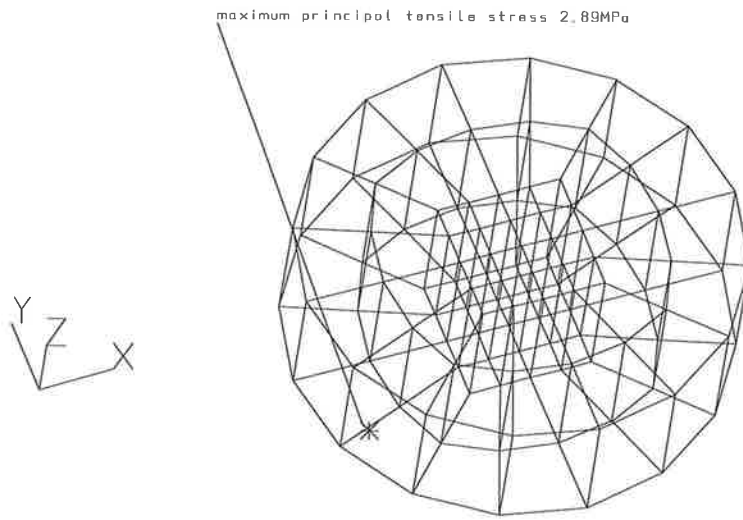
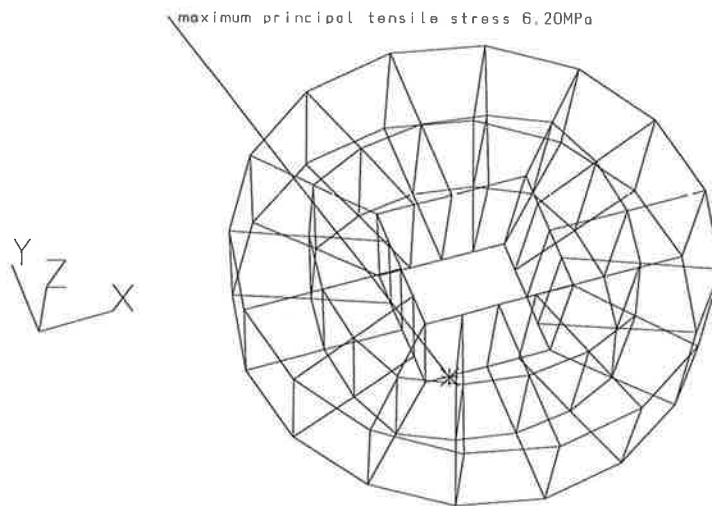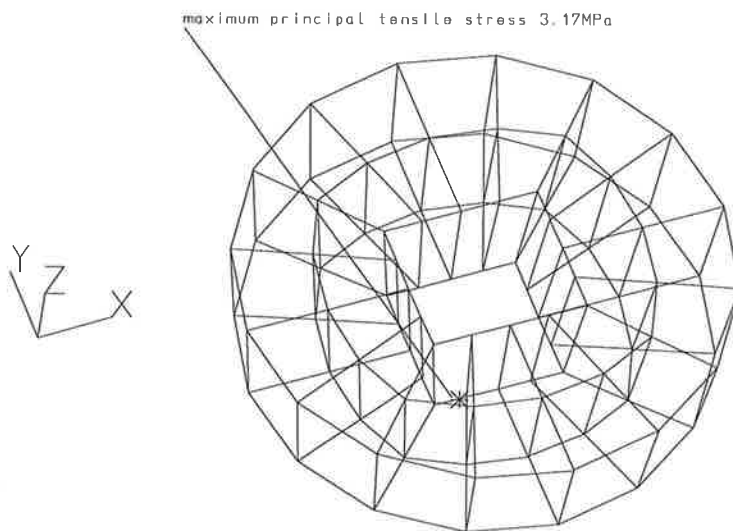(a) Case 1: z = 26 mm, Bonded

(b) Case 2: z = 71 mm, Frictionless

(c) Case 3: z = 71 mm, Coulomb friction

Figure 5.3: Location in xy plane of distal maximum principal tensile cement stress for Cases 1, 2 and 3. No air-gap, elastic cement conditions.

maximum principal tensile stress 1,99MPa

(a) Case 4: z = 128 mm, Bonded

maximum principal tensile stress 6,42MPa

(b) Case 5: z =118 mm, Frictionless

maximum principal tensile stress 4,84MPa

(c) Case 6: z= 118 mm, Coulomb friction

Figure 5.4: Location in the xy plane of proximal maximum principal tensile cement stress for Cases 4, 5 and 6. With an air-gap, elastic cement conditions.

maximum principal tensile stress 2.89MPa

(a) Case 4: z = 26 mm, Bonded

maximum principal tensile stress 6.20MPa

(b) Case 5: z = 71 mm, Frictionless

maximum principal tensile stress 3.17MPa

(c) Case 6: z = 71 mm, Coulomb friction

Figure 5.5: Location in xy plane of distal maximum principal tensile cement stress for Cases 4, 5 and 6. With an air-gap, elastic cement conditions.
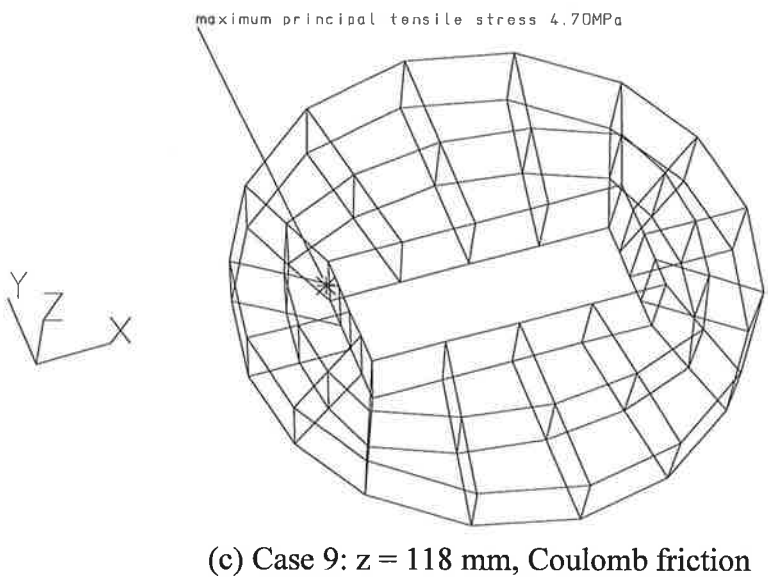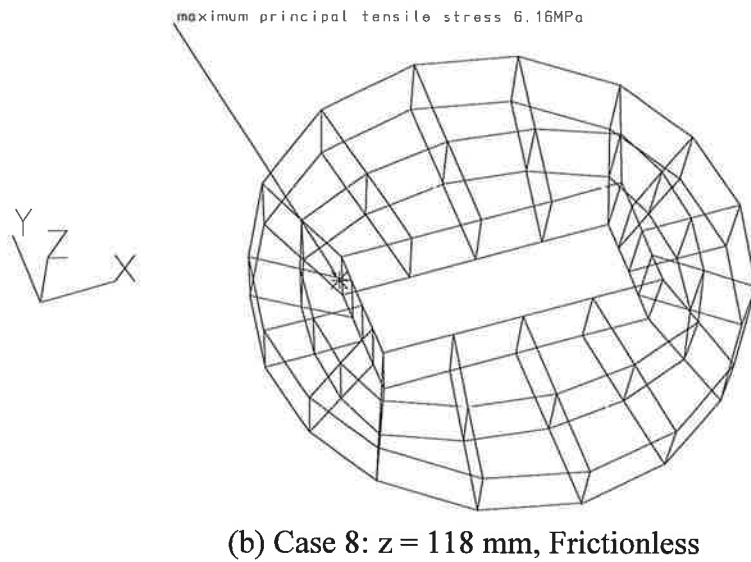
maximum principal tensile stress 1.97MPa

(a) Case 7: z = 128 mm, Bonded

maximum principal tensile stress 6.16MPa

(b) Case 8: z = 118 mm, Frictionless

maximum principal tensile stress 4.70MPa
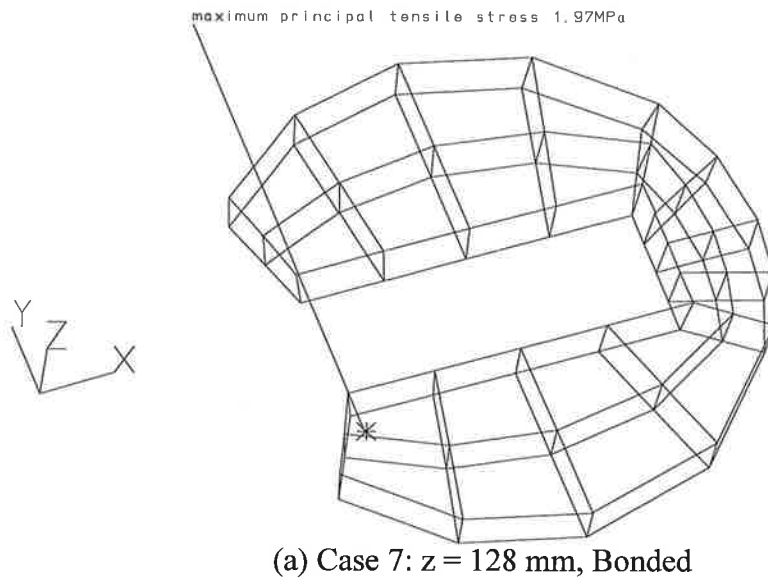

(c) Case 9: z = 118 mm, Coulomb friction

Figure 5.6: Location in xy plane of proximal maximum principal tensile cement stress for Cases 7, 8 and 9. No air-gap, viscoelastic cement conditions.
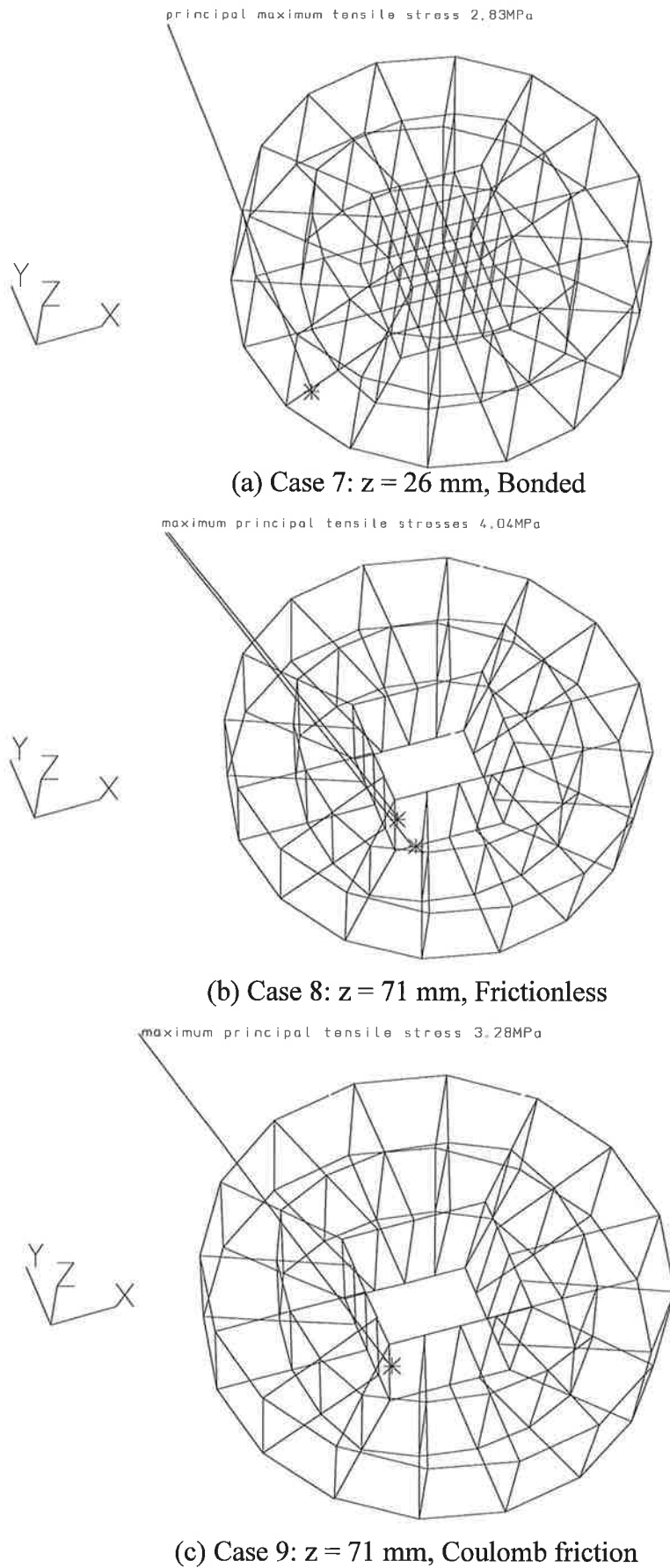
principal maximum tensile stress 2,83MPa

(a) Case 7: z = 26 mm, Bonded

maximum principal tensile stresses 4,04MPa

(b) Case 8: z = 71 mm, Frictionless

maximum principal tensile stress 3,28MPa

(c) Case 9: z = 71 mm, Coulomb friction

Figure 5.7: Location in xy plane of distal maximum principal tensile cement stress for Cases 7, 8 and 9. No air-gap, viscoelastic cement conditions.
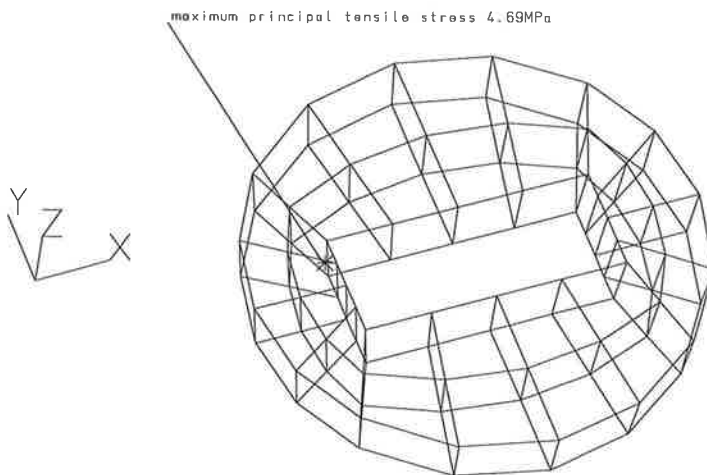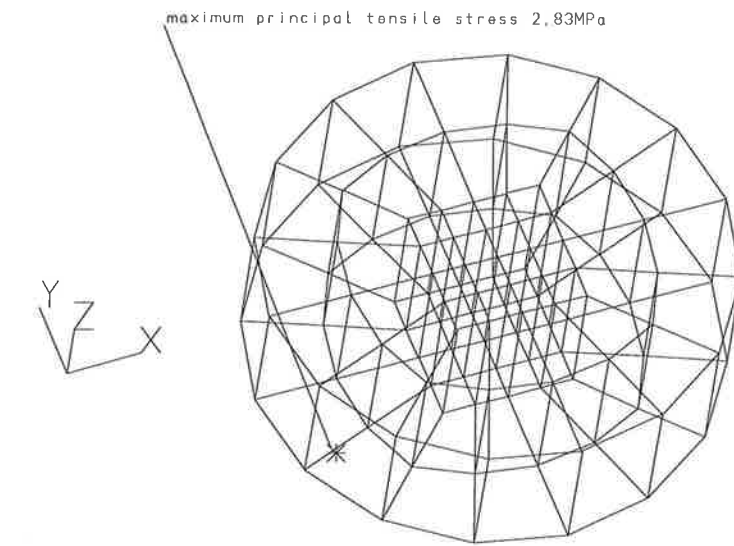
maximum principal tensile stress 1.97MPa

(a) Case 10: z = 128 mm, Bonded
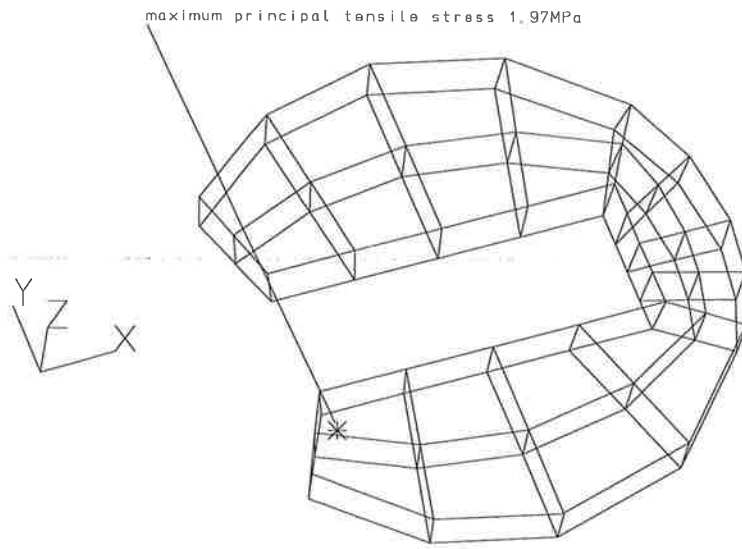
maximum principal tensile stress 6.31MPa
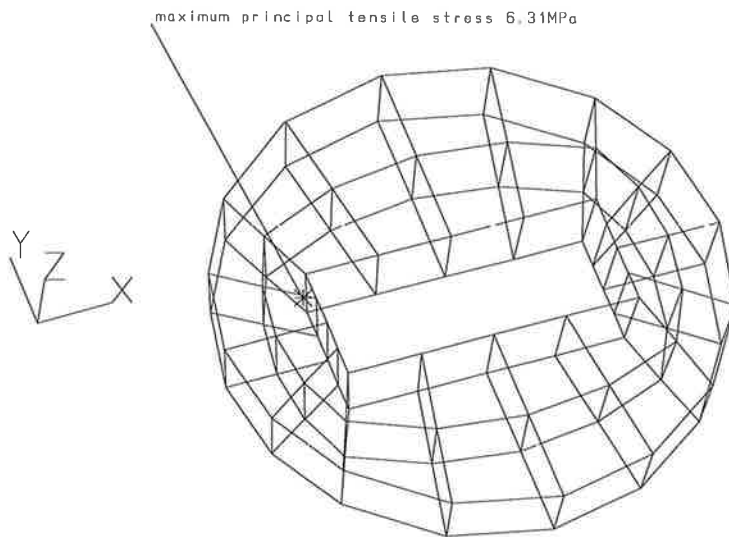
(b) Case 11: z = 118 mm, Frictionless

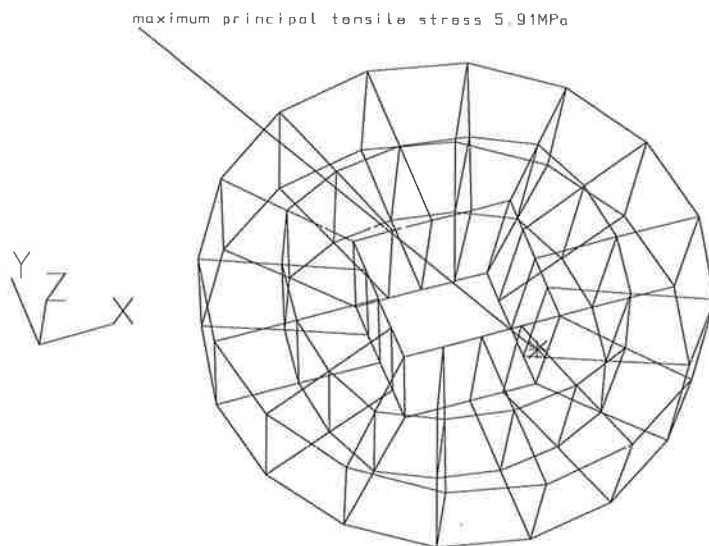maximum principal tensile stress 4.69MPa

(c) Case 12: z = 118 mm, Coulomb friction

Figure 5.8: Location in xy plane of proximal maximum principal tensile cement stress for Cases 10, 11 and 12. With an air-gap, viscoelastic cement conditions.

maximum principal tensile stress 2,83MPa

(a) Case 10: z= 26 mm, Bonded

maximum principal tensile stress 5,91MPa

(b) Case 11: z = 71 mm. Frictionless

maximum principal tensile stress 2.95MPa
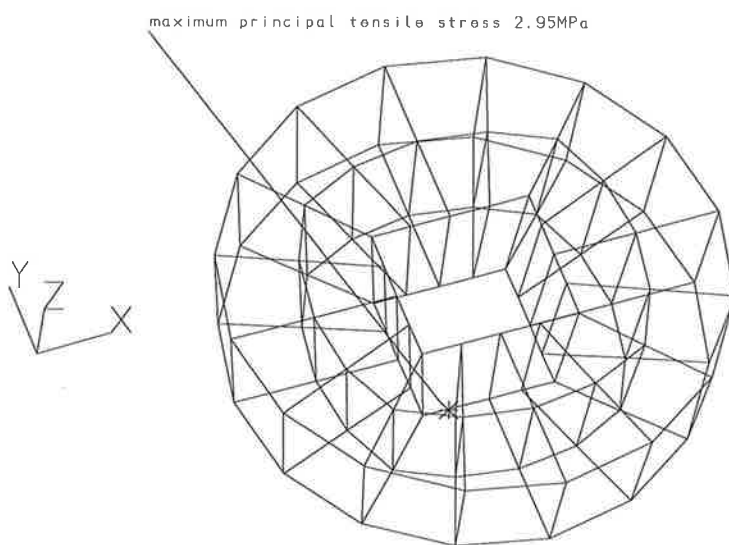

(c) Case 12: z = 118 mm, Coulomb friction

Figure 5.9: Location in xy plane of distal maximum principal tensile cement stress for Cases 10, 11 and 12. With an air-gap, viscoelastic cement conditions.

5.2.3 Summary of cement stress output

The magnitude of the peak tensile stresses in the cement mantle are now presented graphically in Figures 5.10 and 5.11 to allow a convenient comparison between the different analyses. A discussion of the cement stress data and a comparison with other results is presented in Section 5.2.4
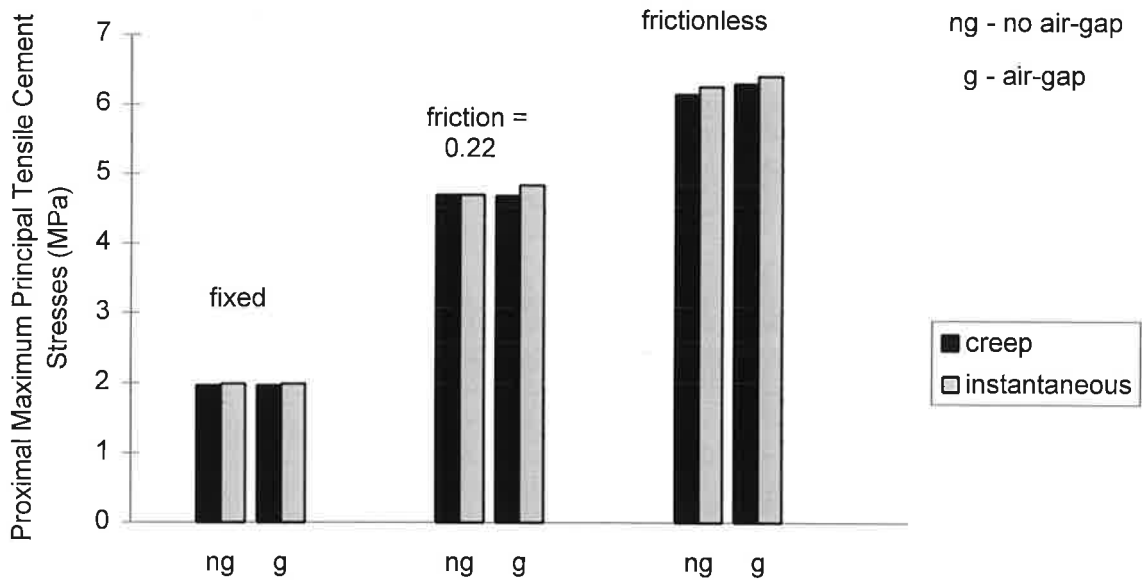

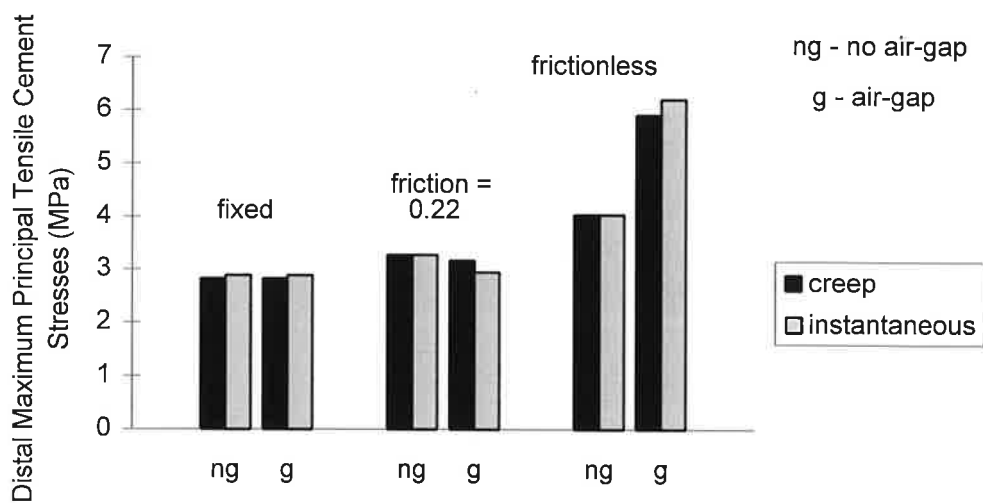**Figure 5.10: Peak proximal tensile cement stresses.**

Figure 5.11: Peak distal tensile cement stresses.

5.2.4 Discussion of cement stress data and comparison with other studies

In this section a general discussion of the cement stress data is presented along with a comparison of the output with other relevant studies. The clinical relevance of the data is also discussed. The biomechanics of the different interface conditions as they relate to cement stresses is presented in Section 5.4.

In the present study, the main feature of the tensile stress distribution was the presence of distinct stress concentrations both proximally and distally. These local concentrations were present for each of the three interface conditions. The stress concentrations can be explained by considering Figure 5.12 which is a simplified longitudinal section of the cemented prosthesis system.
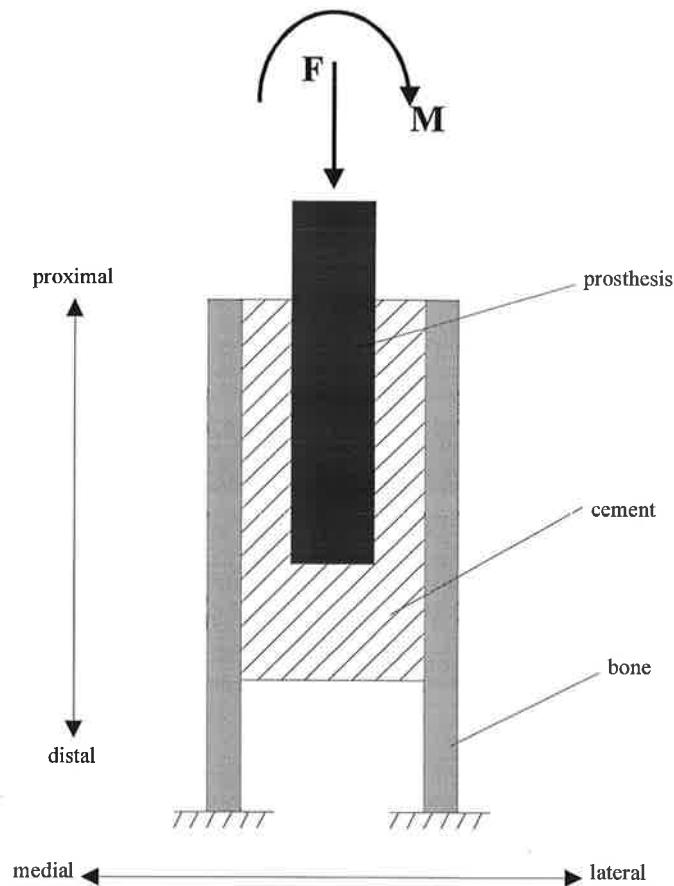

Figure 5.12: Longitudinal simplified section of a cemented total hip replacement

The axial force, F and moment, M are resisted in the plane under consideration. Bending stresses are not transferred to the cement mantle even in the case of the bonded stem-

cement interface. Huiskes (1980) showed that normal elastic beam theory does not apply due to the extremely large difference in elasticity between the stem ($E_{steel} = 200 \times 10^3$ MPa) and cement ($E_{cement} = 2.1 \times 10^3$ MPa). Huiskes suggested that a beam-on-elastic-foundation theory was more appropriate to describe the system, and comparison with finite element results confirmed this theory. Stress concentrations occur proximally and distally due to the rotation of the prosthesis within the medullary canal. This rotation is resisted primarily at two locations, the distal prosthesis tip and the proximal top of the stem.

In this study, for the bonded stem-cement interface, the displacement of the prosthesis produced a radial tensile stress concentration in the proximal anterior region. Distally, the tensile stress concentration presented as a longitudinal bending stress at the most distal section of cement, adjacent to the bone-cement interface. This section is sufficiently distal to the prosthesis tip so that bending stresses dominate over the radial tensile stresses which present more proximally.

For the sliding stem-cement interfaces, both proximally and distally, tensile hoop stresses were dominant. The concept of a sliding stem-cement interface emerged to encourage compression across the bone-cement interface which is a weak interface in tension (Kusleika and Stupp 1983). Although radial compressive stresses did develop to resist the axial and rotational displacement of the prosthesis, they were inevitably accompanied by large tensile circumferential or hoop stresses. The magnitude of these tensile stresses were significantly larger than for the bonded stem-cement interface.

It is pertinent to summarise the relevant biomechanical studies which were detailed in Chapter Three in order to compare the results with the present study.

Svensson *et al.* (1977) also demonstrated that the cement stress distribution altered considerably after considering slip at the stem-cement interface. Sih *et al.* (1981) suggested that the highest probability of cement fracture is either distally near the tip or proximally. It is doubtful however whether a strain energy density failure criteria as used by the authors is appropriate for weak brittle materials such as bone cement. A maximum principal tensile stress failure criteria as used in this study seems more appropriate.

Huiskes (1980) studied the stem-cement interface stresses for a bonded interface and found a large stress concentration proximally and a large shear stress concentration at the distal tip. The author pointed out that torsional effects and hoop stresses could not be considered due to the two dimensional nature of the study.

Crowninshield and Tolbert (1983) found that the "presence of a stem-cement bond was found to reduce proximal cement strain magnitudes", although the authors found little change in the distal peak tensile cement stresses. In the present study peak proximal tensile cement stresses were reduced by 69 %, however peak distal tensile cement stresses were also reduced by 52 % when a bonded stem-cement interface was considered when compared to a frictionless or 'loose' interface. Rosette strain gauges were not used in the Crowninshield and Tolbert study therefore the strains were only recorded in the direction of the gauge. In the present study the peak distal strains presented as tensile hoop strains for the 'loose' interfaces, however the distal strain gauges in the study of Crowninshield and Tolbert were aligned in the longitudinal or proximal-distal direction (z-axis in this study). Hence there was no opportunity to record peak distal tensile cement strains if they occurred in the transverse (xy in this study) plane. This highlights the problem of using *in vitro* strain gauge tests in cemented total hip replacement. Unless rosette strain gauges which measure the three dimensional strains are used *and* gauges are placed in the correct position within the cement mantle, then true *peak* strains occurring within the continuum will not be measured.

Lewis *et al.* (1984) also found tensile stress concentrations both proximally, and distally near the tip. Similar concentrations were found in the study of Weinans *et al.* (1990). Harrigan *et al.* (1991b) showed a debonded prosthesis tip would lead to a distal tensile stress of magnitude 4 MPa. Estok *et al.* (1991) found sharp strain concentrations at the prosthesis tip after simulating both gait and stair-climbing. Estok *et al.* suggested that the magnitude of these strains would predict early failure of the material.

Lee (1990) proposed that a polished prosthesis surface finish would produce tensile hoop stresses in the cement mantle, which the results of this present study confirm. Lee also suggested that these tensile stresses would relax considerably over time. The results from the present study do *not*, however, predict significant levels of cement stress relaxation. Miles (1990) considered only axial loads and the strain gauges were located half way down

the shaft ie neither distally nor proximally where other studies have shown concentrations to occur. The gauges were inserted in such a way as to record both axial and hoop strains. The polished stem showed a large reduction in the axial component of strain however the hoop component did not significantly increase. The present study showed a significant increase in the hoop component of the cement strain when a low friction prosthesis was modelled. The study of Miles (1990) may not have considered the peak location where hoop strains occur with a polished stem due to using strain gauges in only one location.

Harrigan and Harris (1991c) noted a significant increase in the tensile hoop component of the cement stress proximally, as was found in the present study. In the study of Harrigan and Harris the maximum tangential tensile stress at the stem-cement interface increased from 1.4 MPa to 6.5 MPa when a bonded stem-cement interface was compared to a frictionless interface for gait loading. In the present study, considering a distal air-gap and the inclusion of creep, the peak tensile stress increased proximally from 1.97 MPa to 6.31 MPa. These concentrations occurred proximally-medially, as was the case with Harrigan and Harris. The results of Harrigan and Harris show good qualitative and quantitative agreement with the present study. Harrigan and Harris (1991c) also suggested that "regions of cement with pore stresses above 7 MPa are likely to fail *in vivo* if there is a pore present in these regions." Tensile stresses in the present study approach this value for the frictionless stem-cement interface condition which is of concern.

Mann *et al.* (1991) found that "the largest circumferential tensile stresses were three times larger in the model using Coulomb friction" as compared to a bonded stem-cement interface. A large tensile hoop stress of 8.4 MPa was found in the proximal-medial region of the cement.

Mann *et al.* (1992b) found that although a bonded stem-cement interface reduced tensile hoop stresses, the normal tensile stresses at the bone-cement interface (6.1 MPa) increased substantially and may approach the strength (7.5 MPa, Kusleika and Stupp 1983) of the bone-cement interface. In the present study, peak tensile stresses (2.83 MPa for bonded, creep, and air-gap) did not reach this strength limit. This justified the assumption of an intact bonded bone-cement interface in the present study.

McKellop *et al.* (1994) found that the frictionless interface condition produced the highest peak tensile stresses in the cement with a magnitude of approximately 8.0 MPa. McKellop *et al.* found that the tensile stress levels for the bonded interface were higher than for the frictional interface. The peak tensile cement stress relaxation level for the bonded interface was mild (8 %). The frictional interface produced peak tensile cement stress relaxation of 22 %. Considering the frictionless interface, however, the peak tensile cement stresses increased by 16 %. These results are at variance with the present study, which used similar viscoelastic properties. In the present study, considering the presence of a distal air-gap, peak tensile cement stresses reduced after the inclusion of creep for all cases. In the present study, the majority of distal cement stress relaxation creep occurred within the first four hours, however proximally, some further relaxation occurred. A summary of the cement stress reductions for the present study is shown in Table 5.2.

Table 5.2: Cement stress relaxation for loading time of four hours, with distal air-gap.

	Bonded Interface		Friction Coefficient of 0.22		Frictionless Interface	
	Distal	Proximal	Distal	Proximal	Distal	Proximal
Instantaneous	**2.89 MPa**	**1.99 MPa**	**3.17 MPa**	**4.84 MPa**	**6.20 MPa**	**6.42 MPa**
4 hrs. loading	**2.83 MPa**	**1.97 MPa**	**2.95 MPa**	**4.69 MPa**	**5.91 MPa**	**6.31 MPa**
Stress reduction	**2.0 %**	**1.0 %**	**6.9 %**	**3.1 %**	**4.7 %**	**1.7 %**

Lu and McKellop (1995) using the same model as McKellop *et al.* (1994) found that for the bonded and frictionless interface conditions, there was no long-term accumulation of creep ie the creep recovered during the period of rest. The frictional interface did not recover, however with residual stresses presenting as much as 29 % of the maximum. With this interface condition, creep was found to reduce the maximum tensile stress by 25 %.

The difference in results between the present study and the results of McKellop and Lu may be due to differences in loading and restraint conditions. It will be shown in Section 5.4.2 that creep and/or relaxation of bone cement is highly dependent on the restraint condition. Lu and McKellop (1995) also noted that the subsidence of the prosthesis in their study (0.5 mm) did not correspond with clinically observed subsidences of 2.0 mm. The

authors suggested that this could be due to remodelling of the cortex *in vivo* following alterations in the femur's strain energy density field.

Saligrama *et al.* (1996) showed far higher levels of tensile stress relaxation in the cement mantle when the same three interface conditions were considered. The authors also used higher viscoelastic constants than used in the present study, and these differences are highlighted below.

Present study: Creep model - $\varepsilon_{cr} = \dfrac{\sigma^{1.55}t^{0.10}}{45,997}$.
$\qquad\qquad\qquad$ Eq. 4.11 (repeated)

Units; stress, MPa, time, seconds

Saligrama: Creep model - $\varepsilon_{cr} = 1.76 \times 10^{-9}\sigma^{1.858}t^{0.283}$
$\qquad\qquad\qquad$ Eq. (5.1)

Units; stress, psi, time, hours.

ε_{cr} - creep strain

σ - instantaneous stress

t - time

By way of example, Table 5.3 below compares the creep strain increment for various time intervals for a stress of 6.9 MPa or 1000 psi.

Table 5.3: Creep strain increments for bone cement with a constant stress of 6.9 MPa (1000psi).

	Creep strain increment with time intervals in hours.		
time increment	t=10 - t=100	t=1 - t=10	t=0.1 - t=1
Saligrama et al.	0.0012	0.0007	0.0003
Present study.	0.0004	0.0002	0.0003

It can be seen that for increasing time intervals, that the creep strain increment is significantly larger for the Saligrama model, ie the rate of creep is larger. This partly explains the difference in cement relaxation values between the two studies. Different

loading configurations were also used. In the above example, two separate models of cement creep produced quite different results although both models were attempting to mathematically represent the *in vivo* process. It is clearly necessary that more research needs to be done in the area of laboratory testing, in order to clarify the numerical properties of biological systems such as cemented total hip replacement.

It is also important to relate the results obtained in this study to clinical observations. Stauffer (1982) found that the most common type of femoral component (stem) loosening resulted from circumferential splitting of the cement mantle in the proximal region. Jasty *et al.* (1991) found that circumferential cracking of the cement mantle was evident both proximally-medially and distally-laterally and that debonding was frequently associated with crack formation in the cement. Weber and Charnley (1975) found cement cracks to be present in the distal cement mantle in 1.5 % of the patients. The author found that "In all patients but one the cement broke at the level of the distal 2 cm of the femoral stem." The proponents of the Exeter prosthesis (Fowler *et al.* 1988), a highly polished double tapered prosthesis, recommend the employment of a distal air-gap under the prosthesis tip to encourage subsidence of the prosthesis. In the present study, the presence of an air-gap had little effect on the cement stress output except for the frictionless stem-cement interface. For this case there was a significant increase in the peak distal tensile cement stress however proximally there was little change.

A comparison with other strain gauge, finite element and clinical studies indicate the reliability of the present analysis. The cement stress output in the present work compare well both qualitatively and quantitatively with other studies.

5.3 Strain levels in the proximal medial calcar

5.3.1 Output format

It was seen in the literature review that resorption of the proximal medial calcar was a common problem associated with cemented total hip replacement (Charnley, 1964; Beckenbaugh and Ilstrup, 1978; Sutherland *et al.*, 1982). This area of bone provides radial support for the bone cement and its preservation is of prime importance. It was also shown that although a degree of this bone loss may be attributed to adverse tissue reaction from

wear particles, stress shielding is undoubtedly a significant factor. There is a total redistribution of strains in the calcar produced by the implantation of a cemented hip prosthesis. (Oh and Harris, 1978; Jacob and Huggler, 1980; Crowninshield *et al.*, 1980; Lanyon *et al.*, 1981; Huiskes *et al.*, 1987).

Due to Wolff's Law a decrease in stress or strain levels in an area of bone will lead to a decrease in material stiffness at that region and also a geometric thinning. This phenomenon has also been confirmed experimentally (Burkhart and Jowsey, 1967; Heaney, 1962). Wolff's Law is more of a qualitative observation and the actual mechanism by which bone remodels is unclear. It is known qualitatively that bone will align itself along lines of principal strain and will increase in density as the magnitude of principal strain increases. It is therefore of importance to compare both the magnitude and orientation of principal strains in the medial calcar between the different analyses.

It is considered by some that it is the distortional strain energy density which provides the stimulus for bone remodelling (Carter *et al.* 1984). The total strain energy density consists of this distortional component as well as a hydrostatic component. Von mises strains will be used in this study as an index for indicating the level of distortional strain energy density present in the medial calcar. It was assumed in this study that the lower the level of Von mises strain present in the medial calcar, the greater the stimulus for resorptive decay of bone.

For the twelve analyses, the elements representing the proximal medial calcar (highlighted in Figure 5.13 below) are displayed in Figures 5.14 to 5.17, with vectors representing the magnitude and orientation of the principal strains. Table 5.4 displays the principal and Von mises strains present within the medial calcar. The strains were evaluated at the Gauss points, similarly to the cement stress output. A summary of the calcar strains is presented in Section 5.3.3.
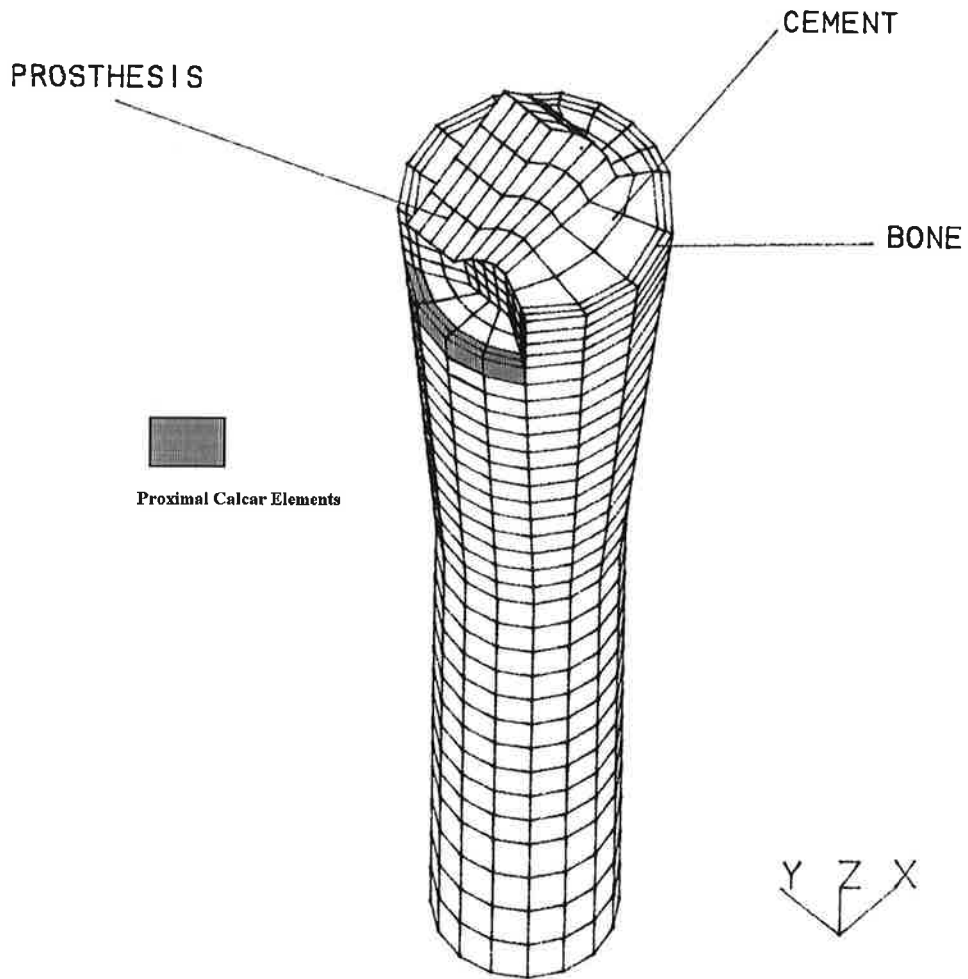
PROSTHESIS

CEMENT

BONE

Proximal Calcar Elements

Y Z X

Figure 5.13: Finite element mesh highlighting proximal medial calcar elements.

5.3.2 Calcar strain data

Table 5.4: Principal tensile and compressive calcar strain range

| Case Number	Principal Strain Range ($\mu\varepsilon$)		Von mises strain range ($\mu\varepsilon$)	Principal strains displayed in Figure
	Tensile	Compressive		
1 (b,ng,e).	37-227	59-253	89-334	5.14
2 (f,ng,e)	29-628	41-329	61-828	5.14
3 (c,ng,e)	26-558	32-295	70-746	5.14
4 (b,g,e)	36-227	59-253	89-334	5.15
5 (f,g,e)	28-662	27-340	49-867	5.15
6 (c,g,e)	18-552	31-274	72-738	5.15
7 (b,ng,v)	37-228	59-255	89-337	5.16
8 (f,ng,v)	30-632	41-331	61-833	5.16
9 (c,ng,v)	26-558	32-295	70-746	5.16
10 (b,g,v)	37-228	59-255	89-337	5.17
11 (f,g,v)	29-668	27-343	49-897	5.17
12 (c,g,v)	26-544	35-286	74-728	5.17

b - bonded, f - frictionless, c - Coulomb friction, ng - no distal air-gap, g - distal air-gap, e - elastic cement conditions, v - viscoelastic cement conditions.
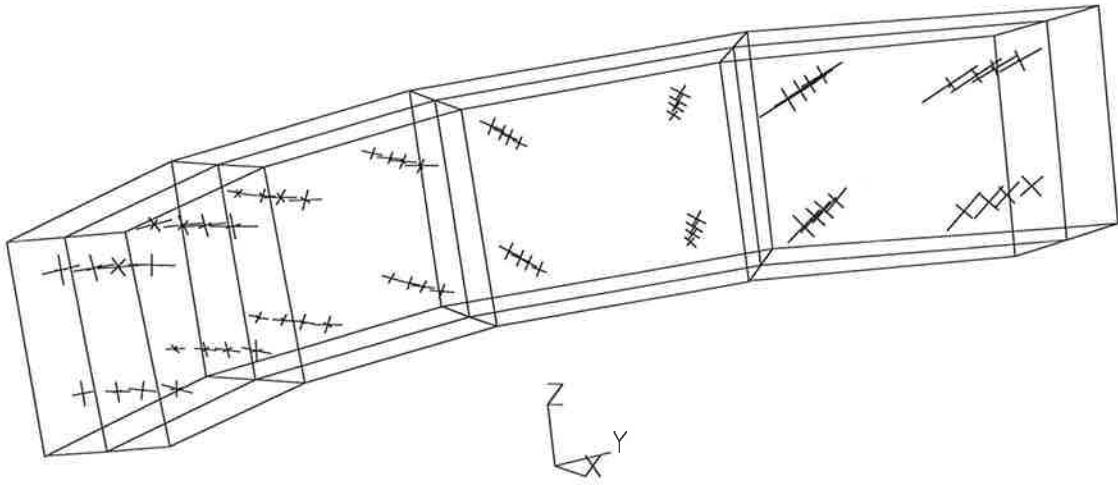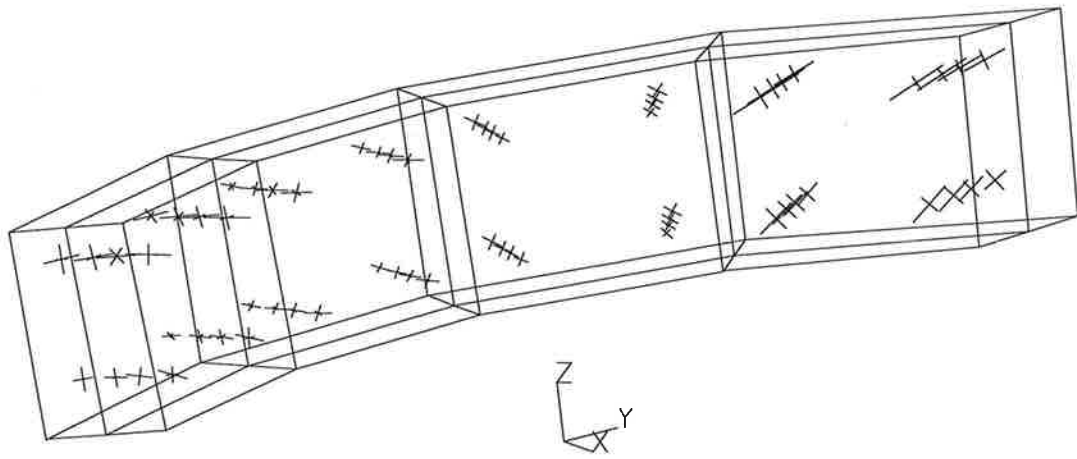
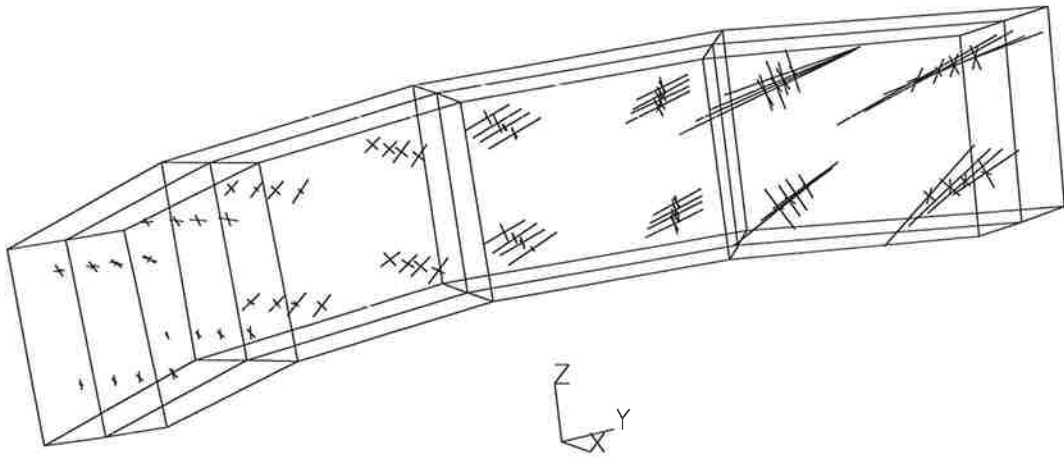(a) Case 1: Bonded
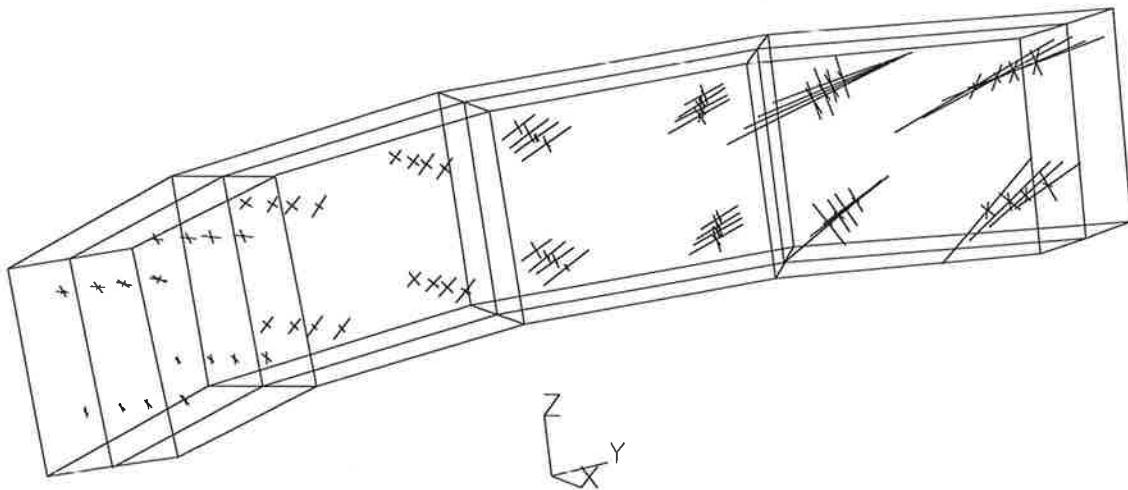
(b) Case 2: Frictionless
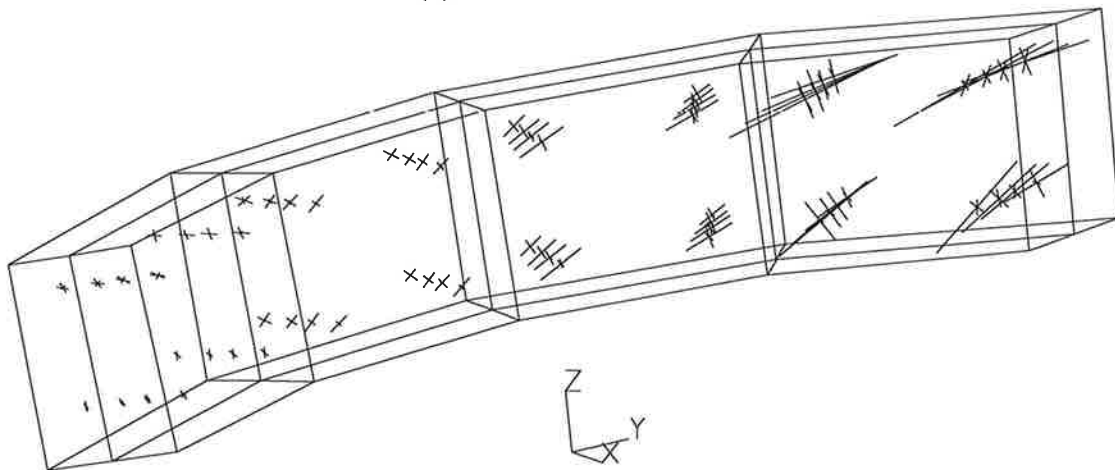
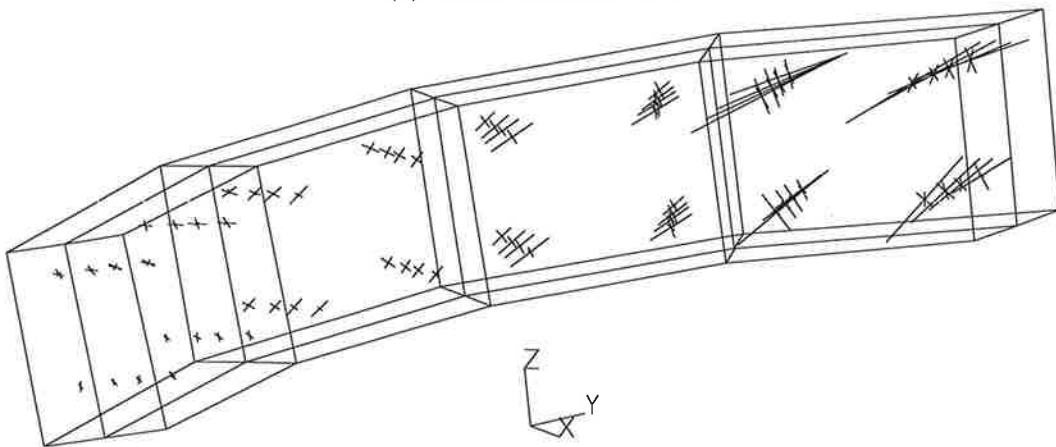(c) Case 3: Coulomb friction

Figure 5.14: Proximal medial calcar elements showing principal strain vectors for Cases 1, 2 and 3. No air-gap, elastic cement conditions.

(a) Case 4: Bonded

(b) Case 5: Frictionless

(c) Case 6: Coulomb friction

Figure 5.15: Proximal medial calcar elements showing principal strain vectors for Cases 4, 5 and 6. With an air-gap, elastic cement conditions.

(a) Case 7: Bonded

(b) Case 8: Frictionless

(c) Case 9: Coulomb friction

Figure 5.16: Proximal medial calcar elements showing principal strain vectors for Cases 7, 8 and 9. No air-gap, viscoelastic cement conditions.
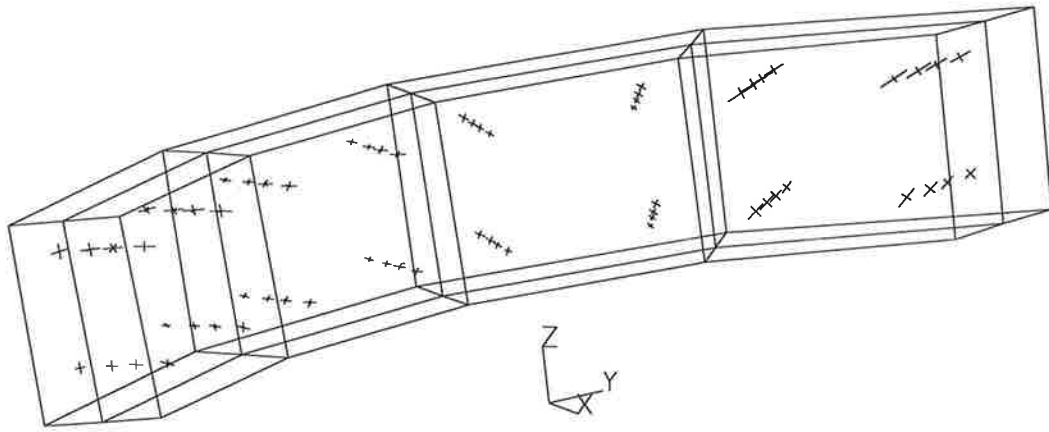
(a) Case 10: Bonded
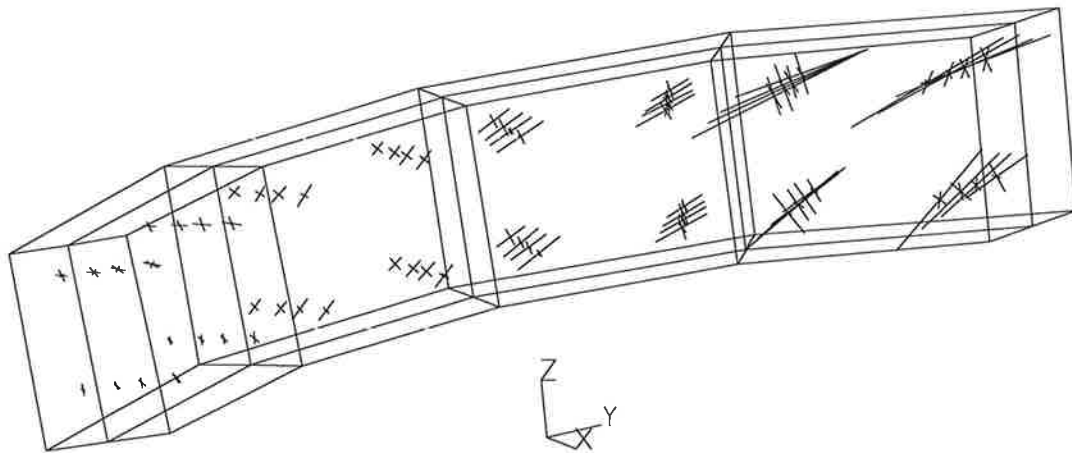
(b) Case 11: Frictionless
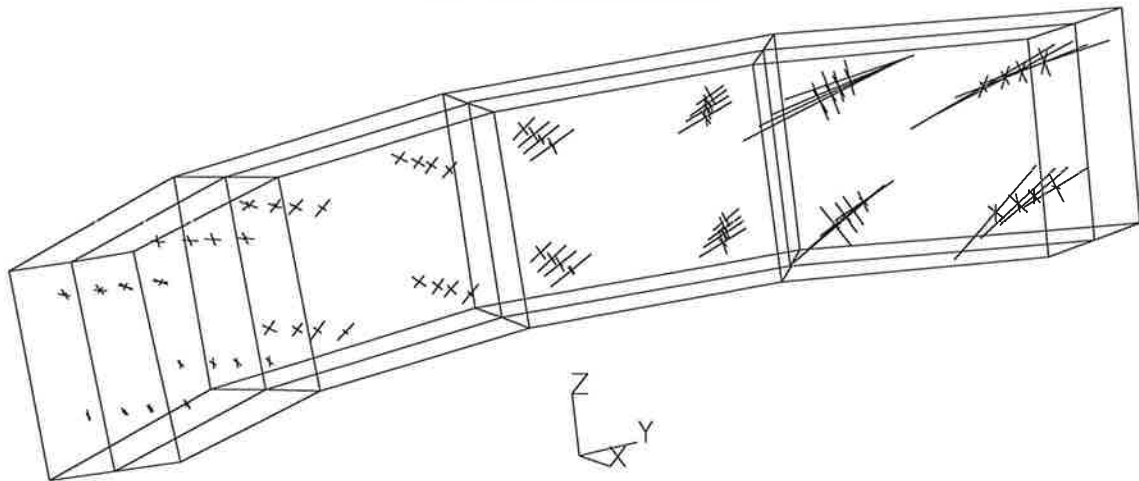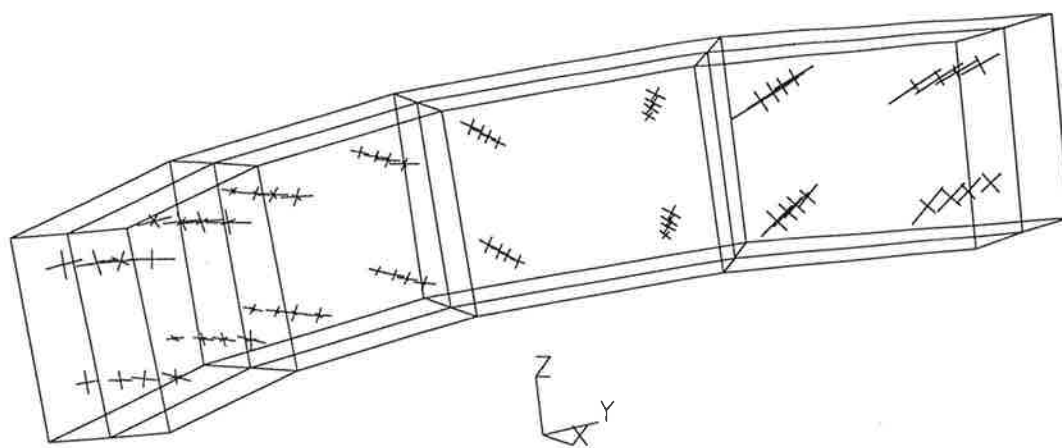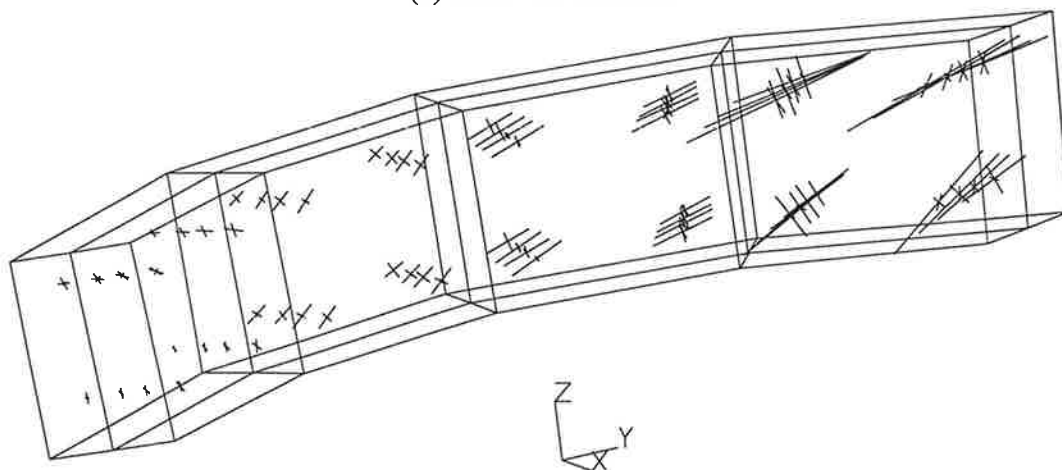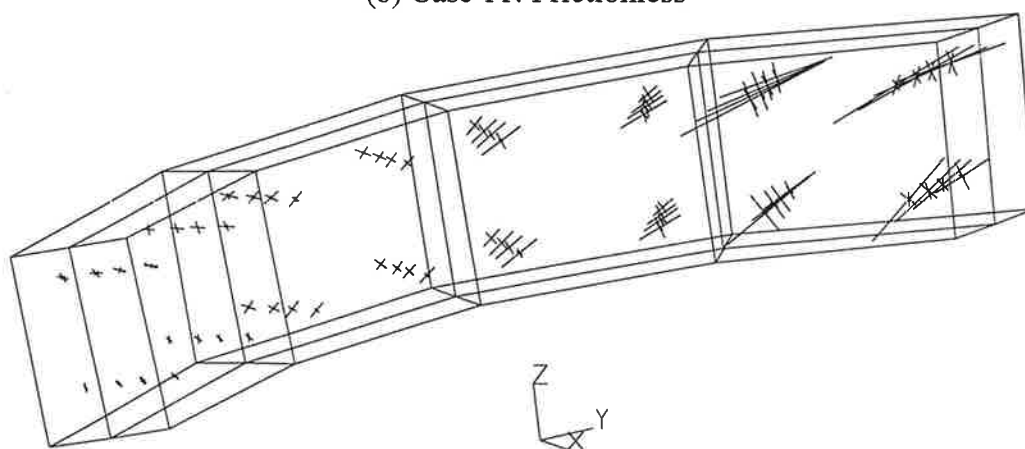
(c) Case 12: Coulomb friction

Figure 5.17: Proximal medial calcar elements showing principal strain vectors for Cases 10, 11 and 12. With an air-gap, viscoelastic cement conditions.

5.3.3 Summary of calcar strain output

The peak Von mises strains in the proximal medial calcar are presented graphically in Figure 5.18 to allow a convenient comparison between the different analyses. A detailed discussion of these results is provided in Section 5.3.4.
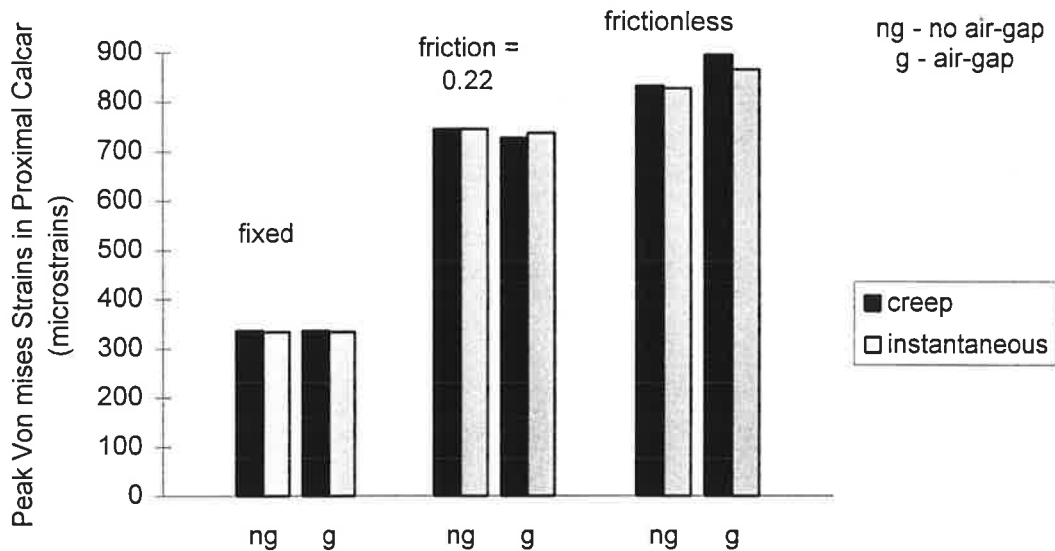
Figure 5.18: Peak Von mises strains within the proximal medial calcar for the twelve analyses.

5.3.4 Discussion of calcar strain data and comparison with other studies

In Section 5.2.4, it was stated that a general discussion of the results would be presented and the results compared to other studies. This also applies to the calcar strain data with a detailed biomechanical discussion reserved for Section 5.4, where the interaction of cement stresses and calcar strains will be detailed.

It was the case with the cement stress data that the main difference in results was produced by altering the surface finish condition of the prosthesis. A similar pattern was noted with the calcar strain output. The inclusion of cement creep and the presence of a distal air-gap had little effect on the results. A comparison between the frictionless and bonded interfaces, however, showed distinct changes in the magnitude and orientation of the principal strains. In the normal pre-operative state, the main strain component is in the

longitudinal (z-axis) direction, (Lanyon *et al.*, 1981). The frictionless stem-cement interface condition produced a large non-physiological tensile hoop component of strain. It is unclear how bone will adapt to this 'unnatural' strain and whether or not resorption will occur. The bonded stem-cement interface also showed a tensile hoop component but of far smaller magnitude. The peak Von mises strain was also significantly smaller for the bonded interface ($337\mu\varepsilon$) when compared to the frictional ($728\mu\varepsilon$) or frictionless ($897\mu\varepsilon$) interface. It appears that a bonded stem-cement interface has a greater opportunity for calcar resorption due to the significant decrease in the distortional strain energy density present in the region.

Oh and Harris (1978) found that strain levels in the femoral calcar reduced massively with the introduction of a cemented hip prosthesis. A reduction from $1800\mu\varepsilon$ for an intact femur down to less than $200\mu\varepsilon$ with a collarless prosthesis was noted. A collared prosthesis is intended to increase strain levels in the proximal medial calcar by transferring load directly to the calcar through bearing. If any resorption of the calcar occurs *in vivo*, however, the collar bears directly onto the cement causing particularly high localised stresses. Oh and Harris concluded that "After insertion of a femoral component, the normal pattern of a progressive proximal-to-distal decrease in strain was reversed, and the strain was maximum near the tip of the prosthesis." It was further concluded that "This severe reduction in strain implies that important metabolic changes may occur and suggests the possibility that extensive disuse osteoporosis may be the result." In the present study, maximum principal strains were in the order of $250\mu\varepsilon$ for the bonded interface analyses, which compare well with the study of Oh and Harris, considering the authors measured strain in the longitudinal direction only ie hoop strains were not considered.

Jacob and Huggler (1980) also found a significant reduction (60 %) in the longitudinal component of strain in the femoral calcar. Crowninshield *et al.* (1980b) noted that with a collarless prosthesis, tensile hoop strains were noted in the proximal calcar that were larger in magnitude than longitudinal compressive strains. A bonded stem-cement interface was assumed in their study.

Lanyon *et al.* (1981) noted a complete reorganisation in the calcar strain pattern between intact and prosthetic femurs. The authors found that compressive strains were reduced from $704\mu\varepsilon$ to $294\mu\varepsilon$ and tensile strains increased from $179\mu\varepsilon$ to $235\mu\varepsilon$ after the introduction of

a cemented hip prosthesis. A bonded stem-cement interface was assumed. The values obtained in their study correspond extremely well with the present finite element study. The present work produced a peak tensile strain of 228$\mu\epsilon$ and a peak compressive strain of 255$\mu\epsilon$ in the medial calcar for the bonded stem-cement interface, including cement creep and an air-gap. The agreement in results between Lanyon *et al.* and the present study is particularly encouraging as a sheep femur was modelled in the present work. The agreement of results with an *in vivo* animal model adds credence to the finite element model constructed in the present study.

Lewis *et al.* (1984) found, based on their theoretical analyses, that "without a collar or effective calcar-collar contact, neither of the metal alloys considered can create stresses greater than about 40 % of those seen in the intact femur." The authors further stated that "Our *in vitro* experimental results for the case of the undercut collar (similar to collarless), and those of others suggest that this percentage may be an optimistic upper bound." The authors assumed a bonded stem-cement interface in their study. The model of Huiskes *et al.* (1987) also predicted large levels of resorption of the proximal calcar. Brown *et al.* (1988) predicted significant (50 %) reductions in the compressive component of stress in the proximal calcar. Brown *et al.* used Von mises equivalent stresses as the "vehicle for reviewing calculated stress fields".

Clinical reviews confirmed the hypothesis that "stress-shielding" leads to calcar resorption. Beckenbaugh and Ilstrup (1978) found resorption of the medial calcar to be evident in 16.1 % of the hips. Blacker and Charnley (1977) found 70 % of long term reviewed hips experienced calcar resorption. Sutherland *et al.* (1982) found a 15 % incidence of calcar resorption in their ten year review.

In each of these reviews, radiographic (X-ray) evidence was used to study calcar resorption, and this resorption was only recorded if there was a geometric decay of the bone area at the medial calcar ie. the bone stock had 'disappeared' in consecutive follow-up radiographs. Recent studies using Tomographic density measurements have shown that losses of less than 20 % of bone mass do not show up on the radiographs. Hence the loss of bone mass may be far more prevalent than indicated by follow-up radiographic reviews.

The strain gauge and finite element studies reviewed in this section show good qualitative and quantitative agreement with the present study. It is obvious that the insertion of a cemented total hip replacement leads to a large decrease in the strain level in the region of the medial calcar. Clinical reviews have confirmed this "stress-shielding" will lead to resorption of bone. This decrease in bone stock will lead to a lack of radial support for the proximal cement mantle increasing the likelihood of failure. It therefore seems of great importance to design a prosthesis system which imparts 'reasonable' levels of strain to the proximal medial calcar to prevent resorption.

The following Section 5.4 will examine the interrelationship between cement stresses and calcar strains and the biomechanical justification behind prosthesis designs using either smooth or rough surface finishes.

5.4 The biomechanical interrelationship between cement stresses and calcar strains

This study has explored the rationale behind the two "schools of thought" regarding surface finish of a cemented hip prosthesis. Some designers and clinicians (Jasty *et al.* 1991) believe that a bonded interface at the stem-cement boundary is of prime importance due to the increase of tensile cement stresses noted with stem-cement debonding. On the other hand, it is considered by some that a bonded stem-cement interface produces a non-physiological strain regime in the femur and that a sliding stem-cement interface will produce a more physiological strain pattern (*Fowler et al.* 1988). It is believed by this group that deleterious tensile hoop stresses induced in the cement mantle will relax over time. This section will examine the biomechanics of these arguments.

5.4.1 The effect of prosthesis surface finish

The biomechanics of load transfer considering different stem-cement interface conditions can be explained with reference to Figure 5.19, which is a schematic view of the cemented THR, considering an axial load, F.
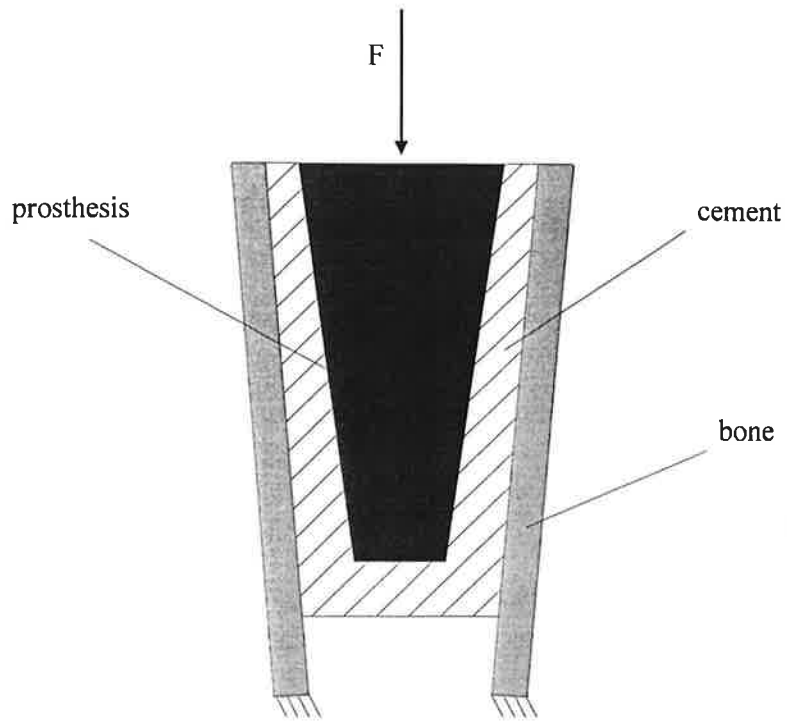
Figure 5.19: Schematic view of cemented THR considering axial load.

The prosthesis is now isolated as a free body and the resistance of the axial force is defined schematically in Figure 5.20.
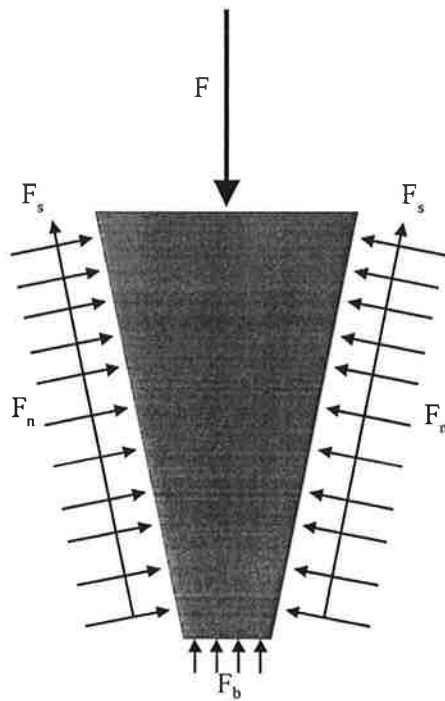

Figure 5.20: Free body diagram of a prosthesis subject to an axial load.

For the case of a no air-gap condition under the prosthesis tip, the axial load F is resisted by a bearing force, F_b, the vertical component of the normal force, F_n, and the vertical component of the shear force, F_s. The biomechanics of the different prosthesis surface finishes will now be examined with reference to this free body diagram.

Bonded stem-cement interface: In this case the shear force, F_s is large and the normal force, F_n is reduced. All longitudinal shear forces are transferred through the stem-cement interface. Some designers and clinicians believe this shear transfer may overstress the bone-cement interface which is weak in shear and tension, however in this study the magnitude of cement stresses did not reach the bone-cement interface strength (7.5 MPa, Kusleika and Stupp 1983).

Frictional stem-cement interface: The presence of Coulomb friction at the stem-cement interface means that some of the applied axial load, F will be transferred as frictional shear. The magnitude of the shear force, F_s, will be less than for the bonded interface. The normal force, F_n, will therefore increase, as will the bearing force, F_b. The higher the coefficient of friction at the stem-cement interface, the higher the magnitude of F_s, and the lesser the magnitude of F_n.

Frictionless stem-cement interface: In the absence of friction at the stem-cement boundary, the axial force, F is resisted purely by the normal force, F_n and the bearing force, F_b. There is no opportunity for shear force to be transmitted across the interface, ie. $F_s = 0$.

These generalised principles were demonstrated quantitatively in the present study. For the frictionless stem-cement interface, the high normal force component led to high tensile hoop stresses being developed in the cement and a large tensile component of strain in the medial calcar. For the frictional interface, these tensile hoop components reduced slightly, as the shear component increased. A low-friction prosthesis was modelled in this study, hence the reductions in the normal component were not overly significant. The bonded interface produced significantly different results in terms of the both the cement stresses and calcar strains. This reflected the significant increase in the shear force, F_s being transmitted across the interface.

The simplified free body diagram (Figure 5.20), considered an axial load only. The bending and torsional loads will also have differing load transfer mechanisms depending on the stem-cement interface condition. For example, a bonded stem-cement interface, will transmit tensile normal forces across the interface in bending whereas a frictionless debonded interface cannot. Torsional loads will be transmitted as shear forces with a bonded stem-cement interface, however a frictionless interface will transmit these loads through the development of normal forces in the cement.

The distal air-gap: When an air-gap is included under the prosthesis tip, the bearing force resisting the applied axial load is zero, ie $F_b = 0$. In the present study the inclusion of an air-gap had little effect on the results except for the frictionless interface. The frictionless interface showed a large increase in the distal peak tensile cement stress. There was little change proximally, however, to either the cement stress or the calcar strain results, even when considering the frictionless interface. This demonstrated that the majority of the load transfer occurs through transmission of shear and normal forces along the prosthesis stem. It does not appear that a distal air-gap increases load shedding to the proximal medial calcar. This is because even without an air-gap the bearing component, F_b is small relative to the shear and normal forces, F_s and F_n. The large distal increase in the peak tensile cement stress with the frictionless interface is due to a localised stress concentration. It may be the case that the removal of *all* cement distal to the prosthesis tip would increase proximal load shedding.

5.4.2 The viscoelastic influence of bone cement

It has been noted clinically that the femoral component of cemented THR can subside up to 2 mm distally in the femoral canal without the occurrence of crack formation in the cement mantle (Fowler *et al.* 1988). Either cracks were not being detected or the cement mantle was creeping over time. The proponents of a highly polished prosthesis surface finish suggested that that the high tensile hoop stresses found in the cement mantle may relax over time. Commercial bone cement or PMMA displays viscoelastic behaviour in the laboratory, however the amount of creep or relaxation *in vivo* depends on the restraint condition.

Consider the following example, Figure 5.21 of a cement bar subject to three different restraint conditions, with an applied axial load P. The cement bar is assumed to have the following properties:

cross-sectional area - A_c

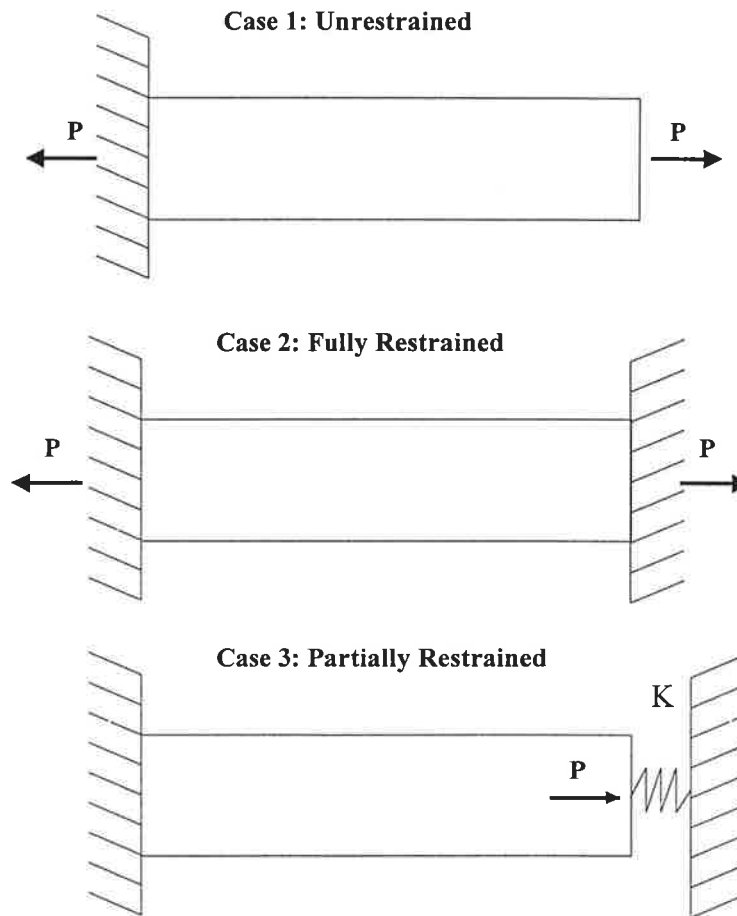length - l_c

Elastic Young's modulus - E_c

Figure 5.21: Different restraint conditions for a viscoelastic cement bar, subject to an axial load, P.

When an axial load, P is applied to the cement bar there is an initial elastic deformation followed by a viscoelastic deformation known as creep. The total strain, therefore consists of an elastic and a creep component. In equation form:

$\varepsilon_{total} = \varepsilon_o + \varepsilon_{cr}$

Where, ε_{total} is the total strain

              ε_o is the elastic strain

              ε_{cr} is the creep strain

Now, ε_o can be expressed as $\varepsilon_o = \sigma/E_o$

where, σ is the instantaneous stress

              E_o is the elastic Young's modulus

and assuming a power law for the creep strain ε_{cr} $\varepsilon_{cr} = A.\sigma^m.t^n$

where,   t is the loading time, A, m, n are viscoelastic constants.

Therefore $\varepsilon_{total} = \sigma/E_o + A.\sigma^m.t^n$ Eq. (5.2)

Consider now the strain response to the application of the axial load, P.

Case 1 - Unrestrained:

Upon application of the load, P, there is an initial elastic strain followed by an unrestrained creep strain. In this case the instantaneous stress remains constant over time, t.

Case 2 - Fully Restrained:

In this case it is assumed that an initial force, P is applied axially to the bar and it is then clamped, producing clamping forces equal in magnitude to P. The total strain in this case is equal to the initial elastic strain for all t. Any additional strain, after t = 0 must be equal to zero for all t due to the restraint condition. As the loading time, t increases, there must be a corresponding decrease in the instantaneous stress component σ to maintain the condition

of zero additional strain. This is what is referred to as stress relaxation. The clamping forces will also therefore decrease.

Case 3 - Partially Restrained:

This situation is analogous to the mechanical condition in total hip replacement. In cemented THR the tensile hoop stresses are resisted by the elastic cortical bone. In this case the total strain is governed by the stiffness of the spring, K.

It can be shown that at t = 0, the stress present in the cement bar, σ_{c0} is given by:

$$\sigma_{c0} = P/A_c \times (K_c/(K_c+K))$$

where K_c is the elastic stiffness of the cement bar given by $K_c = E_c.A_c/L_c$

The lower the spring stiffness K, the higher the value of the tensile cement stress, σ_{c0}. For a high spring stiffness the value of the initial cement stress will approach zero.

After a time, t the strain in the cement bar will increase in accordance with Equation 5.2. This increase in cement strain causes additional displacement of the spring. The force and therefore the instantaneous stress present in the spring is proportional to the spring displacement. The force in the spring therefore must increase over time as the cement creep causes the spring to compress. As the spring force increases over time the instantaneous force, (and therefore stress) in the cement bar must decrease to preserve equilibrium of the internal forces (in the cement and spring) and the external force P. The instantaneous cement stresses will therefore *relax*.

If the spring stiffness is *low*, ie approaching Case 1, the resistance from the spring to any increased displacement caused from creep of the cement bar will not be substantial. There will be a relatively large increase in spring displacement but only a relatively small increase in spring force due to the low spring stiffness (spring force = stiffness x displacement). To maintain equilibrium, there will only be a correspondingly *small* decrease in the cement force and therefore instantaneous cement stress.

If the spring stiffness is *high*, the resistance from the spring to any increased displacement caused from creep of the cement bar is large. There will be a relatively small increase in spring displacement but a relatively large increase in spring force due to the high spring stiffness (spring force = stiffness x displacement). To maintain equilibrium, there will be a correspondingly *large* decrease in the cement force and therefore instantaneous cement stress.

The above discussion has been confined to a qualitative one, as there is no explicit solution for the cement stresses in the cement bar when a spring and creep are considered. Simple numerical examples can be used to demonstrate that, for the same cement properties, an increased spring stiffness will cause a greater percentage reduction in the instantaneous cement stresses.

The previous example can be used as an analogy for tensile hoop stress relaxation in cemented total hip replacement. The degree of restraint for the proximal tensile hoop cement stresses is dependent on the bone stock at the proximal medial calcar.

The largest peak tensile cement stresses in the present study occurred proximally as hoop stresses for the case of the frictionless stem-cement interface. For the frictionless interface condition the loads acting on the head of the prosthesis are transferred as radial compressive forces and are resisted in two ways. The dual resistance can be explained by considering a free body diagram of a half-circle section of cement in the xy plane shown in Figure 5.22.
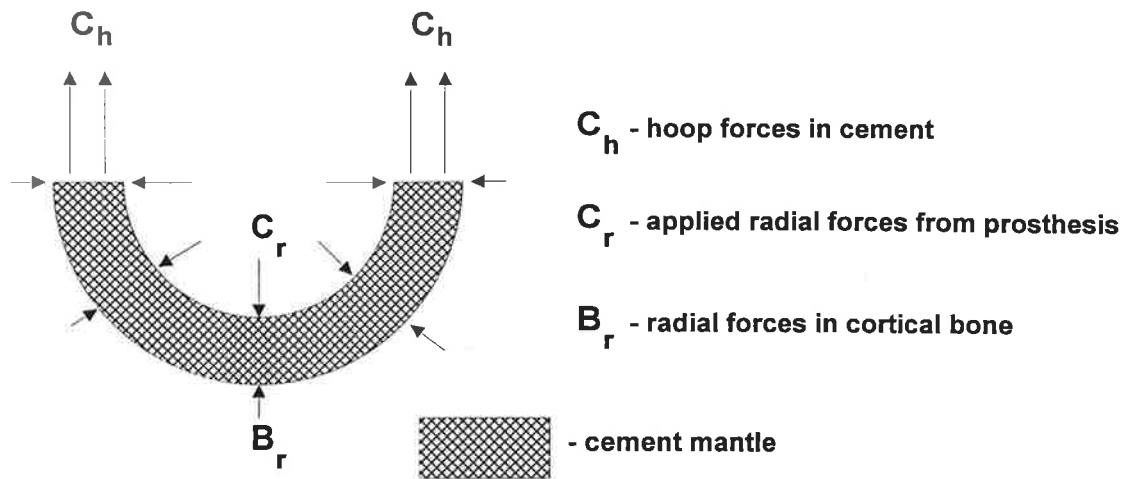
C_h - hoop forces in cement

C_r - applied radial forces from prosthesis

B_r - radial forces in cortical bone

- cement mantle

Figure 5.22: Free body diagram of the cement mantle (transverse plane), showing load transfer.

The compressive radial forces passing through the cement mantle are resisted 1) by radial compressive forces developing in the cortical bone shell and 2) by tensile circumferential or hoop forces developing in the cement mantle. The higher the degree of radial bone restraint, the greater the development of the radial compressive forces in the bone, B_r, and the lesser the development of the tensile hoop forces in the cement, C_h.

In terms of relaxation of the tensile hoop stresses, a high degree of relaxation will occur if the degree of radial bone restraint is high and little relaxation will occur if the degree of radial bone constraint is low.

HIGH RADIAL BONE CONSTRAINT:

The total circumferential or hoop strain of the cement is small due to the high degree of restraint ie ε_{total} is small.

As the loading time increases there must be a relatively large decrease in the instantaneous hoop stress to maintain the condition of a small total strain.

LOW RADIAL BONE CONSTRAINT:

The total circumferential strain of the cement is high due to the low degree of restraint ie. ε_{total} is large.

As the loading time increases, only a relatively slight decrease in the instantaneous hoop stress is necessary to maintain the condition of a large total strain.

The small relaxations in tensile hoop stresses found in this study are due to the low degree of skeletal support provided by the femoral calcar. It was also seen that as the tensile cement hoop stresses decrease, there is a corresponding increase in the Von mises strains in the proximal calcar. This is explained by referring again to Figure 5.22. As the tensile hoop forces which develop in the cement decrease, the radial bone forces must increase to balance the applied force, C_r. The increase in these radial bone forces leads to an increase in both the radial and hoop strains in the proximal calcar. It then follows that the higher the initial radial constraint, the greater the increase of Von mises strains in the supporting proximal bone over time due to cement creep.

The above discussion highlights the importance of the preservation of the proximal medial calcar. A decrease in this radial support will lead to an increase in the instantaneous tensile cement stresses and will reduce the opportunity for further cement stress relaxation.

5.5 The convergence test

Huiskes and Chao (1983) stated that both the accuracy and validity of any finite element model must be tested. A convergence test is one measure of testing the accuracy of the solution. By increasing the number of nodes in the model, the solution should converge towards one particular value. In this model three different element densities were considered and the solution was considered to be the maximum principal tensile stress occurring within the cement mantle. Figure 5.23 shows the values obtained for both the proximal and distal maximum principal stress in the cement mantle. The standard element density used in this study was 45.5 elements/cm^3, corresponding to 2,825 nodes for the bonded interface model and 3,126 nodes for the sliding interface models. Results were also calculated for the bonded stem-cement interface using mesh densities of 5.7 elements/cm^3 corresponding to 421 nodes and 180.1 elements/cm^3 (10,570 nodes) to test for the convergence of the solution.
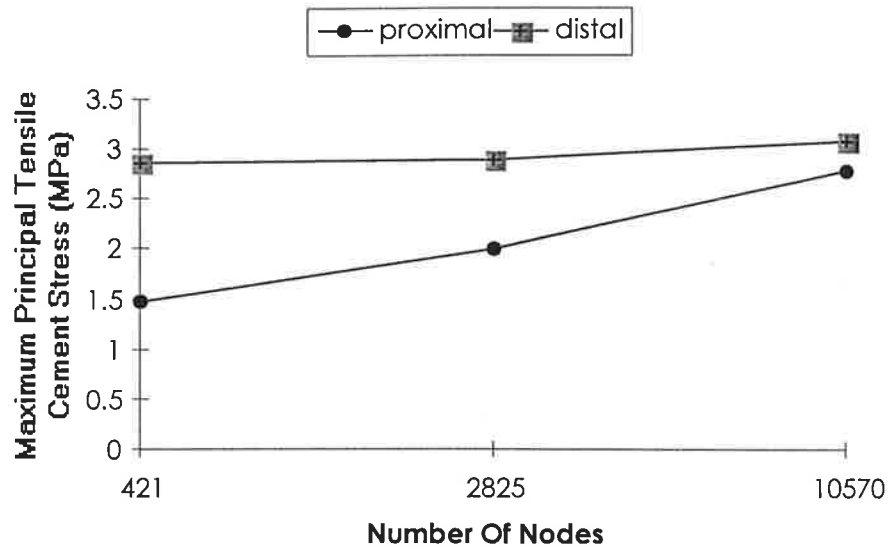
Figure 5.23: The convergence test for the bonded stem-cement interface condition, no creep, no air-gap.

The maximum stress occurred at the same location in the proximal region of the cement mantle for each number of nodes. This location is shown in Figure 5.2a for the intermediate (2,825) number of nodes. The maximum stress at this location presented as a radial tensile stress. The magnitude of this maximum stress increased with the number of nodes and elements as the stress concentration occurred at a boundary. A large element density would be required at this location to accurately determine the "true" maximum stress. Gauss points were used to provide the stress output and the location of the Gauss point will move closer to the true location of the peak stress as the number of elements increase. Computer time however prevented the inclusion of more nodes and the intermediate number (2 825) was used. It is also restated here that the main objective is to compare *qualitative* trends between parameter variation. Therefore if the same number of nodes is used in each analysis, the accuracy of solution will be similar and qualitative comparisons can be made.

For the case of the maximum distal cement stress, the magnitude remained constant and the location remained at the bone-cement boundary. This location is seen in Figure 5.3a for the case of the intermediate number of nodes. This maximum stress presented as a longitudinal tensile stress for each number of nodes.

134

5.6 Model validity

Two features of the finite element model were checked for validity; 1) the effect of extended cement creep and 2) the effect of restraining the femur at the knee, instead of the cut-off level as was used in this study.

5.6.1 The effects of extended creep

McKellop *et al.* (1994) showed that the majority of cement stress relaxation occurred in the first four hours of loading. The same loading time was used in this study as the creep properties of cement were the same as used in the study of McKellop *et al.* (1994). It was decided to test the effects of extended cement creep by considering a loading period of six months. Figure 5.24 compares the effect of short and long term creep.
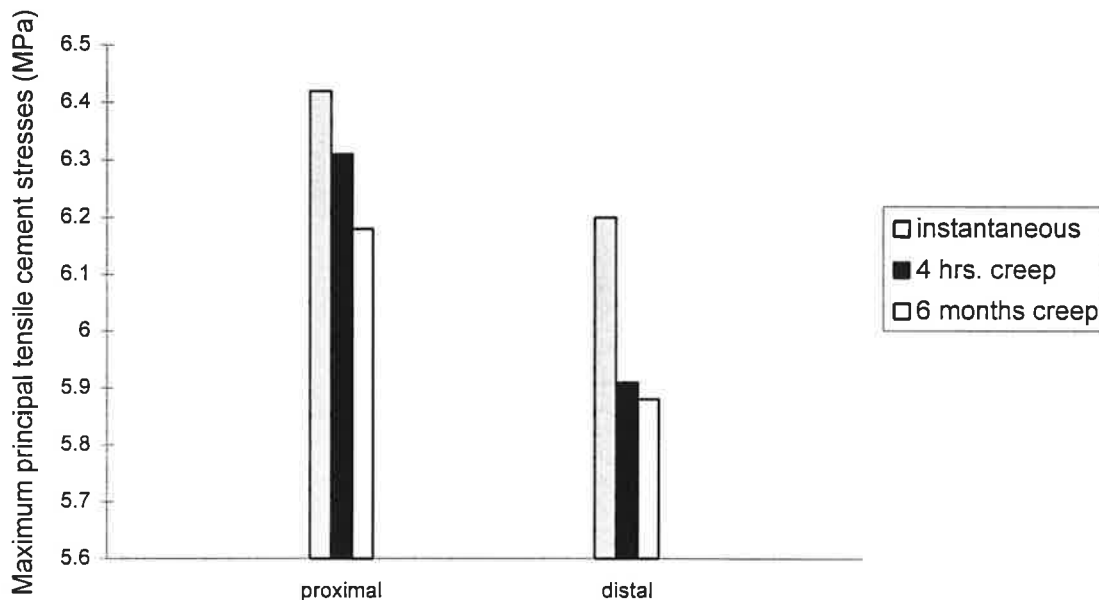
Figure 5.24: The effect of extended creep on peak tensile cement stresses for a frictionless stem-cement interface with an air gap.

It can be seen that the majority of stress relaxation had occurred distally in the first four hours of loading with only a small further decrease in the peak tensile cement stress distally. The peak proximal stress did show some further relaxation however it was decided for computational efficiency to terminate all viscoelastic analyses after loading times of

four hours. It was noted that even after six months, there was not a significant reduction in the peak proximal cement stress level.

5.6.2 Restraint at the knee level

In Chapter Four it was stated that to save computational expense the femur would be modelled as being restrained 50 mm proximal to the knee level. To test if this would affect the maximum tensile stresses in the cement mantle an analysis was conducted assuming distal support at the knee level. ie z = -50 mm. The model was adjusted for this analysis by altering the position of the Level 0 surfaces (Section 4.3.2) so that they were located at z = -50 mm. This analysis was for the bonded stem-cement interface and caused virtually no change in the maximum principal tensile stress, as shown in Table 5.5 below.

Table 5.5 The effect of distal restraint at the knee.

	Femur restrained 50 mm above knee level, ie z = 0.	Femur restrained at knee level, ie z = -50 mm.
Maximum proximal principal tensile cement stress.	1.99 MPa	1.99 MPa
Maximum distal principal tensile cement stress.	2.89 MPa	2.87 MPa

A summary of the study, with relevant conclusions and recommendations is presented in Chapter Six.

Chapter Six

Conclusions and Recommendations

6.1 Summary

The aims of this study were to examine the biomechanics of cemented total hip replacement, and assess the mechanical influence of the stem-cement interface.

The literature review revealed the complexity of aseptic loosening of the femoral prosthesis component and showed that the causes behind this loosening were multi-factorial. Several finite element and strain gauge studies have explored the mechanical behaviour of cemented THR. Many of the early studies were two-dimensional and linear in nature. This was mainly due to inadequate computing capabilities, both in terms of the available software and hardware. Another limitation in modelling cemented THR systems was the lack of knowledge regarding the numerical characterisation of the physical variables *in vivo*. These variables included the mechanical properties of bone and bone cement, the interface behaviour, both at the bone-cement and stem-cement boundaries, and the nature of the joint loading.

In the late 1980s, significant improvements in computing capabilities led to three dimensional analyses and non-linear considerations, such as debonded interfaces and anisotropic material properties. The extent of how accurately these models reflected *in vivo* mechanical conditions was still questionable, however the inadequacy of two-dimensional

137

linear models became clear. The more realistic simulations demonstrated a completely different stress distribution present in the composite structure.

In the 1990s, viscoelastic properties of the bone cement were considered in the analyses as well as more complex loading arrangements such as stair-climbing and sophisticated muscle involvement. The present study has included a non-linear stem-cement interface, a realistic three dimensional loading pattern based on an *in vivo* animal model, a viscoelastic cement mantle and a double tapered femoral stem which is a common feature of many modern designs. Quasi-anatomical skeletal support was also included, based on CT scans from an adult sheep. This model produced results which compared well both qualitatively and quantitatively with other relevant studies. The main difficulty in assessing the reliability of results was the lack of data from *in vivo* studies. Several *in vitro* studies have used strain gauges to measure the strain levels in the femur and to a lesser extent the stress levels in the cement mantle, however the *in vivo* conditions may be substantially different. The present study compared well, in terms of strain levels in the medial calcar, with an *in vivo* strain gauge study performed by Lanyon *et al.* (1981). Finite element studies such as the present analysis should be used mainly for qualitative comparison between design parameters.

The present study indicated that significant changes occur in the cement stresses and medial calcar strains produced by altering the interface conditions at the stem-cement interface. For the most realistic case of including creep and an air-gap, maximum proximal principal tensile cement stresses varied from 6.31 MPa, to 4.69 MPa to 1.97 MPa for the respective interface conditions of frictionless, frictional with coefficient of 0.22 and bonded. Maximum distal principal tensile cement stresses varied from 5.91 MPa, to 2.95 MPa to 2.83 MPa for the three respective conditions.

The location and orientation of these stresses altered with the inclusion of sliding interfaces producing peak hoop cement stresses in both the distal and proximal regions, whereas the bonded interface produced a peak radial tensile stress proximally, and a longitudinal bending stress distally. The peak Von mises strain in the proximal calcar varied from 897$\mu\varepsilon$, to 728$\mu\varepsilon$ to 337$\mu\varepsilon$ for the three respective interface conditions, again considering the presence of creep and an air-gap.

The inclusion of cement creep in the model was not significant in reducing peak tensile stresses in the cement mantle. Although PMMA demonstrates significant creep in unconstrained tests (McKellop *et al.* 1988), little change in actual cement stress values was noted in this study. This may be explained by the degree of radial constraint modelled in this study.

The inclusion of an air-gap, designed to encourage subsidence and proximal load shedding, did not significantly affect the results except for the case of the frictionless interface. For this case, including cement creep, a 32 % increase in the distal maximum principal tensile cement stress was noted. Clinical reviews have shown the distal region of the cement mantle to be particularly susceptible to cracking hence the inclusion of the air-gap in modelling considerations seems necessary.

6.2 Conclusions

It is apparent that there is a "trade-off" between design objectives in cemented THR. The results of this study suggest a higher coefficient of friction between the stem and cement will reduce the peak tensile principal stresses in the cement mantle, however there will be lower levels of strain in the proximal medial calcar which may lead to resorption. It is also noted that the orientation of these calcar strains are not physiological. The normal physiological strain pattern shows a large longitudinal compressive component, however the insertion of a highly polished prosthesis produced a strain pattern in the femoral calcar with a large circumferential or hoop component. It is unclear whether this reorganisation of the strain pattern will lead to resorption, or whether bone stock will be preserved to a greater degree, relative to a bonded stem-cement interface, due to the higher strain energy density levels. Further work examining retrieved prosthetic sheep femurs should "shed light" on the clinical reality of bone loss from "stress-shielding".

It is reasonable to suggest, following the arguments presented in this study, that decreasing proximal radial bone support must increase the tensile hoop stresses present in the cement mantle. The magnitude of tensile cement stresses found in this study, for the frictionless interface, approach the fatigue endurance limit (6.89 MPa at one million cycles) for PMMA (Freitag and Cannon, 1977).

Jasty *et al.* (1991) concluded that the initial event in the failure of cemented THR does not occur at the bone-cement interface, but exists as a crack in the cement mantle originating at a void or at the stem-cement interface. It therefore seems ominous for the long-term mechanical survival of the prosthesis system, if there is decreasing radial cement support due to calcar resorption, leading to increased tensile cement stresses. In a review of the Exeter prosthesis (Fowler *et al.* 1988), a low coefficient of friction prosthesis, a very low incidence of calcar resorption was noted and the brief introduction of a matt-surfaced prosthesis was later regarded as retrograde as there was found to be an increased incidence of loosening with the higher coefficient of friction.

The results from this study have clinical implications. The quality of bone stock at the medial calcar at the time of implantation may influence the choice of design. A polished prosthesis surface may prevent calcar resorption by increased proximal load shedding, however there must be enough initial restraint to prevent excessively high tensile hoop stresses. Miles (1990) found that "a high degree of mechanical interlock at the interface (stem-cement) results in greater interfacial shear stress at the bone-cement interface, reduced radial compression and a marginally lower hoop stress. The hoop strain, however, is strongly influenced by the quality of the radial restraint offered by the surrounding skeleton." The results from the present study agree with this synopsis.

It is interesting to note that in this study for the case of including cement creep and an air-gap, peak proximal tensile cement stresses decreased by 25.7 %, and peak distal tensile cement stresses decreased by 50.0 % when the coefficient of friction was increased from 0.0 to 0.22. The peak Von mises strain in the calcar only decreased by 18.8 %. There may be an optimal condition at the stem-cement interface which leads to acceptable levels of proximal load shedding to the femoral calcar, but also maintains acceptably low levels of tensile hoop stresses in the cement mantle.

6.3 Recommendations

Further studies should address different bone stock conditions at the proximal medial calcar to account for osteoporotic ("thin-boned") patients. Another area of investigation which relates to the bone stock condition at the proximal calcar is that of impaction grafting. This involves grafting bone from other areas of the body to the deficient bone

stock area. Finite Element Analysis could be used to study the effect of impaction grafting in THR, on cement stresses and calcar strains.

It is also clear that further research must be carried out in terms of the numerical modelling of the materials comprising the composite system. For example the results of this study showed far lower levels of cement stress relaxation than a recent similar study (Saligrama *et al.* 1996). In their study, however, higher coefficients of viscoelasticity were used to model the cement. It is unclear which model most accurately reflects the actual *in vivo* situation. A parametric analysis of the stem-cement friction coefficient should also be considered.

A further area of consideration is the numerical modelling of calcar resorption, included in a study of the stem-cement interface. Strain energy density can be used as a feedback to the finite element model to predict regions of calcar resorption due to "stress-shielding". The decreasing stiffness of certain bone elements may affect the cement stresses. It has been suggested by Lu and McKellop (1995) that remodelling of cortical bone *in vivo* may account for the difference between finite element models and *in vivo* observations of distal subsidence of the prosthesis. Correlation between FEM models and animal experiments must also continue in order to improve the validity of FEM models which have the potential to replace animal experiments in the long term (Weinans *et al.* 1993).

Exploration of these areas may lead to more realistic simulations of *in vivo* total hip replacement behaviour, and the design of prostheses which are mechanically sustainable for the remainder of the patient's life.

References

Ahmed, A.M., Raab, S. and Miller, J.E. (1984) Metal/cement interface strength in cemented stem fixation. *J. Orthop.Res.* 2, 105-118.

Andriacchi, T.P., Galante, J.O., Belytschko, T.B. and Hampton, S. (1976) A stress analysis of the femoral stem in total hip prostheses. *J. Bone Jt. Surg.* 58-A, 618-624.

Astleford, W.J., Asher, M.A., Lindhold, V.S. and Rockwood, C.A. (1975) Some physical and mechanical factors affecting the shear strength of Methylmethacrylate. *Clin. Orthop.* 108, 145-148.

Bayne, S.C., Lautenschlager, E.P., Compere, C.L. and Wildes, R. (1975) Degree of polymerisation of acrylic bone cement. *J. Biomed. Mat. Res.* 9, 27-34.

Beaumont, P.W.R. and Plumpton, B. (1977) The strength of acrylic bone cements and acrylic cement-stainless steel interfaces. *J. Mat. Sci.* 12, 1853-1856.

Beckenbaugh, R.D. and Ilstrup, D.M. (1978) Total Hip Arthroplasty. A review of three hundred and thirty-three cases with long follow-up. *J. Bone Jt. Surg.* 60-A, 306-313.

Bergmann, G., Siraky, J. and Rohlmann, A. (1984) A comparison of hip joint forces in sheep, dog and man. *J. Biomechanics* 12, 907-921.

Bergmann, G., Graichen, F. and Rohlmann, A. (1992) Loading of hip implants by torsional moments. *Proc. 38th Ann. Meet. Orthop. Res. Soc.* p.19. Washington ORS.

Blacker, G.J. and Charnley, John (1977) Long-term changes in the upper femur after low-friction arthroplasty. *Orthop. Trans.* 1, 92.

Bonfield, W. and Datta, P.K. (1974) Young's Modulus of compact bone. *J. Biomechanics* 7, 147-149.

Brockhurst, P. (1975) Design for total hip prosthesis - the femoral stem. *Centre for Biomedical Engineering Report*, University of New South Wales, July.

Brown, T.D. and Ferguson, Jr., A.B. (1978) The development of a computational stress analysis of the femoral head - mapping tensile, compressive and shear stress for the varus and valgus positions. *J. Bone Jt. Surg.* 60-A, 619-629.

Brown, T.D. and Ferguson, Jr., A.B. (1980) Mechanical property distributions in the cancellous bone of the proximal femur. *Acta. Orthop. Scand.* 51, 429-437.

Brown, T.D., Pedersen, D.R., Radin, E.L. and Rose, R.M. (1988) Global mechanical consequences of reduced cement/bone coupling rigidity in proximal femoral arthroplasty: A three dimensional finite element analysis. *J. Biomechanics* 21, 115-129.

Brumby, S.A., Howie, D.W., Wang, A.W., Pearcy, M.J. and Nawana, N.S. (1996) The effect of surface roughness and a collar on fixation of cemented femoral stems *in vivo*. *Proc. 42nd Ann. Meet. Orthop. Res. Soc.* p.281. Atlanta ORS.

Bugbee, W.D., Barrera, D.L., Lee, A.C. and Convery, F.R. (1992) Variations in shear strength of the bone-cement interface in the proximal femur. *Proc. 38th Ann. Meet. Orthop. Res. Soc.* p.22. Washington ORS.

Burkhart, J.M. and Jowsey, J. (1967) Parathyroid and thyroid hormones in the development of immobilisation osteoporosis. *Endocrinol.* 81, 1053-1062.

Burstein, A.H., Currey, J.D., Frankel, V.H. and Reilly, D.T. (1972) The ultimate properties of bone tissue: The effects of yielding. *J. Biomechanics* 5, 34-44.

Carter, D.R. and Hayes, W.C. (1977) The compressive behaviour of bone as a two-phase porous structure. *J. Bone Jt. Surg.* 59-A, 954-962.

Carter, D.R. and Spengler, D.M. (1978) Mechanical properties and composition of cortical bone. *Clin. Orthop. Rel. Res.* 135, 192-210.

Carter, D.R., Vasu, R. and Harris, W.H. (1984) Stress changes in the femoral head due to porous ingrowth surface replacement arthroplasty. *J. Biomechanics* 17, 737-747.

Charnley, J. (1960) Anchorage of the femoral head prosthesis to the shaft of the femur. *J. Bone Jt. Surg.* 42-B, 28-30.

Charnley, J. (1964) The bonding of prosthesis to bone by cement. *J. Bone Jt. Surg.* 46-B, 518-529.

Charnley, J. (1965a) The elimination of slip between prosthesis and femur. *J. Bone Jt. Surg.* 47-B, 56-60.

Charnley, J. (1965b) A biomechanical analysis of the use of cement to anchor the femoral head prosthesis. *J. Bone Jt. Surg.* 47-B, 354-363.

Clarke, I.C.C. (1990) Micro-motion, consequences of material choices, implant design and fit. In *Implant bone interface*. Ed. John Older. Springer-Verlag. London. pp 123-129.

Cook, S.D., Klawitter, J.J. and Weinstein, A.M. (1980) The influence of design parameters on calcar stresses following femoral head arthroplasty. *J. Biomed. Mat. Res.* 14, 133-144.

Crowninshield, R.D., Johnston, R.C., Andrews, J.G. and Brand, R.A. (1978) A biomechanical investigation of the human hip. *J Biomechanics* 11, 75-85.

Crowninshield, R.D., Brand, R.A., Johnston, R.C. and Milroy, J.C. (1980a) The effect of femoral stem cross-sectional geometry on cement stresses in total hip reconstruction. *Clin. Orthop. Rel. Res.* 146, 71-77.

Crowninshield, R.D., Brand, R.A., Johnston, R.C. and Milroy, J.C. (1980b) An analysis of femoral component stem design in total hip arthroplasty. *J. Bone Jt. Surg.* 62-A, 68-78.

Crowninshield, R.D., and Tolbert, J.R. (1983) Cement strain measurement surrounding loose and well-fixed femoral component stems. *J. Biomed. Mat. Res.* 17, 819-828.

Davy, D.T., Kotzar, G.M., Brown, R.H., Heiple, K.G., Goldberg, V.M., Heiple, Jr., K.G., Berilla, J. and Burstein, A.H. (1988) Telemetric force measurements across the hip after total arthroplasty. *J. Bone Jt. Surg.* 70-A, 45-50.

Estok, D.M., Harrigan, T.P. and Harris, W.H. (1991) Finite element analysis of cement strains at the tip of an idealised cemented femoral component. *Proc. 37th Ann. Meet. Orthop. Res. Soc.*, p.504. ORS. Anaheim.

Estok, D.M. and Orr, T.E. (1992) The strain gradient across the cement mantle in a cemented femoral component, a detailed mapping. *Proc. 38th Ann. Meet. Orthop. Res. Soc.*, p.371. ORS. Washington.

Fornasier, V.L. and Cameron, H.U. (1976) The femoral stem/cement interface in total hip replacement. *Clin. Orthop.* 116, 248-252.

Fowler, J.L., Gie, G.A., Lee, A.J.C. and Ling, R.S.M. (1988) Experience with the Exeter total hip Since 1970 *Orthop. Clin. North Am.* 19, 477-489.

Freitag, T.A. and Cannon, S.L. (1977) Fracture characteristics of acrylic bone cements 2. Fatigue. *J. Biomed. Mat. Res.* 11, 609-624.

Gibson, L.J. (1985) The mechanical behaviour of cancellous bone. *J. Biomechanics* 18, 317-328.

Goldstein, S.A. (1987) The mechanical properties of trabecular bone: Dependence on anatomic location and function. *J. Biomechanics* 20, 1055-1061.

Greenwald, A.S., Wilde, A.H. and Matejczyk, M.B. (1977) Clinical applications and properties of acrylic bone cement. *Orthopaedics Digest* 5, 16.

Gruen, T.A., McNeice, G.M. and Amstutz, H.C. (1979) "Modes of Failure" of cemented stem-type components: A Radiographical Analysis of Loosening. *Clin. Orthop.* 141, 17-27.

Haas, S.S., Brauer, G.M., and Dickson, G. (1975) A characterisation of polymethylmethacrylate bone cement. *J. Bone Jt. Surg.* 57-A, 380-391.

Hampton, S.J., Andriacchi, T.P. and Galante, J.O. (1980) Three dimensional stress analysis of the femoral stem of a total hip prosthesis. *J. Biomechanics* 13, 443-448.

Harrigan, T.P. and Harris, W.H. (1991a) Collar-calcar stress transfer decreases cement stresses in femoral total hip replacements under rotatory loads. *Proc. 37th Ann. Meet. Orthop. Res. Soc.*, p.501. ORS. Anaheim.

Harrigan, T.P. and Harris, W.H. (1991b) Mechanical consequences of cement-metal interface disruption (debonding) at the distal tip of femoral total hip prostheses. *Proc. 37th Ann. Meet. Orthop. Res. Soc.*, p.503. ORS. Anaheim.

Harrigan, T.P. and Harris, W.H. (1991c) A three-dimensional non-linear finite element study of the effect of cement-prosthesis debonding in cemented femoral total hip components. *J. Biomechanics* 24, 1047-1058.

Harrigan, T.P., Kareh, J. and Harris, W.H. (1991) Initial loosening mechanisms in cemented femoral stems: Debonding at the cement-metal interface. *Proc. 37th Ann. Meet. Orthop. Res. Soc.*, p.520. ORS. Anaheim.

Harrigan, T.P., Kareh, J.A., O,Connor, D.O., Burke, D.W. and Harris, W.H. (1992) A finite element study of the initiation of failure of fixation in cemented femoral total hip components. *J. Orthop. Res.* 10, 133-144.

Harris, W.H., McCarthy, J.C. and O'Neill, D.A. (1982) Femoral component loosening using contemporary techniques of femoral cement fixation. *J. Bone Jt. Surg.* 64-A, 1063-1067.

Harris, W.H. and McGann, W.A. (1986) Loosening of the femoral component after use of the medullary-plug cementing technique. *J. Bone Jt. Surg.* 68-A, 1064-1066.

Heaney, R.P. (1962) Radiocalcium metabolism in disuse osteoporosis in man. *Am. J. Med.* 33, 188-200.

Helmke, H.W., Lednicky, C.L. and Tullos, H.S. (1992) Porosity of the cement/metal interface following cemented hip replacement. *Proc. 38th Ann. Meet. Orthop. Res. Soc.*, p.364. ORS. Washington.

Holm, N.J. (1977) The modulus of elasticity and flexural strength of some acrylic bone cements. *Acta. Orthop. Scand.* 48, 436-442.

Holm, N.J. (1980) The relaxation of some acrylic bone cements. *Acta. Orthop. Scand.* 51, 727-731.

Huiskes, R. (1980) Some fundamental aspects of joint replacement. *Acta. Orthop. Scand. Suppl.* 185.

Huiskes, R. and Chao, E.Y.S. (1983) A survey of finite element analysis in orthopaedic biomechanics: The first decade. *J. Biomechanics* 16, 385-409.

Huiskes, R., Weinans, H., Gootenboer, H.J., Dalstra M., Fudala, B. and Slooff, T.J. (1987) Adaptive bone-remodelling theory applied to prosthetic-design analysis. *J. Biomechanics* 20, 1135-1150.

Huiskes, R. (1990) The various stress patterns of press-fit, ingrown, and cemented femoral stems. *Clin. Orthop. Rel. Res.* 261, 27-38.

Inman, V.T. (1947) Functional aspects of the abductor muscles of the hip. *J. Bone Jt. Surg.* 29, 607-619.

Jacob, H. A. C. and Huggler, A. H. (1980) An investigation into biomechanical causes of prosthesis stem loosening within the proximal end of the human femur. *J. Biomechanics* 13, 159-173.

**Jasty, M., Maloney, W.J., Bragdon, C.R., O'Connor, D.O., Haire T. and Harris W.H.
(1991)** The initiation of failure in cemented femoral components of hip arthroplasties. *J. Bone Jt. Surg.* 73-B, 551-558.

Keller, J.C., Lautenschlager, E.P., Marshall, Jr., G.W. and Meyer, Jr., P.R. (1980)
Factors affecting surgical alloy/bone cement interface adhesion. *J. Biomed. Mat. Res.* 14, 639-651.

Keller, T.S., Mao, Z. and Spengler, D.M. (1990) Young's Modulus, bending strength, and tissue physical properties of human compact bone. *J. Orthop. Res.* 8, 592-603.

Krause, W.R., Krug, W. and Miller, J. (1982) Strength of the cement-bone interface. *Clin. Orthop. Rel. Res.* 163, 290-299.

**Ku, J.L., Goldstein, S.A., Choi, K.W., London, M., Herzig, M.A. and Matthews, L.S.
(1987)** The mechanical properties of single trabeculae. *Proc. 33rd Ann. Meet. Orthop. Res. Soc.*, p.48. ORS.

Kusleika, R and Stupp, S.I. (1983) Mechanical strength of polymethylmethacrylate cement-human bone interfaces. *J. Biomed. Mat. Res.* 17, 441-458.

Kusy, R.P. (1978) Characterisation of self-curing acrylic bone cements. *J. Biomed. Mat. Res.* 12, 271-305.

Lanyon, L.E., Magee, P.T. and Baggott, D.G (1979) The relationship of functional stress and strain to the processes of bone remodelling. An experimental study on the sheep radius. *J Biomechanics* 12, 593-600.

**Lanyon, L.E., Paul, I.L., Rubin, C.T., Thrasher, E.L., DeLaura, R., Rose, R.M. and
Radin, E.L. (1981)** *In vivo* strain measurements from bone and prosthesis following total hip replacement. *J. Bone Jt. Surg.* 63-A, 989-1001.

Lautenschlager, E.P., Moore, B.K. and C.M. Schoefeld, C.M. (1974) Physical characteristics of setting of acrylic bone cements. *J. Biomed. Mat. Res. Symp.* 5, 185-196.

Lautenschlager, E.P., Marshall, G.W., Marks, K.E., Schwartz, J. and Nelson, C.L. (1976) Mechanical strength of acrylic bone cements impregnated with antibiotics. *J. Biomed. Mat. Res.* 10, 837-845.

Lee, A.J.C., Ling, R.S.M. and Vangala, S.S. (1977) The mechanical properties of bone cements. *J. Med. Eng. Tech.* 2, 137-140.

Lee, A.J.C. (1990) Differential movement between implant and bone. In *Implant bone interface*. Ed. John Older. Springer-Verlag. London. pp 131-135.

Lewis, J.L., Askew, M.J., Wixson, R.L., Kramer, G.M and Tarr, M.S. (1984) The influence of prosthetic stem stiffness and of a calcar collar on stresses in the proximal end of the femur with a cemented femoral component. *J. Bone Jt. Surg.* 66-A, 280-286.

Ling, R.S.M., Halawa, M., Lee, A.J.C. and Vangala, S.S. (1981) Total hip replacement using the Exeter prosthesis. *J. Bone Jt. Surg.* 63-B, 283.

Lu, Z., Ebramzadeh, E., McKellop, H., Zahiri, C. and Sarmiento, A. (1992) The influence of the stem-cement bonding strength on the cement stresses in total hip arthroplasty. *Proc. 38th Ann. Meet. Orthop. Res. Soc.*, p.377. ORS. Washington.

Lu, Z. Ebramazadeh, E. and Sarmiento, A. (1993) The effect of failure of the cement interfaces on gross loosening of cemented total hip femoral components. *Proc. 39th Ann. Meet. Orthop. Res. Soc.*, p.519. ORS. San Francisco.

Lu, Z. and McKellop, H. (1995) The effect of creep on cement stress and subsidence of a hip prosthesis. *Proc. 21st Ann. Meet. Soc. Biomat.* San Francisco.

LUSAS user manual. (1990) FEA Ltd. Surrey. United Kingdom.

Maloney, W.J, Jasty, M., Burke, D.W., O'Connor, D.O., Zalenski, E.B., Bragdon, C. and Harris, W.H. (1989) Biomechanical and histologic investigation of cemented total hip arthroplasties. *Clin. Orthop. Rel. Res.* 249, 129-140.

Mann, K.A., Bartel, D.L., Wright, T.M. and Ingraffea, A.R. (1990) The role of friction at the Stem-PMMA cement interface. *Proc. 36th Ann. Meet. Orthop. Res. Soc.*, p.231. ORS New Orleans.

Mann, K.A., Bartel, D.L., and Wright, T.M. (1991) Cement stresses in a femoral hip component with coulomb friction at the stem-cement interface. *Proc. 37th Ann. Meet. Orthop. Res. Soc.*, p.107. ORS Anaheim.

Mann, K.A., Wright, T.M., Klein, R.W. and Ingraffea, A.R. (1992a) Mechanical characteristics and constitutive modelling of the plasma-sprayed stem-cement interface. *Proc. 38th Ann. Meet. Orthop. Res. Soc.*, p.21. ORS Washington.

Mann, K.A., Bartel, D.L., and Wright, T.M. (1992b) The effect of using a plasma-sprayed stem-cement interface on stresses in a cemented femoral hip component. *Proc. 38th Ann. Meet. Orthop. Res. Soc.*, p.317. ORS Washington.

Markolf, K.L. and Amstutz, H.C. (1976) A comparative experimental study of stresses in femoral total hip replacement components: The effects of prosthesis orientation and acrylic fixation. *J Biomechanics* 9, 73-79.

Martens, M., Aernoudt, E., de Meester, P., Ducheyne, P., Mulier, J.C., de Langh, R. and Kestelijn, P. (1974) Factors in the mechanical failure of the femoral component in total hip prosthesis. *Acta. Orthop. Scand.* 45, 693-710.

Martens, M., Van Audekercke, R., Delport, P., de Meester, P. and Mulier, J.C. (1983) The mechanical characteristics of cancellous bone at the upper femur region. *J. Biomechanics* 16, 971-983.

McCoy, T.H., Salvati, E.A., Ranawat, C.S. and Wilson, Jr., P.D. (1988) A fifteen-year follow up study of one hundred Charnley low-friction arthroplasties. *Orthop. Clin. North Am.* 19, 467-476.

McElhaney, J., Fogle, J., Byars, E. and Weaver, G. (1964) Effect of embalming on the mechanical properties of beef bone. *J. Appl. Physiol.* 19, 1234-1236.

McElhaney, J.H. and Byars, E. (1965) Dynamic response of biological materials. *ASME* 65. WA/HUF-9.

Mente, P.L. and Lewis, J.L. (1987) Young's modulus of trabecular bone tissue. *Proc. 33rd Ann. Meet. Orthop. Res. Soc.*, p.49. ORS.

Miles, A.W. (1990) A preliminary report on the stem-cement interface and its influence on the bone-cement interface. In *Implant bone interface*. Ed. John Older. Springer-Verlag. London. pp 137-145.

McKellop, H., Narayan, S., Ebramzadeh, E. and Sarmiento, A. (1988) Viscoelastic creep properties of PMMA surgical cement. *3rd World Biomaterials Congress*, p.328.

McKellop, H., Narayan, S., Lu, B. Ebramzadeh, E. and Sarmiento, A. (1989) Creep of PMMA surgical cement under constant stress and stress rate. *Proc. 15th Ann. Meet. Soc. Biomat.*, p.48. Lake Buene Vista.

McKellop, H, Lu, Z., Ebramzadeh, E. and Sarmiento, A. (1994) Variation of stress in the cement mantle of total hip replacements as a result of creep. *Proc. 40th Ann. Meet. Orthop. Res. Soc.*, p.798. ORS. New Orleans.

Oh, I., and Harris, W.H. (1978) Proximal strain distribution in the loaded femur. *J. Bone Jt. Surg.* 60-A, 75-85.

Oh, I., Carlson, C.E., Tomford, W.W. and Harris, W.H. (1978) Improved fixation of the femoral component after total hip replacement using a methacrylate intramedullary plug. *J. Bone Jt. Surg.* 60-A, 608-613.

Pal, S. and Saha, S. (1982) Stress relaxation and creep behaviour of normal and carbon fibre reinforced acrylic bone cement. *Biomaterials* 3, 93-96.

Paterson, M., Fulford, P. and Denham, R. (1986) Loosening of the femoral component after total hip replacement. *J. Bone Jt. Surg.* 68-B, 392-397.

Paul, J.P. (1971) Load actions on the human femur in walking and some resultant stresses. *Exper. Mech.* March, 121-125.

Pilliar, R.M., Blackwell, R., MacNab, I. and Cameron, H.U. (1976) Carbon fibre-reinforced bone cement in orthopaedic surgery. *J. Biomed. Mat. Res.* 10, 893-906.

Pugh, J.W., Rose, R.M. and Radin, E.L. (1973) A structural model for the mechanical behaviour of trabecular bone. *J Biomechanics* 6, 657-669.

Raab, S., Ahmed, A.M. and Provan, J.W. (1981) The quasistatic and fatigue performance of the implant/bone-cement interface. *J. Biomed. Mat. Res.* 15, 159-182.

Reilly, D.T., Burstein, A.H. and Frankel, V.H. (1974) The elastic modulus for bone. *J. Biomechanics* 7, 271-275.

Reilly, D.T. and Burstein, A.H. (1974) The mechanical properties of cortical bone. *J. Bone Jt. Surg.* 56-A, 1001-1022.

Reilly, D.T. and Burstein, A.H. (1975) The elastic and ultimate properties of compact bone tissue. *J. Biomechanics*, 393-405.

Rohlmann, A., Mossner, U., Bergmann, G. and Kobel, R. (1983) Finite-element-analysis and experimental investigation in a femur with hip endoprosthesis. *J. Biomechanics* 16, 727-742.

Rydell, N.W. (1966) Forces acting on the femoral head-prosthesis. *Acta. Orthop. Scand. Suppl.,* 1-128.

Saha, S., Pal, S. and Albright, J.A. (1981) Time dependent mechanical properties of normal and carbon fiber reinforced bone cement. *Proc. 27th Ann. Meet. Orthop. Res. Soc.* p.296. ORS.

Saha, S. and Pal, S. (1984) Mechanical properties of bone cement: A review. *J. Biomed. Mat. Res.* 18, 435-462.

Saha, S. and Warman, M.L. (1979) Compressive and shear properties of graphite fiber reinforced bone cement. *Orthop. Trans.* 3, 169.

Saligrama, V.C., Norman, T.L., Blaha, J.D. and Gruen, T.A. (1996) 3D finite element analysis of the stem-cement interface in a femoral hip prosthesis with a viscoelastic cement mantle. *Proc. 42nd Ann. Meet. Orthop. Res. Soc.* p.422. ORS. Atlanta.

Schaffler, M.B. and Burr, D.B. (1988) Stiffness of compact bone: Effects of porosity and density. *J. Biomechanics* 21, 13-16.

Schoenfeld, C.M., Lautenschlager, E.P. and Meyer, Jr., P.R. (1974) Mechanical properties of human cancellous bone in the femoral head. *Med. Biol. Eng.* 12, 313-317.

Sih, G.C. and Berman, A.T. (1980) Fracture toughness concept applied to Methyl Methacrylate. *J. Biomed. Mater. Res.* 14, 311-324.

Sih, G.C., Matic, P. and Berman, A.T. (1981) Failure prediction of the total hip prosthesis system. *J. Biomechanics.* 14, 833-841.

Simkin, A. and Robin, G. (1973) The mechanical testing of bone in bending. *J. Biomechanics* 6, 31-39.

Simo, J.C. and Rifai, M.S. (1990) A class of mixed assumed strain methods and the method of incompatible modes. *Int. J. Num. Meth. Eng.* 29, 1595-1638.

Skinner, H.B., Cook, S.D., Weinstein, A.M. and Haddad, Jr., R.J. (1982) Stress changes in bone secondary to the use of a femoral canal plug with cemented hip replacement. *Clin. Orthop. Rel. Res.* 166, 277-283.

Stauffer, R.N. (1982) Ten-year follow-up study of total hip replacement. *J. Bone and Jt. Surg.* 64-A, 983-990.

Sutherland, C.J., Wilde, A.H. and Borden, L.S. (1982) A ten-year follow-up of one hundred consecutive Muller curved-stem total hip-replacement arthroplasties. *J. Bone Jt. Surg.* 64-A, 970-982.

Svensson, N.L., Valliappan, S. and Wood, R.D. (1977) Stress analysis of human femur with implanted Charnley prosthesis. *J Biomechanics* 10, 581-588.

Taitsman, J.P. and Saha, S. (1977) Tensile strength of wire-reinforced bone cement and twisted stainless steel wire. *J. Bone Jt. Surg.* 59-A, 419-425.

Timoshenko, S.P. and Young, D.H. (1965) *Theory of Structures* 2nd. ed., McGraw-Hill.

Townsend, P.R., Raux, P., Rose, R.M., Miegel, R.E. and Radin, E.L. (1975) The distribution and anisotropy of the stiffness of cancellous bone in the human patella. *J. Biomechanics.* 8, 363-367.

Treharne, R.W. and Brown, N. (1975) Factors influencing the creep behaviour of polymethylmethacrylate cements. *J. Biomed. Mat. Res.* 6, 81-88.

Weber, F.A. and Charnley, J. (1975) A radiological study of fractures of acrylic cement in relation to the stem of a femoral head prosthesis. *J. Bone Jt. Surg.* 57-B, 297-301.

Weightman, B., Freeman, M.A.R., Revell, P.A., Braden, M., Albrektsson, B.E.J. and Carlson, L.V. (1987) The mechanical properties of cement and loosening of the femoral component of hip replacements. *J. Bone. Jt. Surg.* 69-B, 558-564.

Weinans, H., Huiskes, R. and Grootenboer, H.J. (1990) Trends of mechanical consequences and modelling of a fibrous membrane around femoral hip prostheses. *J. Biomechanics* 23, 991-1000.

Weinans, H., Huiskes, R., van Rietbergen, B., Sumner, D.R., Turner, T.M. and Galante, J.O (1993) Adaptive bone remodelling around bonded noncemented total hip arthroplasty A comparison between animal experiments and computer simulation. *J. Orthop. Res.* 11, 500-513.

Wilde, A.H. and Greenwald, A.S. (1974) The shear strength of Polymethylmethacrylate. *Proc. 41st Ann. Meet. Am. Acad. Orthop. Surg.*, Dallas.

Williams, J.L. and Lewis, J.L. (1982) Properties and an anisotropic model of cancellous bone from the proximal tibial epiphysis. *J. Biomech. Eng.* 104, 50-56.

Wilson, J.N.; and Scales, J.T. (1970) Loosening of total hip replacements with cement fixation. Clinical findings and laboratory studies. *Clin. Orthop.* 72, 145-160.

Wright, T.M. and Trent, P.S. (1979) Mechanical properties of Aramid fibre reinforced acrylic bone cement. *J. Mater. Sci.* 14, 503-505.

Yettram, A.L. and Wright, K.W. (1979) Biomechanics of the femoral component of total hip prostheses with particular reference to the stresses in the bone-cement. *J. Biomed. Eng.* 4, 281-285.

Zienkiewicz, O.C. and Taylor, R.L. (1971) *The finite element method.* 2nd ed. McGraw-Hill.